EPSC2018

TP1 abstracts

EPSC Abstracts
Vol. 12, EPSC2018-163, 2018
European Planetary Science Congress 2018

Hollows and their relationship with geochemical terrains

Alice Lucchetti (1), Maurizio Pajola (1), Marco Merusi (2), Gabriele Cremonese (1), Valentina Galluzzi (3), Lorenza Giacomini (3), Cristian Carli (3) Giuseppe A. Marzo (4), Sabrina Ferrari (5), Matteo Massironi (6), Pasquale Palumbo (7).

(1) INAF-OAPD Astronomical Observatory of Padova, Italy (alice.lucchetti@inaf.it) (2) Dept of Physics and Astronomy, University of Padova, Italy, (3) INAF-IAPS Roma, Istituto di Astrofisica e Planetologia Spaziali di Roma, Rome, Italy; (4) ENEA Centro Ricerche Casaccia, 00123 Rome, Italy, (5) CISAS, University of Padova, Italy, (6) Dept. of Geosciences, University of Padova, Italy, (7) Università degli Studi di Napoli "Parthenope", Italy.

1. Introduction

One of the most surprising discoveries revealed by the MESSENGER (Mercury Surface, Space, Environment, Geochemistry, and Ranging, [1]) spacecraft was the presence of shallow irregular and rimless flat-floored depressions with bright interiors, called hollows, at the Mercury surface. These features are widespread on the surface of the planet [2-4] and since they are fresh in appearance, they may be actively forming today via a mechanism that could involve depletion of subsurface volatiles [2-4], whose nature is not yet known. In this work, we want to characterize in deeper detail the behaviour of hollows located in three different craters, applying a spectral clustering technique [5] to understand if there are similarities among them from a compositional point of view.

2. Dataset and Methodology

We chose three different craters hosting hollows: (i) the **Dominici crater** (1.38N, 323.5°E, Kuiper quadrangle) with a diameter of 20 km [6]; (ii) an **un-named crater** (25.62°N, -3.4°W, Victoria quadrangle) with a diameter of 25 km; (iii) the **Velazquez crater** (37.74°N, 304.77°E, Victoria quadrangle) with a diameter of 128 km. For each crater, we chose a WAC dataset of different filters in order to apply a spectral clustering technique based on a K-mean algorithm [7-9]. This allows us to separate our studying area in clusters (as reported in [5]), each one characterized by an average multi-color spectrum and its associated variability, as shown in Fig. 1.

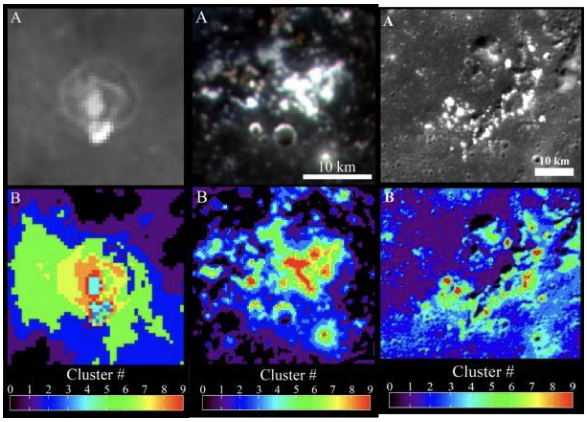

Fig. 1. *A:WAC reference images (EW0210848973D) (EW1017269227D) (EW1020781879D) for Dominici, un- named and Velazquez crater respectively. B: The relative 10 clusters identified in the MDIS datasets.*

3. Results

From the clusters' spectra we managed to separate areas associated to hollows from both the surroundings and intermediate terrains. Within all craters, we were then able to identify a unique hollows' representative spectrum that is characterised by a wide absorption band between 0.558 and 0.828, with a possible hint of absorption towards 1 μm (top of Fig. 3). Our analysis suggests that the spectral behavior of hollows cannot be explained by sulfides alone (CaS, MnS and MgS, [10]), as reported from the comparison between spectra in Fig. 3. Even if the mechanism forming hollows likely involves the loss of volatiles from the surface, we have to take into account other minerals that could be in part responsible of the absorption. In this context, we consider bedrock-forming material contributing to the spectral identified hollow behavior, in particular pyroxene presenting transitional elements (Cr and Ti) and clynopyroxenes in which Ni is substituting Mg (Ni-diopside) [11,12] seem to be particularly well suited.

Figure. 3 *On top the continuum removed hollows spectra found in our crater cases, while on bottom left the continuum removed MgS*

and MnS spectra reported in [10], which are already cited candidates for hollows composition in literature. The comparison shows that sulfides alone cannot be considered as the only responsible of the absorption found in hollows spectra.

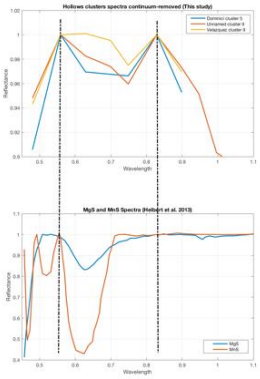

4. Conclusion and future work

In this work we suggest that hollows terrains are the expression of both the remnant material coming from a process that involve degassing and the bedrock-forming material in which they formed. Indeed, all the considered hollows show a similar spectral behaviour, suggesting that their location is not strictly associated to the presence of a particular element. In order to understand if the 0.558 and 0.828 μm band is present on all hollows, independently from the location, the next step will be the analysis of other hollows features located in the high rich Mg-region [13]. Here, 80 hollows groups were previously found [4]. We are currently investigating them in order to understand if the presence of Mg in high concentration within the bedrock could affect the hollows' spectral behaviour in that region.

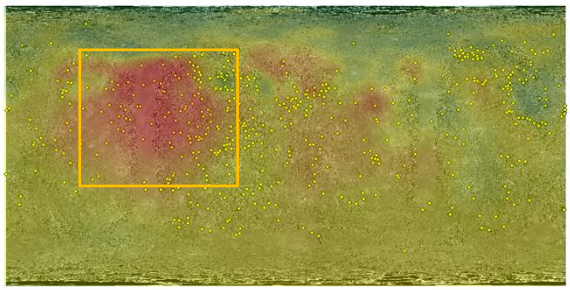

Figure 4*: High Mg-region [13] highlighted by the orange square on Mercury basemap. Yellow dots are the location of hollows group as reported by [4].*

Acknowledgements

This activity has been realized under the BepiColombo ASI-INAF agreement no. 2017-47-H.

References

[1] Hawkins, S. E. et al. (2007), The Mercury Dual Imaging System on the MESSENGER *Space Sci. Rev.*, 131, 247-

[2] Blewett D. T, et al. (2011) Hollows on Mercury: MESbSENGER evidence for geologically recent volatile-related activity. *Science*, 333, 1856–1859

[3] Blewett D. T. et al. (2013), Mercury's hollows: Constraints on formation and composition from analysis of geological setting and spectral reflectance. *JGR Planets*, 118, 1013-1032.

[4] Thomas R. J. et al. (2014), Hollows on Mercury: Materials and mechanisms involved in their formation. *Icarus*, 229, 221–235.

[5] Lucchetti, A. et al. (2018). Mercury: current and future science of the innermost planet. Abstract #6028.

[6] Vilas, F. et al. (2016), Mineralogical indicators of Mercury's hollows composition in MESSENGER color observations. *GRL*, 43, 1450-1456.

[7] Marzo et al. (2006), Cluster analysis of planetary remote sensing spectral data. J. Geophys. Res. 111. E03002.

[8] Marzo et al. (2008), Statistical exploration and volume reduction of planetary remote sensing spectral data. J. Geophys. Res. 113. E12009.

[9] Marzo et al. (2009), Automated classification of visible and infrared spectra using cluster analysis. J. Geophys. Res. 114. E08001.

[10] Helbert et al. (2013). Visible and near-infrared reflectance spectra of thermally processed synthetic sulfides as a potential analog for the hollow forming materials on Mercury. Earth Planet. Earth Planet. Sci. Lett. 369-370, 233–238.

[11] Cloutis et al., (2002), Pyroxene reflectance spectra: Minor absorption bands and effects of elemental substitutions. *JGR: Planets*, *107*(E6).

[12] White et al. (1971), Optical spectra of chromium, nickel and cobalt-containing pyroxenes. Am Mineral 56:72–89.

[13] Weider et al. (2015), Evidence for geochemical terranes on Mercury: Global mapping of major elements with MESSENGER's X-Ray Spectrometer. Earth Planet. Sci. Lett. 416, 109–120.

EPSC Abstracts
Vol. 12, EPSC2018-164-1, 2018
European Planetary Science Congress 2018

Spectral clustering on Hermean hollows located on pyroclastic deposits

Maurizio Pajola (1), Alice Lucchetti (1), Giuseppe A. Marzo (2), Gabriele Cremonese (1), Matteo Massironi (3)
(1) INAF, Osservatorio Astronomico di Padova, Vicolo dell'Osservatorio 5, 35122, Padova, Italy (maurizio.pajola@inaf.it), (2) ENEA C. R. Casaccia, 00123, Roma, Italy, (3) Dipartimento di Geoscienze, Università di Padova, via G. Gradenigo 6, 35131 Padova, Italy.

Abstract

By means of the Mercury Dual Imaging System (MDIS [1]) onboard the NASA MESSENGER mission (Mercury Surface, Space Environment, GEochemistry, and Ranging [2]) the Hermean surface has been imaged both in colours and with unprecedented spatial scales. Indeed, the MDIS instrument was equipped with a multiband Wide Angle Camera (WAC) that could observe the Mercury surface up to 11 filters (in the 0.43 – 1.01 μm range) and with a monochromatic Narrow Angle Camera (NAC) that returned images of multiple Mercury's areas with resolutions of 10s to 100s meters.

We here decided to make use of the wealth of multiband WAC imagery to study the hollows located in proximity to two previously identified pyroclastic deposits [3] inside the Tyagaraja crater (a 97 km wide crater, centered at 3.89°N, 148.9° W in the Tolstoj quadrangle) and the Lermontov crater (a 166 km wide crater, centered at 15.24°N, 48.94° W in the Kuiper quadrangle). Hollows are shallow, irregular and rimless flat-floored depressions characterised by bright interiors and halos with bluish colours, often found on crater walls, rims, floors and central peaks [3-5]. The main aim of this work is to assess similarities and differences between the Visible spectra of the hollows located in Tyagaraja and Lermontov craters and to compare them with the spectral properties of the neighbouring pyroclastic deposits.

The resolution for each datacube used, as well as the multiband filters used for each observations are presented in Table 1. All images have been photometrically corrected with Hapke methods following [6], using the parameters derived in [7], i.e. incidence angle of 30°, emission angle of 0° and phase angle of 30°. On the photometrically corrected full datasets we applied a statistical clustering based on a K-means partitioning algorithm developed and evaluated by [8]. This makes use of the Calinski and Harabasz criterion [9] in order to find the intrinsically natural number of clusters, hence making the process unsupervised. Such technique has been extensively validated using different spectral data sets on different areas of Mars [8,10,11], Iapetus [12,13], Phobos [14], and Charon [15] as well as on other Herman hollows [16,17]. On both datasets, each of the identified clusters is characterised by an average multi-colour spectrum, and its associated variability. In addition, the relative geographical information of each spectrum is maintained in the process, hence the resulting clusters can be geolocated on the studied surface and correlations with geographical features can be investigated.

For the specific case of the Tyagaraja crater (Fig. 1A), a natural number of 10 clusters was identified (Fig. 1B); instead, 11 clusters were identified on Lermontov crater. As it is possible to see from Fig. 1B-C, the clustering technique separates the different spectral trends between the pyroclastic material,

	Tyagaraja	Lermontov
Resolution (m)	383	266
Filters used (μm)	0.4332	0.4332
	-	0.4799
	0.5589	0.5589
	0.6288	0.6288
	-	0.6988
	0.7487	0.7487
	0.8284	0.8284
	-	0.8988
	0.9470	0.9470
	0.9962	0.9962
	1.0126	1.0126

Table 1. The resolutions and filters used for the two MDIS cubes used in this work.

located both inside and outside the crater and the hollow deposits. Clusters 8 and 9, i.e. those associated with the hollow fields, show distinct shallower/bluer spectra with respect to those associated with the pyroclastic deposits (clusters 3-5) and the surrounding dark terrains (clusters 0-2). The clusters unrelated to hollows are all characterised by distinct steeper/redder spectral slopes, typical of the pyroclastic deposits observed on Mercury [4]. Instead, clusters 6 and 7 of Fig. 1B are transitional deposits where hollows' halos intermix with the pyroclastic deposits.

We point out that hollows' spectra present a distinctive, wide absorption band (0.558-0.828 μm) that was already observed on other different hollows (all unrelated to pyroclastic deposits) located inside the Dominici, Velazquez and an Unnamed crater [16,17]. This suggests that despite being located on different hosting terrains, hollows present a similar composition.

Eventually, the same spectral trends characterising the Tyagaraja crater are observed both on the pyroclastic deposits and the hollowed terrains of the Lermontov crater as well, with the main difference that the Lermontov pyroclastic deposits show steeper spectral slopes than the Tyagaraja's ones.

Acknowledgements

This activity has been realized under the BepiColombo ASI-INAF agreement no. 2017-47-H.

References

[1] Hawkins, S. E. et al. (2007), *Space Sci. Rev.*, 131, 247- 338 [2] Solomon, S. C. et al. (2001), *Planet. Space Sci.*, 49, 1445-1465. [3] Blewett D. T. et al. (2013) *JGR Planets*, 118, 1013-1032. [4] Blewett D. T, et al. (2011) *Science*, 333, 1856– 1859. [5] Thomas R. J. et al. (2014), *Icarus*, 229, 221–235. [6] Hapke, B. (2002), *Icarus*, 157, 523-534. [7] Domingue, D. et al. (2015), *Icarus*, 257, 477-488. [8] Marzo, G. et al. (2006) *JGR*, 111, E03002. [9] Calinski, T., Harabasz, J., (1974), *Commun. Statist.* 3, 1–27. [10] Marzo, G. et al. (2008), *JGR*, 113, E12009. [11] Marzo, G. et al. (2009), *JGR*, 114, E08001. [12] Pinilla-Alonso, N. et al. (2011), *Icarus*, 215, 1, 75. [13] Dalle Ore, C. et al. (2012), *Icarus*, 221, 2, 735. [14] Pajola, M. et al., 2018. *Planet. Space Sci.* 154, 63-71. [15] Dalle Ore, C., et al., 2018. *Icarus* 300, 21–32. [16] Lucchetti, A. et al. (2017), *48th LPSC*, 1964. [17] Lucchetti, A. et al. (2017), *EPSC 2017*,188.

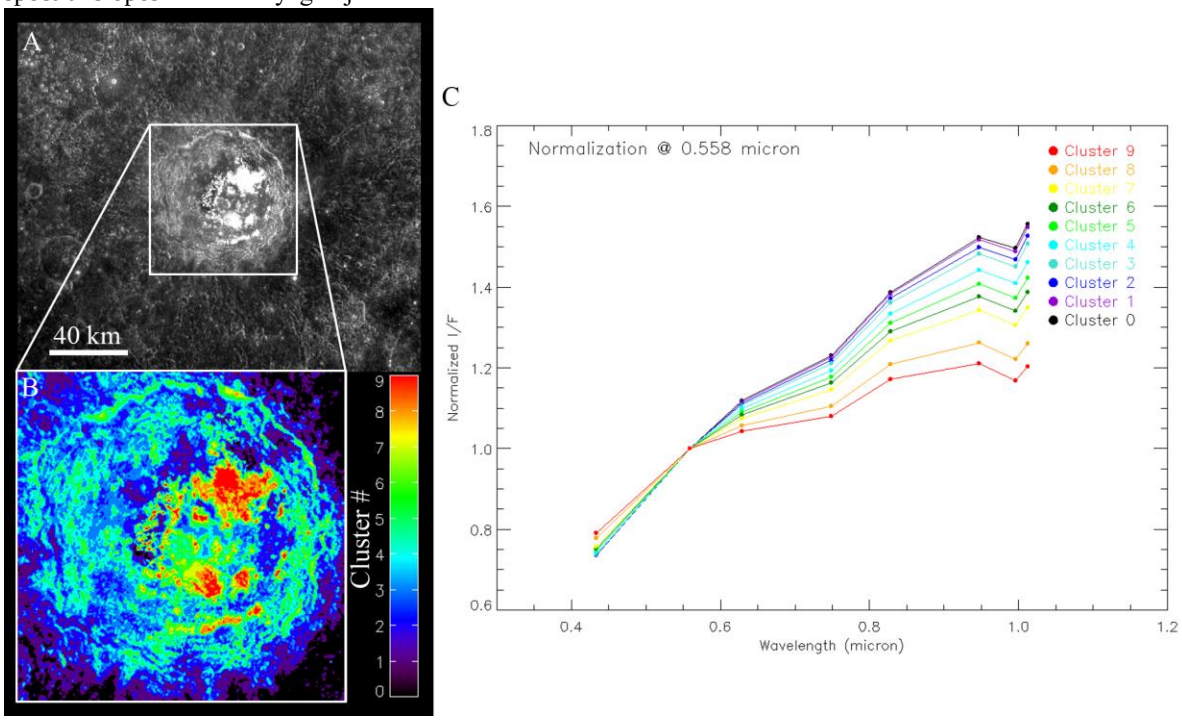

Fig. 1: A) The MDIS WAC image (EW1009232936D) of the Tyagaraja crater. B) The 10 clusters identified on the dataset. C) The average I/F normalised spectra (at 0.558 μm) of the clusters identified in B. Colours refer to B.

EPSC Abstracts
Vol. 12, EPSC2018-219, 2018
European Planetary Science Congress 2018

Preparing for the epic adventures of BepiColombo

Emily Baldwin, Claudia Mignone and Markus Bauer. European Space Agency (ESA/ESTEC), Keplerlaan 1, Postbus 299, 2200 AG Noordwijk, The Netherlands. (emily.baldwin@esa.int)

Abstract

The joint European Space Agency (ESA) and Japan Aerospace Exploration Agency (JAXA)'s BepiColombo mission to Mercury is almost ready for launch, and the outreach and communications efforts to raise awareness about the project are gearing up. The social media landscape is very different now to what it was at the time of Rosetta's launch in 2004 for example, when popular social media channels such as Facebook and Twitter were only just conceived; today we have the opportunity to engage with different audiences on a vast range of platforms from the early stages of a mission. We draw on the experiences of our Rosetta communications campaign between 2013 and 2016 [1] to help shape our outreach activities for BepiColombo. This includes the introduction of a new cartoon series and first person Twitter accounts for the three spacecraft that comprise the mission, alongside traditional media relations and event organisation.

1. Mission profile

The BepiColombo mission is Europe's first mission to Mercury, the smallest and least explored terrestrial planet in our Solar System. It consists of two scientific orbiters: ESA's Mercury Planetary Orbiter (MPO) and JAXA's Mercury Magnetospheric Orbiter (MMO), and ESA's Mercury Transfer Module (MTM). The three spacecraft will launch together on an Ariane 5 from Europe's Spaceport in Kourou in late 2018 and voyage to Mercury as a single composite spacecraft, with the MTM providing power and propulsion. It will use the gravity of Earth, Venus and Mercury in a total of nine flybys, in combination with the thrust provided by electric propulsion, to reach Mercury orbit at the end of 2025. When approaching Mercury, the MTM will separate and the two science orbiters, still together, will be captured into a polar orbit around the planet, before separating and entering into their own respective orbits.

BepiColombo is set to build on the achievements of NASA's Messenger mission (completed in 2015), in order to provide the best understanding of the Solar System's innermost planet to date. The technology preparations needed to fly to and operate at Mercury, the science that will be performed once at the planet, and the journey itself provide talking points and opportunities for public engagements along the way.

1.1 Preparing our audience for launch

We have followed the construction and testing of the mission through our traditional channels [2], and hosted a media event in July 2017 at ESA's technical centre in the Netherlands to present the completed spacecraft stack (figure 1), allowing journalists to 'meet' the spacecraft – the last time this would be possible in Europe. In March/April 2018 we started ramping up our communications activities in preparation for the shipment of the spacecraft modules to Kourou in late April/early May, marking the start of six months of launch preparations. This included the release of traditional artist impressions of the spacecraft and video footage of the packing activities, and the launch of the cartoon [3] and three new Twitter accounts: @ESA_Bepi, @ESA_MTM and @JAXA_MMO (the latter is managed by JAXA). We have also produced a simple 'print-and-play' memory game to familiarise our younger audience with the mission and its long journey. After a successful launch we intend to release an interactive tool where users can find out where the spacecraft is on its way to Mercury.

Figure 1: Completed spacecraft stack, July 2017. Top: MMO, Middle: MPO, Bottom: MTM.

2. New friends, new adventures

Following the success of the "Once upon a time" cartoon series that told the story of Rosetta and Philae's escapades at Comet 67P/Churyumov Gerasimenko [4], we have embarked on "The Epic Adventures of BepiColombo". This is again a close partnership between ESA on the script-writing side and Design & Data [5] on the visualisation and production side. As with Rosetta and Philae, the BepiColombo characters provide an obvious opportunity for a dialogue – this time with two science orbiters and one transport 'robot', giving a different dimension to the story telling.

2.1 Twitter personalities

The first person Twitter account of @ESA_Rosetta captured a wide audience with its endearing conversations with @Philae2014 [6]. Therefore, we have chosen to personify the three BepiColombo characters on Twitter, which again take the visual identity of the cartoon characters. The personified accounts complement the more traditional voice of the existing @bepicolombo account. The @ESA_Bepi account is a key storyteller in the English language, complemented by the Japanese/English-speaking @JAXA_MMO account. The ESA-JAXA partnership offers a unique opportunity for cultural exchange, which will be portrayed through the two characters as their journey progresses. Meanwhile the MTM character, pitched rather as a robot, only speaks Emoji – picture icons with drive from Japanese – the first time a space agency account is presented in this way and although somewhat lighthearted, is very much in keeping with the global emoji phenomenon. [7].

The accounts follow the real-time mission activities as closely as possible, which in recent months has covered the preparation activities in the Spaceport, building excitement and momentum as they prepare for their journey to Mercury. They utilise materials posted on ESA's traditional channels to populate their timelines, and it is the aim to post complementary multi-media material on each account to give variety and maintain interest.

3. Existing audiences

We will prioritise our communications on the main ESA web portal, esa.int/bepicolombo, and through the social media channels, rather than host a dedicated blog, for example. Similarly, for Facebook, Instagram, and YouTube, ESA's other primary social media accounts alongside Twitter, we use the existing audiences of these accounts to highlight key announcements and messages. The mission will also be covered by ESA TV and ESA Web TV at key moments, and media events will be organised around certain milestones, such as launch.

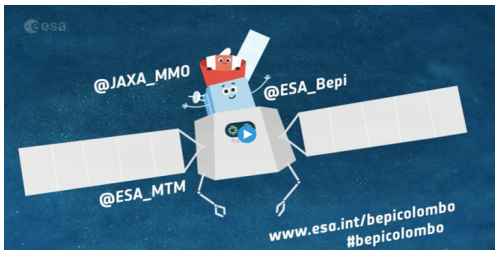

Figure 2: BepiColombo cartoon characters

4. Summary and future outlook

The Rosetta mission allowed us to explore various new methods of communications for the first time – such as the use of a cartoon to communicate important milestones and scientific results, and the complementary first-person Twitter accounts. This shaped our decision to pursue these activities again for telling the story of our BepiColombo mission in the current communications landscape. The seven year journey to Mercury, augmented by nine flybys, gives plenty of talking points and opportunities for engagement activities in the future. We will present a more detailed overview of our activities in the planning around launch, as well as our ideas for the future.

References

[1] Bauer. M et al. The Strategy and Implementation of the Rosetta Communication Campaign, CAPj, 19, 2016
[2] http://sci.esa.int/bepicolombo/
[3] All via www.esa.int/bepicolombo
[4] Mignone, C. How a Cartoon Series Helped the Public Care about Rosetta and Philae CAPj, 19, 2016
[5] https://designdata.de
[6] Baldwin. E "Hello, World!" Harnessing Social Media for the Rosetta Mission, CAPj, 19, 2016
[7] Evans. V, The Emoji Code, 2017

EPSC Abstracts
Vol. 12, EPSC2018-312-1, 2018
European Planetary Science Congress 2018

Deciphering the conditions of formation of Mercury

Thomas Ronnet, Pierre Vernazza, Olivier Mousis and Bastien Brugger
Laboratoire d'Astrophysique de Marseille, Aix Marseille Univ, CNRS, CNES, LAM, Marseille, France
(thomas.ronnet@lam.fr)

Abstract

The Earth, Venus and Mars all have approximately chondritic ratios of the major rock-forming elements (Si, Mg, Fe, S, Ca, Al, and Ni) and are characterized by metallic cores (mostly made of iron) comprising ∼30% of their total mass surrounded by a silicate mantle accounting for the remaining ∼70% of their mass. In stark contrast, Mercury's high density suggests that the planet has a large metallic core accounting for 70% of its total mass and hence a much less massive silicate mantle as compared to other terrestrial planets. The origin of the high metal/silicate ratio of Mercury is a longstanding puzzle and the data recently collected by the MESSENGER mission revealed that the planet's surface and mantle is also more reduced than almost any known Solar System material [2].

It is unlikely that the composition of Mercury is a direct result of condensation processes due to the narrow temperature range within which gas should be removed to match the metal/silicate ratio of the planet. Moreover, MESSENGER's data indicate that Mercury is not depleted in moderately volatile elements such as S, Na, Cl or K relative to Mg, which is in contradiction with a scenario where condensation temperature controlled the planet's composition [1]. Scenarios based on removal of Mercury's mantle after its completion (following an impact or due to evaporation from a young hot Sun) are difficult to achieve because debris or vaporized silicates tend to re-accrete or recondense onto the planet, yielding only moderate metal/silicate fractionation [3, 1].

Here we investigate the conditions of formation of Mercury's precursor material and the processes that could have led to the planet's peculiar properties. We consider the early evolution of the protosolar nebula and the conditions for the formation of planetesimals in the inner Solar System. We show that the innermost planetesimals (at distances $\lesssim$0.5 au from the Sun) could have formed from material that was sublimated and subsequently condensed, implying very reduced compositions consistent with that of Mercury (Mercury's inferred oxygen fugacity is close to that of a solar composition vapor). Planetesimal formation further out from the Sun would however be the result of the pile-up of material coming from the outer regions of the disk and would therefore involve material with much more oxidized compositions. The subsequent thermal/collisional evolution of the planetesimals is considered where we argue that metal/silicate fractionation is rendered easier in the early phases of terrestrial planets formation (rather than in the late giant impact phase) due to the smaller masses of the objects involved.

References

[1] Ebel, D. S. and Stewart, S. T.: To appear in *Mercury: The view after MESSENGER*, S. C. Solomon, B. J. Anderson, L. R. Nittler (editors), Cambridge University Press.

[2] Nittler, L. R., Chabot, N. L., Grove, T. L., and Peplowski, P. N.: To appear in *Mercury: The view after MESSENGER*, S. C. Solomon, B. J. Anderson, L. R. Nittler (editors), Cambridge University Press.

[3] Stewart, S. T., Lock, S. J., Petaev, M. I., et al. 2016, Lunar and Planetary Science Conference, 47, 2954

EPSC Abstracts
Vol. 12, EPSC2018-344, 2018
European Planetary Science Congress 2018

Discovering Rembrandt basin's subsurface and Enterprise Rupes: 3D-model based on stratigraphic mapping and structural analysis

Andrea Semenzato (1), Matteo Massironi (1), Riccardo Pozzobon (1), Valentina Galluzzi (2), David A. Rothery (3), Sabrina Ferrari (4)
(1) Dipartimento di Geoscienze, Università di Padova, Italy, (2) INAF, Istituto Nazionale di Astrofisica e Planetologia Spaziali, Rome, Italy, (3) Department of Physical Science, The Open University, Milton Keynes, UK, (4) CISAS, Università di Padova, Italy. (andrea.semenzato.3@studenti.unipd.it)

Abstract

This work is part of the Horizon 2020 - PLANMAP project and in support of the Bepi-Colombo mission. It aims at realizing a geologic map of the Rembrandt basin and the surrounding area focusing on the stratigraphy of its interior plains, to finally reconstruct a subsurface 3D geological model of the basin itself and of the Enterprise Rupes cross-cutting it. This will allow to better infer the infilling history of the basin and the kinematic evolution of the scarp.

1. Introduction

The ~715-km-diameter Rembrandt basin is known as the second largest well-preserved basin on Mercury after the almost coeval Caloris basin (~1500 km). Rembrandt is peculiarly cross-cut by an extensive and possibly multi-phase lobate scarp, i.e. Enterprise Rupes, whose activity is thought to be initiated prior to the impact event and subsequently reactivated during the emplacement of the inner volcanic smooth plains [2]. The improvements of imagery data provided by NASA MESSENGER spacecraft offer the possibility to unravel this complex turn of events and observe a variety of spectrally distinct units within and outside the basin. Hence, in this work we propose a more comprehensive stratigraphic and geologic interpretation of these events.

2. Data and Methods

We have produced a map layer focused on geomorphology and morpho-stratigraphy (Figure 1) following the methods and symbology adopted by many authors while mapping the quadrangles of Mercury [4, 5, 6]; the second layer is based on the main chrono-stratigraphic units, which can be related to different events and therefore different ages (Figure 1B), distinguished by their model ages and spectral characteristics (i.e. different false colours based on MESSENGER MDIS 3-colour, 8-colour and PCA – enhanced colour images, which are consistent with a different composition of the material on the surface). Within the latter we took into consideration the colour units on the base of their stratigraphic position inferred by the crater excavations. For this reason, crater floors and ejecta are classified in function of the color-stratigraphic unit they are constituted of. In particular, the smooth plains were distinguished into two different units inside it, based on spectral distinctions as well as the thickness and age constraints described below.
We have estimated the thickness of the smooth plains units inside the basin with three methods. The first one used by [1] allows to link the depth of origin of spectrally distinct ejecta and central peak structures associated with impact craters. The second method applied on Mercury by [2] provides an estimation of the depth of boundary between two distinct volcanic plains inside the basin by performing a crater-age determination. The crater counting includes partially buried craters, and relates the deflection of an S-shaped kink that occurs at larger diameters with the minimum and maximum thickness of the younger unit. The third method allows to estimate the thickness of the upper smooth plains by comparing the measured rim heights of embayed craters with the rim heights expected by morphologic relationships for mercurian craters (following [7]).
These layers have provided the basis for subsurface 3D geological modelling, and additional map layers have been produced for surface features (such as secondary crater chains and bright rayed ejecta) and linear features (such as faults and crests of crater rims). In addition, new measurements of fault geometry and kinematic properties of Enterprise Rupes have been obtained by using the method of [3], analyzing three main craters cross-cut and deformed

by the lobate scarp. To this aim we used MESSENGER MDIS Global Basemap BDR and Global DEM data.
Finally, the 3D model has been developed using the Midland Valley's MOVE software.

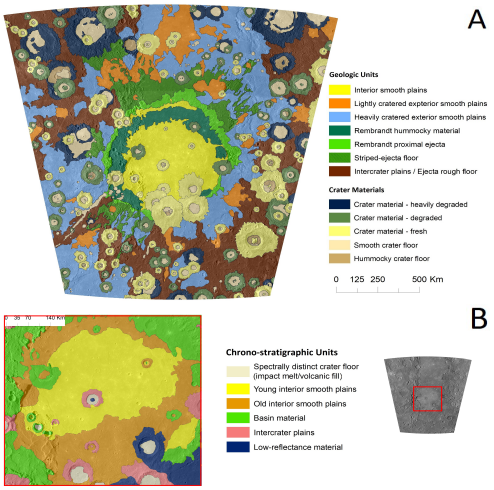

Figure 1: Preview of the map layers. A) Geomorphologic mapping. B) Close view within the Rembrandt basin showing the chrono-stratigraphic mapping, which displays the main stratigraphic units. (Lambert conformal conic projection)

3. Results and future work

After combining the map layers with the methods described above, we distinguished two different volcanic plains inside the Rembrandt basin and estimated the thickness of these two units: we obtained a maximum thickness for the younger smooth plains of 0.34-0.44 km (thickening towards the centre of the basin), which is consistent with the values observed from the S-shaped kink by [2], and a maximum depth for the older smooth plains of 1.73-2 km. Furthermore, we have modelled the fault plane of Enterprise Rupes (Figure 2) based on the measured fault parameters and interpolating multiple sections cross-cutting the basin and the lobate scarp. We measured low angles for the portion of the frontal thrust inside the basin (plunge 14-23°) and high angles for the lateral ramp outside the basin (up to 40°).
As a follow up of our work, we aim at modelling also the smooth plains inside the basin by using similar techniques, to provide not only a better understanding of the Rembrandt basin's evolution and stratigraphy, in connection with Enterprise Rupes.

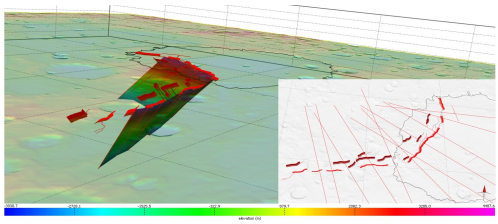

Figure 2. Preliminary 3D model of Enterprise Rupes, obtained with the MOVE software. Red ribbons represent the main fault segments of Enterprise Rupes, mapped on the surface and inclined by the measured angles, whereas brown ribbons are the main backthrusts (or "backscarp"). The vertical scale is exaggerated x2.5. Bottom right: cross sections drawn for modelling the scarp.

Acknowledgments

This research was supported by European Union's Horizon 2020 under grant agreement No 776276-PLANMAP.

References

[1] Ernst C.M. et al. (2010): Exposure of spectrally distinct material by impact craters on Mercury: Implications for global stratigraphy, Icarus, 209, 210-223, 2010.

[2] Ferrari S. et al. (2015): Age relationships of the Rembrandt basin and Enterprise Rupes, Mercury, Geological Society, London, 401, 159-172, 2014.

[3] Galluzzi V. et al. (2015): Faulted craters as indicators for thrust motions on Mercury, Geological Society, London, 401, 313-325, 2014.

[4] Galluzzi V. et al. (2016): Geology of the Victoria quadrangle (H02), Mercury, J. of Maps, 12, 227-238, 2016.

[5] Guzzetta L. et al. (2017): Geology of the Shakespeare quadrangle (H03), Mercury, J. of Maps, 12, 227-238, 2016.

[6] Mancinelli P. et al. (2016): Geology of the Raditladi quadrangle (H04), Mercury, J. of Maps, 12, 190-202, 2016.

[7] Whitten J.L. and Head J.W. (2015): Rembrandt impact basin: Distinguishing between volcanic and impact-produced plains on Mercury, Icarus, 258, 350-365, 2015.

EPSC Abstracts
Vol. 12, EPSC2018-386, 2018
European Planetary Science Congress 2018

Scientific Performance of the BepiColombo Laser Altimeter (BELA) at Mercury

Hauke Hussmann (1), Gregor Steinbrügge (1), Alexander Stark (1), Jürgen Oberst (1), Nicolas Thomas (2) and Luisa Lara (3)
(1) DLR Institute of Planetary Research, Rutherfordstr. 2, 12489 Berlin, Germany (hauke.hussmann@dlr.de), (2) Physikalisches Institut, University of Bern (UBE), Sidlerstrasse 5, 3012 Bern Switzerland, (3) CSIC, Instituto de Astrofísica de Andalucía (IAA), Glorieta de la Astronomia s/n, 18008 Granada, Spain

Abstract

The BepiColombo Laser Altimeter (BELA) is one of 11 instrument onboard the Mercury Planetary Orbiter (MPO) which is part of the BepiColombo mission scheduled for launch in October 2018. Here the prospects for the BELA experiment, in particular with respect to Mercury's topography, interior structure and evolution will be discussed.

1. BELA: Scientific Performance

Mercury is an intriguing planetary object with respect to its dynamical state and evolution. The planet is differentiated and contains a large iron core overlain by a relatively thin silicate mantle and crust. Mercury is locked in a unique 3:2 spin-orbit coupling and its intrinsic magnetic dipole field tells us that at least part of Mercury's iron core is liquid. From libration measurements it has been concluded that Mercury's outer core is liquid, decoupling the silicate mantle from the deep interior. Phases of global contraction and phases of volcanic activity occurred in the thermal history of the planet.

The BepiColombo joint mission by the European Space Agency (ESA) and the Japan Aerospace Exploration Agency (JAXA) consists of two spacecraft, the Mercury Planetary Orbiter (MPO) and the Mercury Magnetospheric Orbiter (MMO). The spacecraft stack will be launched in October 2018 and conduct a one year nominal mission in Mercury orbit, with the possibility of an extension by one additional year [1]. Here the prospects for investigations with the BepiColombo Laser Altimeter (BELA) [2] will be discussed. We present an updated semi-analytical instrument performance model estimating the signal to noise ratio, single shot probability of false detection, range error and pulse-width reconstruction accuracy. The model is generally applicable to laser altimeters using matched filter algorithms for pulse detection and has been validated against the recently tested BELA flight model after integration on the MPO spacecraft. Further, we present numerical simulations of the instrument performance expected in orbit about Mercury. In particular, we study the measurement accuracy of topography, slopes and surface roughness, which will allow us to estimate local and global topographic coverage based on the current trajectory design. We also assess the potential for measuring the tidal Love number h_2 using cross-over points, which we estimate to be constrained with an absolute accuracy of 0.14 corresponding to a relative accuracy of about 18% after two years in Mercury orbit.

References

[1] Benkhoff et al (2010) Planetary and Space Science 58, 1-20.

[2] Thomas et al. (2007) Planet. Space Sci., 55, 1398-1413.

EPSC Abstracts
Vol. 12, EPSC2018-404, 2018
European Planetary Science Congress 2018

Characterizing the deviations of Mercury's bulk composition from solar abundances

B. Brugger, O. Mousis, M. Deleuil, and T. Ronnet
Aix Marseille Univ, CNRS, LAM, Laboratoire d'Astrophysique de Marseille, Marseille, France (bastien.brugger@lam.fr)

Abstract

Mercury is characterized as an iron-rich planet, who experienced particular chemical conditions during its formation. From the latest MESSENGER data and laboratory experiments, we investigate the interior of this planet with a precise description of both core and mantle materials. We show that the measured moments of inertia of the planet favor a dense mantle, possibly containing a non-negligible fraction of iron, and a core containing silicon rather than sulfur. We finally derive the bulk composition of the planet fitting both the moments of inertia and the solar S abundance.

1. Introduction

Compared to the other terrestrial planets of the solar system, Mercury presents several unique characteristics. It is both the smallest and densest (uncompressed) planet, indicative of a composition significantly rich in iron. Formation scenarios specific to Mercury thus invoked different methods of fractionation between iron and silicates. Recent studies revealed another unique feature of this planet, namely that it formed in chemically reducing conditions [1]. This has strong implications on the materials forming Mercury, favoring the formation of metallic iron and silicon, and of sulfides in the mantle. The mantle of Mercury is thus believed to be strongly depleted in silicate iron, enriched in sulfur, and the core believed to harbor both silicon and sulfur as alloying elements. Several of these characteristics were strengthened by results of the MESSENGER mission, who analyzed the surface composition of the planet, but also derived constraints on its structural parameters.

2. Modeling the interior

We use a model designed for exploring the interior of terrestrial planets [2], that we adapt to the case of Mercury. The modeled body is differentiated into a metallic core surrounded by a silicate mantle, whose respective sizes are governed by the core mass fraction (CMF). The model varies the CMF to converge towards the planetary mass and radius of Mercury. Modeling the metallic core is done with an equation of state of the complete Fe-S-Si system, as both silicon and sulfur are potential alloying elements present in the core of Mercury. Coupling our model to the PerpleX code [3] allows us to use a complete description of the mineralogy of the silicate mantle. We can thus study the impact of both core and mantle compositions on the internal structure of Mercury, and derive the bulk elemental composition of the planet.

We employ a Monte-Carlo approach to constrain Mercury's bulk parameters, by launching a large number of simulations with different bulk compositions. The ternary diagram of the Fe-S-Si system is uniformly explored, whereas we select a set of five compositions for the mantle, chosen to span large ranges of density and composition (estimates of the Earth mantle, Mercury mantle, and meteorites). The results obtained for all explored compositions are then refined by selecting only simulations that reproduce Mercury's moments of inertia, as deduced from MESSENGER data [4].

3. Reproducing Mercury

Our results confirm previous estimates of Mercury's structural parameters, with a CMF within the 72–76% range, corresponding to a mantle thickness of 430±40 km. The constraints placed by the moments of inertia tend to favor a dense mantle, as our best fit is obtained with an Earth mantle, the only investigated composition with a significant fraction of silicate iron (7.5wt%). This density could however also be revealing of a lower mantle temperature compared to previous estimates. Although a large fraction of light elements can theoretically be incorporated in the core, the moments of inertia are only reproduced with 1–9wt% of Si or 2–16wt% of S.

The relative abundances of Fe, Mg, and Si in Mercury can give important hints for the formation of

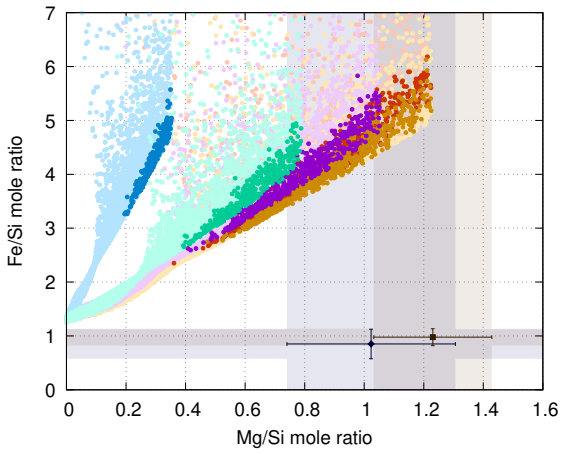

Figure 1: Map of the Fe/Si ratio as a function of the Mg/Si ratio, for all simulations (light) and those compatible with the moments of inertia (dark). Colors denote the different mantle compositions (see text). Two solar estimates are shown for reference.

the planet, as these refractory elements have similar condensation temperatures in protosolar nebula conditions. We thus aim at quantifying the deviations of Mercury's ratios from the solar values. Figure 1 shows the areas of the Mg/Si-Fe/Si map that are covered by our simulations. A pure Fe core thus yields a solar Mg/Si ratio but an Fe/Si ratio enriched $\sim$5 times the solar value. Incorporating S in the core does not change the planetary Mg/Si ratio, but Fe/Si increases towards higher values. On the opposite, Fe/Si is brought closer to solar values when the core contains Si, but this also reduces the Mg/Si ratio to sub-solar values. On the planetary scale, Mercury was suggested to be strongly enriched in S, but we show that solar abundances can be reached, especially since Si can replace S in the core. Moreover, the moments of inertia are best reproduced with an Fe-Si core than with Fe-S. We thus derive the bulk composition of Mercury which fits the solar S abundance, that we obtain for a core containing 4.4wt% of Si and 1.8wt% of S (see Figure 2).

4. Discussion

The presence of a significant amount of Si in Mercury's core, at the expense of S which was the first candidate for an alloying element, are in agreement with the latest studies on Mercury's composition from laboratory experiments. The mantle of this planet is thus likely to be rich in S, in contrast to the core, allowing to

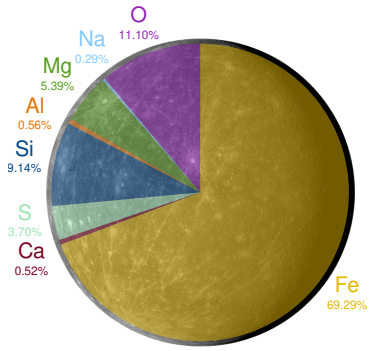

Figure 2: Bulk composition obtained for a Mercury mantle with addition of 9wt% S, and an Fe-$_{1.8\%}$S-$_{4.4\%}$Si core (values are in wt%). *Picture credits: NASA*

reach a bulk abundance of S similar to the solar value. This favors a formation scenario invoking a depletion of mantle material, increasing the planetary Fe/Si ratio, and decreasing both Mg/Si and S/Si ratios. Such characteristics could thus be revealing of a particular formation mechanism which could be extended to the study of exoplanets sharing one of Mercury's feature, namely a high mean density. A finer knowledge of Mercury's interior is thus essential to allow for a better characterization of these "super-Mercuries".

Acknowledgements

The project leading to this publication has received funding from Excellence Initiative of Aix-Marseille University - A*MIDEX, a French "Investissements d'Avenir" program. O.M. and M.D. acknowledge support from CNES.

References

[1] Nittler, L. R., Starr, R. D., Weider, S. Z., et al. 2011, Science, 333, 1847

[2] Brugger, B., Mousis, O., Deleuil, M., & Deschamps, F. 2017, ApJ, 850, 93

[3] Connolly, J. A. D. 2009, Geochemistry, Geophysics, Geosystems, 10, Q10014

[4] Margot, J.-L., Peale, S. J., Solomon, S. C., et al. 2012, Journal of Geophysical Research (Planets), 117, E00L09

EPSC Abstracts
Vol. 12, EPSC2018-420, 2018
European Planetary Science Congress 2018

BepiColombo – The next step of Mercury Exploration with two orbiting spacecraft

Johannes Benkhoff (1), **Joe Zender** (1), Go Murakami (2)

(1) ESA/ESTEC, Noordwjk, The Netherlands (Joe.Zender, Johannes.Benkhoff@esa.int) (2) Institute of Space and Astronautical Science , Japan Aerospace Exploration Agency, 3-1-1 Yoshinodai, Chuo, Sagamihara, Kanagawa 252-5210, Japan (go@stp.isas.jaxa.jp)

Abstract

The BepiColombo mission is ready for launch from the European spaceport in French Guyana. A mission overview is provided with the latest information from the launch site, followed by an overview of the science objectives of the mission,

1. Introduction

Mercury is in many ways a very different planet from what we were expecting. In October 2018 BepiColombo [1] will be launched to follow up on answering the fundamental questions about the evolution history of the planet nearest to the sun.

BepiColombo is a joint project between the Euro- pean Space Agency (ESA) and the Japanese Aero- space Exploration Agency (JAXA). The Mission con- sists of two orbiters, the Mercury Planetary Orbiter (MPO) and the Mercury Magnetospheric Orbiter (MMO). From their dedicated orbits the two space- craft will be studying the planet and its environment.

The mission has been named in honor of Giuseppe (Bepi) Colombo (1920–1984), who was a brilliant Italian mathematician, who made many significant contributions to planetary research and celestial mechanics.

2. Science goals

BepiColombo will study and understand the composition, geophysics, atmosphere, magnetosphere and history of Mercury, the least explored planet in the inner Solar System. In particular, the mission objectives are:

• to understand why Mercury's uncompressed density is markedly higher than that of all other terrestrial planets, Moon included

• to understand and determine the nature of the core of Mercury

• to understand why such a small planet pro- cesses an intrinsic magnetic field and investigate Mercury's magnetized environment

• to investigate if the permanently shadowed craters of the Polar Regions contain Sulphur or water ice

• to study the production mechanisms of the exosphere and to understand the interaction between planetary magnetic field and the solar wind in the absence of an ionosphere

• to obtain new clues about the composition of the primordial solar nebula and about the formation of the solar system

• to test general relativity with improved accu- racy, taking advantage of the proximity of the Sun. Since and considering that the advance Mercury's perihelion was explained in terms of relativistic space-time curvature.

3. Science Payload

The MPO scientific payload comprises eleven instruments/instrument packages and the MMO comprises 5 instruments/instrument packages to study the planet itself and its environment,

respectively. The MPO will focus on a global characterization of Mercury through the investigation of its interior, surface, exosphere and magnetosphere. In addition, it will be testing Einstein's theory of general relativity. The MMO will focus on the plasma and particle environment and the magnetosphere.

4. Expected results

Together, the scientific payload of both spacecraft will provide the detailed information necessary to understand Mercury and its Magnetospheric environment and to find clues to the origin and evolution of a planet close to its parent star. The BepiColombo mission will complement and follow up the work of NASA's MESSENGER [2] mission by providing a highly accurate and comprehensive set of observations of Mercury. In addition, the BepiColombo mission will provide a rare opportunity to collect multi-point measurements in a planetary environment. This will be particularly important at Mercury because of short temporal and spatial scales in the Mercury's environment. The foreseen orbits of the MPO and MMO will allow close encounters of the two spacecraft throughout the mission.

References: [1] Benkhoff, J., et al. (2010) *Planet. Space Sci.* 58, 2-20. [2] McNutt R.L., S.C. Solomon, R.E. Gold, J.C. Leary and the MESSENGER Team (2006) *Adv. in Space Res. 38*, 564-571

EPSC Abstracts
Vol. 12, EPSC2018-451, 2018
European Planetary Science Congress 2018

Mercury Science Objectives and Traceability within the BepiColombo project: Optimizing the Science Output of the next mission to Mercury

Sebastien Besse[1], Johannes Benkhoff[2], Mark Bentley[1], Thomas Cornet[1], Richard Moissl[1], Claudio Munoz[1], Joe Zender[2]
(1) ESA/ESAC, BepiColombo Science Ground Segment, Madrid Spain, (2) ESA/ESTEC, BepiColombo Science Ground Segment, Noordwijk, The Netherlands (sbesse@sciops.esa.int)

Abstract

BepiColombo is Europe's first mission to Mercury. It will set off in 2018 on a journey to the smallest and least explored terrestrial planet in our Solar System. When it arrives at Mercury in late 2025, it will gather data during its 1 year nominal mission, with a possible 1-year extension. The mission comprises two spacecraft: the Mercury Planetary Orbiter (MPO) and the Mercury Magnetospheric Orbiter (MMO). BepiColombo is a joint mission between ESA and the Japan Aerospace Exploration Agency (JAXA), executed under ESA leadership..

1. Science at Mercury

The scientific interest in going to Mercury lies in the valuable information that such a mission can provide to enhance our understanding of the planet itself as well as the formation of our Solar System; information which cannot be obtained with observations made from Earth. The science mission will consist of two separate spacecraft that will orbit the planet. ESA is building one of the main spacecraft, the Mercury Planetary Orbiter (MPO), and the Institute of Space and Astronautical Science (ISAS) at the Japan Aerospace Exploration Agency (JAXA) will contribute the other, the Mercury Magnetospheric Orbiter (MMO).

The BepiColombo mission relies on the valuable observations and science discoveries obtained by the MESSENGER and Mariner 10 missions in the past years and decades. Those discoveries shape the description of science objectives to be performed by the 11 instruments onboard the MPO spacecraft, and the 5 instruments onboard the MMO. In order to optimize the science planning and outcome of the mission, the BepiColombo Science Ground Segment (SGS) is developing strategies, tools, and workflows that will enable the science teams of the MPO spacecraft to maximize the science to be performed at Mercury.

2. Science Objectives and Traceability

As for every mission, the overall scientific goals are discussed in numerous documents. For Bepicolombo, those objectives are well summarized in [1]. They cover three main areas of scientific investigation of Mecury: Surface, Interior, and Exosphere. The BepiColombo Science Working Team (SWT) is supported by three scientific Working Groups (WG) that represents these science themes, 1) Surface and Composition, 2) Geodesy and Geophysics, and 3) Hermean Environment. Following the mission science objectives, those working groups provide a more detailed Science Traceability Matrix (WG-TMX) that helps to define the observation strategies and priorities.

To close the gap between the WG-TMX and the implementation of observations performed by individual instrument teams, the SGS is developing, in collaboration with the instrument teams, targeted science traceability matrix of each instruments (Inst-TMX). These Inst-TMX (linked to the WG-TMX) represent the essence of the science objectives of Bepicolombo. The SGS is using the TMX concept in a similar way to other projects (e.g., Cassini, JUICE), with an emphasisis on tracking them.

The Inst-TMX are defined in such a way that they can be tracked (using specific IDs) during the observation lifecycle (request, planning, commanding to the spacecraft, and downlink) until product generation. For instance, requirements on the spacecraft and instruments operations are listed (e.g., pointing, duration, etc..). This information is critical to ensure:

- the evaluation of observations success needed to perform science investigations, and
- a progress report on the evolution of the observations, in order to reschedule if needed and optimize the planning

In addition, measurements performed and received data will be analysed, quality checked, and traced back to the TMX.

During the conference, we will present the developement status of the science-observation tracking system for BepiColombo. The SGS welcomes any suggestions, improvements, and new or refined science goals that will help improving the science done at Mercury.

References

[1] Benkhoff et al. (2010) *PSS*.

EPSC Abstracts
Vol. 12, EPSC2018-511, 2018
European Planetary Science Congress 2018

Constraining the Early History of Mercury and its Core Dynamo by Studying the Crustal Magnetic Field

Joana S. Oliveira (1,2) and Lon L. Hood (3)
(1) ESA/ESTEC, SCI-S, Keplerlaan 1, 2200 AG Noordwijk, Netherlands, (2) CITEUC, Geophysical & Astronomical Observatory, University of Coimbra, Coimbra, Portugal, (3) Lunar & Planetary Lab, 1629 E. University Blvd., Univ. of Arizona, Tucson, AZ 85721, USA (joliveira@cosmos.esa.int)

Abstract

We study crustal magnetic field anomalies associated with impact craters on Mercury. The sources of these anomalies likely consist of impact melt, enriched in impactor iron, that was thermoremanently magnetized in the ancient Mercury dynamo field. Results show that paleopoles are not always located near the present-day north magnetic pole, which lies near the south geographic pole. This provides further evidence that anomalies are not induced but are remanent, and represent useful constraints on the early history of Mercury and its dynamo magnetic field.

1. Introduction

Crustal magnetic field maps were obtained using low altitude MESSENGER MAG data, obtained during the last months of the mission [1, 2, 3, 4]. Though some of the anomalies are related to the Hermean topography structures, others are not. The measured crustal field can be explained through or by a combination of various sources such as thermoremanent magnetization, shock remanent magnetization or even induced fields. Distinguishing among those different sources that are contributing to a given anomaly is challenging when lacking in situ measurements. Here, we study the different anomalies that are found on Mercury that are clearly related with craters or basins. Their interior subsurfaces are thought to have cooled very slowly in a presence of a constant global magnetic field, and have been thermoremanently magnetized. The anomaly sources most probably consist of impact melt rocks that were enriched in iron from the impactor [5]. We use a unidirectional magnetization model which assumes that the melt impact rocks recorded the constant core magnetic field present when the crater was formed. The results will help to constrain the early history of Mercury, as they give insights on true polar wander event, and on the early dynamo morphology and dynamics.

2. Method

We invert for crustal magnetization by making use of a method developed by Parker for studying seamount magnetism on Earth [6], and which was recently applied to lunar crustal magnetism by [7, 8]. The only assumption that this method makes is that the magnetization within the crust is unidirectional, which is the case when the material cools below the Curie temperatures in the presence of a steady main field. As shown by Parker, a unidirectional distribution of dipoles within the crust is equivalent to unidirectional dipoles placed on the surface. Therefore, no assumptions about the source geometry are made. Many dipoles are placed within a circle over a region that encompasses the isolated anomaly, usually of the same size of the crater rim. For an assumed direction of magnetization, we solve for the magnetic moments of the dipoles and determine the misfit between the model and observations using a non-negative least squares inversions approach [9]. For our inversions we use the global gridded magnetic field maps at 40 km altitude from [4] based on MESSENGER magnetometer observations.

3. Results

We study five anomalies associated with craters: the two main magnetic anomalies related to the craters Rustaveli (200 km in diameter, centered at 83ºE, 52ºN), and Vyasa (300 km in diameter, centered at 275ºE, 50ºN); and three anomalies related with smaller unnamed craters centered at (289ºE, 57ºN), (295ºE, 46ºN), and (282ºE, 41ºN). For the Rustaveli anomaly, we find the best paleopole position at (269ºE, 13ºN), with a misfit value of 0.85 nT (see Figure 1).

Considering the uncertainties on the paleopole position the solution includes the South pole, where the present-day magnetic North pole is believed to be located. For the Vyasa anomaly, we find the best paleopole at (230ºE, 50ºS), with a misfit of 0.81 nT. These results, even showing an equatorial best solution, do not allow one to argue for a thermoremanent source, as the uncertainty also includes the present magnetic North pole (located near the south geographic pole).

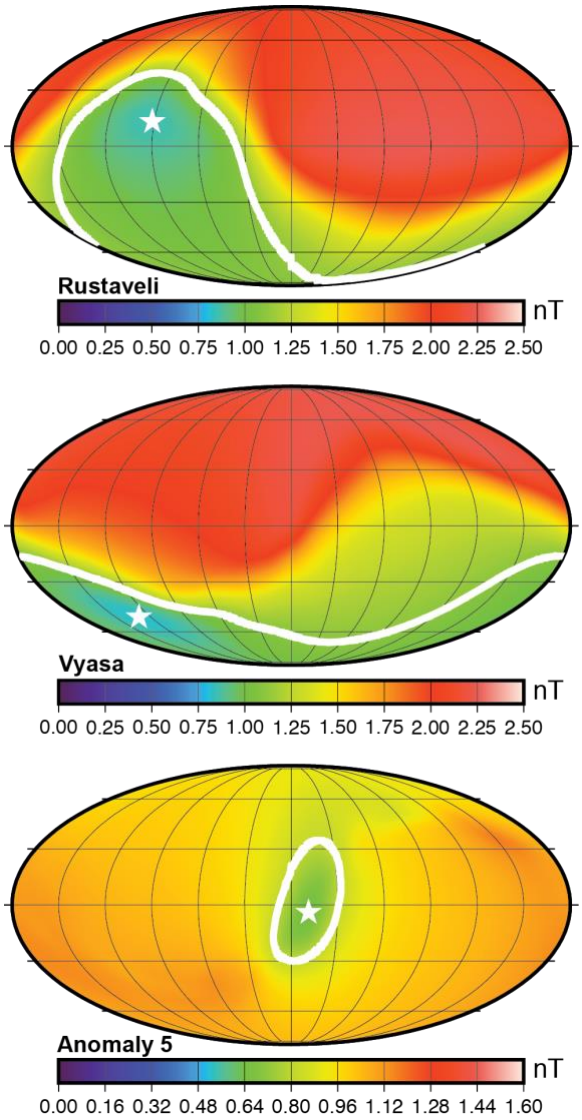

Figure 1: Misfit as a function of the paleopole position for three different magnetic anomalies associated with craters. The star symbol denotes the best fit solution and the solid white line its uncertainty.

For those cases, an induced field due to a permeability enhancement beneath the crater's interior surface process cannot be ruled out. However, anomalies with small uncertainty solutions are obtained at the equator of the planet, proving that at least some of the anomalies are thermoremanently magnetized (see Anomaly 5 from Figure 1).

4. Summary and Conclusions

Results prove that at least some of Mercury's crustal anomalies have a thermoremanent magnetization origin, implying information about the early history of Mercury's core dynamo. In particular, inferred paleomagnetic poles for some anomaly sources are not located near the south geographic pole, indicating that they are not induced in the present-day dynamo field.

Acknowledgements Supported at the University of Arizona by the NASA DDAP.

References **[1]** Johnson C. et al.: Low-altitude magnetic field measurements by MESSENGER reveal Mercury's ancient crustal field, Science, Vol. 348, pp. 892-895, 2015. **[2]** Hood L.: Initial mapping of Mercury's crustal magnetic field: Rela- tionship to the Caloris impact basin, Geophys. Res. Lett., Vol. 42, pp. 10565-10572, 2015. **[3]** Hood L.: Magnetic anomalies concentrated near and within Mercury's impact basins: Early mapping and interpretation, J. Geophys. Res. Planets, Vol. 121, pp. 1016-1025, 2016. **[4]** Hood L. L., Oliveira J. S., Galluzzi V., Rothery D. A.: Investigating Sources of Mercury's Crustal Magnetic Field: Further Mapping of MESSENGER Magnetometer Data, J. Geophys. Res. Planets, Submitted. **[5]** Wieczorek, M. A., Weiss, B. P., Stewart, S. T.: An Impactor Origin for Lunar Magnetic Anomalies, Science 335, pp.1212, 2012. **[6]** Parker R.: A theory of ideal bodies for seamount magnetism, J. Geophys. Res., Vol. 96, pp. 16101–16112, 1991. **[7]** Oliveira J. S. and Wieczorek M. A., Testing the axial dipole hypothesis for the Moon by modeling the direction of the crustal magnetization, J. Geophys. Res. Planets, Vol. 122, pp. 383–399, 2017. **[8]** Oliveira, J. S., Wieczorek, M. A., and Kletetschka, G.: Iron abundances in lunar impact basin melt sheets from orbital magnetic field data. J. Geophys. Res. Planets, Vol. 122, pp. 2429–2444, 2017. **[9]** Lawson, C. L., and Hanson R. J.: Solving Least Squares Problems, Series in Automatic Computation, Prentice-Hall, Englewood Cliffs, N. J., 1974.

EPSC Abstracts
Vol. 12, EPSC2018-522-1, 2018
European Planetary Science Congress 2018

Mapping Low-Reflectance Material on Mercury

R. Klima (1), D. Blewett (1), B. Denevi (1), C. Ernst (1), S. Murchie (1), and P. Peplowski (1). (1) Johns Hopkins University Applied Physics Laboratory, Laurel, MD, USA. (Rachel.Klima@jhuapl.edu / Fax: +1-443-778-8939

Abstract

Distinctive low-reflectance material (LRM) was first observed on Mercury in Mariner 10 flyby images [1]. Visible to near-infrared reflectance spectra of LRM are flatter than the average reflectance spectrum of Mercury, which is strongly red sloped (increasing in reflectance with wavelength). From Mariner 10 and early MErcury, Surface, Space, ENvironment, GEochemistry, and Ranging (MESSENGER) flyby observations, it was suggested that a higher content of ilmenite, ulvöspinel, carbon, or iron metal could cause both the characteristic dark, flat spectrum of LRM and the globally low reflectance of Mercury [1,2]. Once MESSENGER entered orbit, low Fe and Ti abundances measured by the X-Ray and Gamma-Ray Spectrometers ruled out ilmenite and ulvöspinel as important surface constituents [3,4] and implied that LRM was darkened by a different phase, such as carbon or small amounts of micro- or nanophase iron or iron sulfide dispersed in a silicate matrix. Low-altitude thermal neutron measurements of three LRM-rich regions confirmed an enhancement of 1–3 wt% carbon over the global abundance, supporting the hypothesis that the darkening agent in LRM is carbon [5].

1. Distribution of LRM

LRM is distributed across Mercury, typically having been excavated from depth by craters and basins. In contrast to the brighter high reflectance plains (HRP) and smooth plains deposits, which exhibit morphological evidence of volcanism [e.g., 6-8], LRM is not associated with flow features or other evidence of a volcanic origin. Older LRM boundaries are generally diffuse, and grade into low-reflectance blue plains (LBP). Because of the common lack of sharp geologic boundaries, LRM has been defined primarily based on albedo and spectral shape, isolated through principal components (PC) analyses of MDIS color images [9]. LRM is the darkest material on Mercury, with an albedo of 4–5% at 560 nm, and it exhibits a spectral slope that is substantially less red (increases less in brightness with increasing wavelength) than the rest of Mercury. The low iron content of Mercury's surface results in a lack of the spectral absorption bands typically used to map mafic minerals on planets and asteroids. Thus, mathematical transformations such as PC analysis are required to map subtle spectral differences. For example, the second principal component (PC2), captures a combination of spectral slope and curvature, isolating LRM and hollows as one endmember, with red material and HRP as the other end member. LBP and intermediate plains (IP) are transitional from LRM to HRP [10]. In [5], concentrated LRM exposures were defined as regions with a photometrically corrected reflectance of <5% (at 560 nm wavelength) and a PC2 value of <0.023. This value corresponds with the lower ~25% of the range of PC2 values for the whole planet. The resulting LRM map, overlain on the global color mosaic, is shown in Fig. 1a. There are some regional concentrations where many moderate sized craters or several larger basins excavated LRM in close proximity to one another. LRM is most immediately recognizable visually when excavated by craters and deposited onto high-reflectance red plains (HRP, as in Caloris basin), due to the contrasting reflectance and spectral slopes of the different stratigraphic layers. However, it is also abundant throughout the oldest, rough terrains, where its boundaries are more difficult to delineate as they grade into LBP. In these older terrains LRM is still apparently associated with crater ejecta, but the high density of craters excavating LRM results in a patchy distribution of low-reflectance, low-PC2 material.

2. Mapping LRM Directly

Because PC analyses are calculated using the spectral range over a given data set, a PC2 constraint cannot be directly translated to individual targeted color images, except in the rare case of images that contain the full range of Mercury's spectral diversity. The broad, shallow band centered near 600 nm that is observed in LRM (and also often in hollows material) can be isolated directly by dividing the planet as a whole by a reference spectrum and then calculating a band depth ratio. Murchie et al. [11] found that the most successful ratio for mapping the LRM was calculated by first dividing the full mosaic by a

reference spectrum of the northern volcanic plains, and then calculating the ratio as:

$$\sim 600\ nm\ band\ depth = 1 - \left| \frac{(R560 + R630 + R750 + R830)/4}{(R900 + R480)/2} \right|$$

where R is photometrically corrected reflectance in each of the given filters. Mapping this feature with the calibrated 8-color mosaic [12] clearly highlights the regions identified by the LRM map (Fig. 1b). However, isolating the LRM deposits also requires combining this band depth with an albedo constraint. We are currently developing a new 'LRM' parameter that captures the aspects of both the albedo and the spectral shape observed in the LRM and so far best parameterized by the 600 nm band depth calculation.

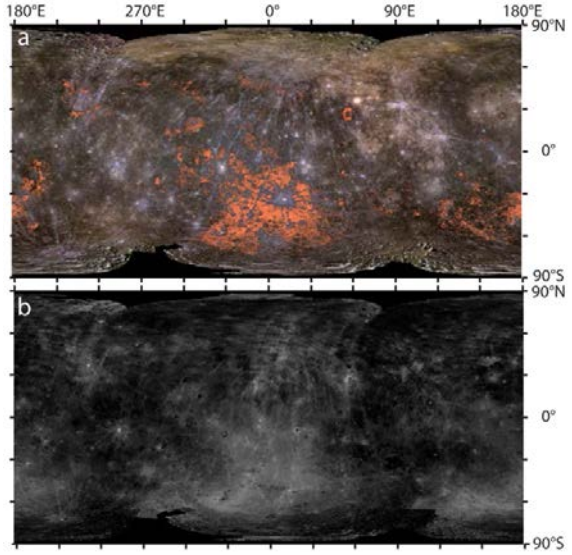

Fig. 1. (a) False color global map of Mercury with R=1000 nm, G=750 nm and B=430 nm. LRM shows up as dark bluish-black material, and grades into the slightly brighter LBP. The LRM map using albedo, PC2 and slope constraints as detailed in the text is overlain in orange. **(b)** ~600-nm broad band depth map. From Klima et al., 2018.

3. Carbon Content of LRM

In [5], 600-nm band depth ratio in LRM was found to correlate with abundance of carbon as measured during low-altitude neutron detector measurements. Although there were only three locations that could be measured, within uncertainty, there is a clear linear relationship between the average ~600 nm band depth for each LRM deposit (mapped using the PC constraints previously described) and the measured carbon content. Based on the derived band-depth to carbon relationship, we estimated carbon contents for other LRM deposits (Fig. 2). Our results suggest that some regions may contain as much as 5 wt% carbon above the global mean, a value consistent with the carbon content required to produce their low reflectances [11].

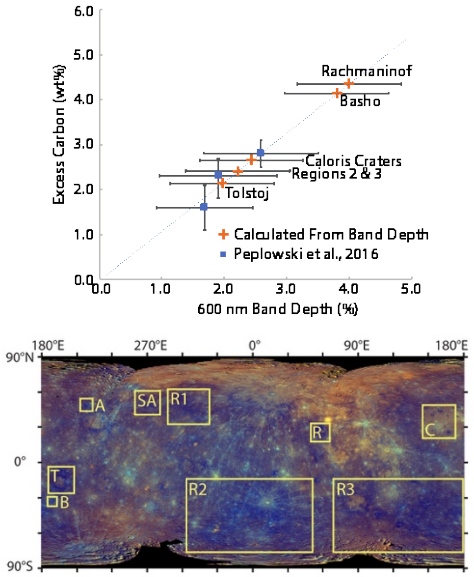

Fig. 2. (top) Extrapolated carbon content for different regions of the surface. Blue squares were measured directly in [5], orange plusses were calculated from the derived band depth relationship. (bottom) Enhanced color composite of Mercury with R=PC1, G=PC2, B=430/1000 nm slope. Locations of LRM-enriched craters measured in [5] A-Akutagawa, SA-Sholem-Aleichem, and R1-region LRM-A are shown, along with derived values for B-Basho, T-Tolstoj, R-Rachmaninoff and C-Craters within Caloris and two additional regional enhancements (R2, R3). From Klima et al., 2018.

Acknowledgements

We are grateful to the NASA PMDAP program for supporting this work (#NNX14AM93G).

References

[1] Hapke, B. et al. (1975) *JGR* 80, 2431. [2] Robinson, M.S. et al. (2008) *Science* 321, 66. [3] Nittler, L.R. et al., (2011) *Science* 333, 1847. [4] Evans, R.G. et al. (2012) JGR 117, E00L07. [5] Peplowski, P.N. et al. (2016) *Nat. Geosci.* 9, 273-278. [6] Head, J.W. et al., (2011) *Science* 333, 1853–1856. [7] Whitten, J. L., et al. (2014) *Icarus* 241, 97-113. [8] Denevi, B.W. et al., (2013) *JGR Planets* 118, 891–907. [9] Klima, R.L., et al. (2016), *LPSC* 47, Abstract#1195. [10] Denevi, B. et al., (2016), *LPSC* 47, Abstract#1624. [11] Murchie, S.L. et al. (2015) *Icarus* 254, 287. [12] Denevi et al., (in press) DOI: 10.1007/s11214-017-0440-y. [13] Klima et al. [2018] GRL.

EPSC Abstracts
Vol. 12, EPSC2018-533, 2018
European Planetary Science Congress 2018

Re-examination of the population, stratigraphy, and sequence of Mercurian basins: Implications for Mercury´s early impact history and comparison with the Moon

Csilla Orgel (1), Caleb I. Fassett (2), Greg Michael (1), Carolyn H. van der Bogert (3), Harald Hiesinger (3)
(1) Freie Universität Berlin, Institute of Geological Sciences, Berlin, Germany (orgel.csilla@fu-berlin.de) (2) NASA Marshall Space Flight Center, Alabama, USA (3) Westfälische Wilhelms-Universität, Münster, Germany

1. Introduction

The Mercury has the second best preserved impact record in the inner Solar System due to the absence of an atmosphere, but a much higher rates of surface modification than on the Moon [1-3]. The earliest geological mapping of the planet revealed a variety of important differences from the Moon, regarding the impact basin (≥ 300 km) and cratering record as well as extensive volcanic plains of Mercury [1-3]. It has been shown [3] that the bombardment history of the terrestrial planets is lunar-like and linked in term of impactor population(s) and impact rates. Recent studies suggest that Mercury and Moon had the same early impactor populations based on the similarity of the crater size-frequency distributions (CSFD), however the impact rates on Mercury are higher than on the Moon [4, 5]. Fassett et al. [6] catalogued and characterized the basin population on Mercury using early orbital data obtained by the MESSENGER spacecraft and found 46 certain and probable impact basins, as well as a few more uncertain suggested basins. Many of these suggested basins were proposed on the basis of Mariner 10 but could not be verified with the available new data.

In this study, we are re-investigating the number of the mercurian impact basin (≥ 300 km) and their superposed crater populations. Moreover, we will revisit the stratigraphic relationships of basins based on N(20) and N(64) crater frequencies, absolute model ages, and observation data. Finally, we intend to infer potential projectile populations and compare the findings to the Moon.

2. Data and Methods

The primary data for this study are optical images mosaicked into a 166 m/pixel global data set and topography (665 m/pixel) from MESSENGER's Mercury Dual Imaging System (MDIS) and Mercury Laser Altimeter (MLA) (250 m/pixel). All data products are available from the Planetary Data System (PDS). The data was analysed in ESRI ArcGIS 10.3 environment. The CraterTools extension in ArcMap [9] was used to map the basins and their related crater population. We classified basins as either certain, probable or suggested. We use two different mapping approaches by (1) counting craters on the basin rim excluding all resurfaced areas by the smooth plains, and (2) mapping all craters inside the basin cavity, which provides a lower limit crater density and absolute model age (AMA) for the basins. Most commonly we apply the second approach, because the basins are fully or partially covered by plains in various thicknesses [6]; the degree of basin resurfacing is evidently much more substantial than on the Moon. To derive the CSFD of impact basins we will use the CSFD_Tools from [10], and apply the buffered crater counting technique [7] (first and second mapping approaches) and the buffered non-sparseness correction technique (first mapping approach) as in our previous study on the Moon [8]. We will also consider AMA of the impact basins by applying the CraterStats software [11].

3. Preliminary Results

We identified 80 certain or probable basins on Mercury, twice as much as in the previous study [6]. This increase in number will have substantial implications for the early history of Mercury´s crust. Most of the basins are buried by smooth plains, intercrater plains, or both. In addition, there are complex interactions of basins with lobate scarps and other tectonic landforms. Candidate basins are often surrounded by scarps, rather than obvious intact rims. Thus topography data is extremely useful to find

“hidden” basins which were not identified by earlier studies [1, 3, 6].

Some of the more remarkable candidate new basins are candidate landforms stratigraphically beneath Caloris, which have never been described by earlier studies (e.g., Fig. 1). These basins are similar in character to Mendel-Rydberg on the Moon, which is directly superposed by Orientale ejecta, although the additional complication on Mercury is they are also buried by abundant smooth plains.

In summary, our initial results and future work should greatly enhance the understanding of the early Mercury impact record.

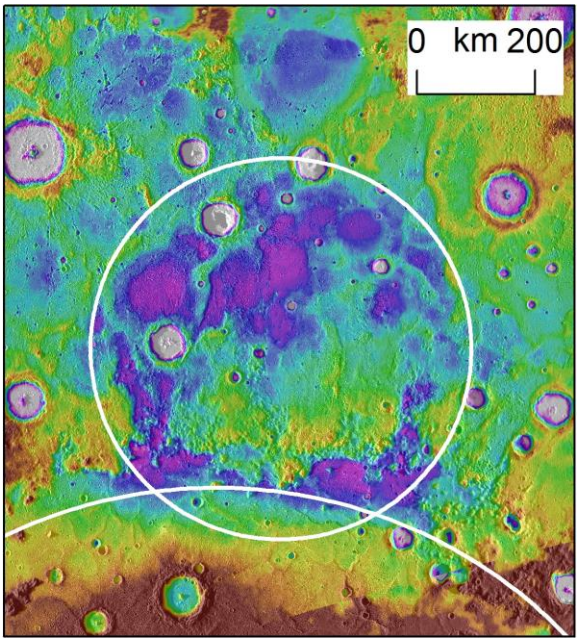

Figure 1: Candidate impact basin beneath Caloris on MLA DEM 250 m/pixel data (165E, 54N).

Acknowledgements

This work was funded by the Deutsche Forschungsgemeinschaft (SFB-TRR 170, subproject A3-3). CIF was supported by a NASA DDAP grant.

References

[1] Spudis, P. D., and J. E. Guest, Stratigraphy and geologic history of Mercury, in Mercury, edited by F. Vilas, C. R. Chapman, and M. S. Matthews, pp. 118–164, Univ. of Ariz. Press, Tucson, 1988. [2] Strom, R. G., and G. Neukum, The cratering record on Mercury and the origin of impacting objects, in Mercury, edited by F. Vilas, C. R. Chapman, and M. S. Matthews, pp. 336–373, Univ. of Ariz. Press, Tucson, 1988. [3] Neukum, G. et al., Geologic evolution and cratering history of Mercury, Planetary and Space Science, 49, 1507-1521, 2001. [4] Strom, R. et al., Mercury crater statistics from MESSENGER flybys: Implications for stratigraphy and resurfacing history, Planetary and Space Science, 59, 1960-1967, 2011. [5] Fassett et al., The global population of large craters on Mercury and comparison with the Moon, Journal of Geophysical Research Letters, 38, L10202, 2011. [6] Fassett et al., Large impact basins on Mercury: Global distribution, characteristics, and modification history from MESSENGER orbital data, Journal of Geophysical Research, 117, E00L08, 2012. [7] Fassett, C. I., and Head, J. ~W., The timing of martian valley network activity: Constraints from buffered crater counting, Icarus, 195, 61–89, 2008. [8] Orgel et al., Ancient bombardment of the inner Solar System - Reinvestigation of the "fingerprints" of different impactor populations on the lunar surface. Journal of Geophysical Research, 123, doi.org/10.1002/2017JE005451. [9] Kneissl, T., van Gasselt, S., and Neukum, G., Map-projection-independent crater size-frequency determination in GIS environments--New software tool for ArcGIS, Planetary and Space Science, 59, 1243-1254, 2011. [10] Riedel et al., An ArcGIS independent application to conduct crater size-frequency measurements with respect to crater obliteration effects, 49th Lunar and Planetary Science Conference, LPI Contrib. Nr. 2083, #1478. [11] Michael, G., and Neukum, G., Planetary surface dating from crater size-frequency distribution measurements: Partial resurfacing events and statistical age uncertainty, Earth Planet. Sci. Lett., 294, 223-229, 2010.

EPSC Abstracts
Vol. 12, EPSC2018-610, 2018
European Planetary Science Congress 2018

Viscoelastic Tides of Mercury and Implications for its Inner Core Size

G. Steinbrügge[1,3] (gregor.steinbruegge@dlr.de), S. Padovan[1], H. Hussmann[1], T. Steinke[2], A. Stark[1] and J. Oberst[1].
[1]German Aerospace Center (DLR), Institute of Planetary Research, Berlin, Germany, [2]Delft University of Technology, Delft, Netherlands, [3]Institute for Geophysics, University of Texas at Austin, Austin, TX, USA

1. Introduction

This work studies the tidal deformation of Mercury based on the currently published geodetic constraints from the MESSENGER mission and shows that a future determination of the tidal Love number h_2 can yield important constraints on the inner core when combined with the available (or future) measurements of k_2. We further studied the potential range of tidal phase-lags and resulting tidal heat dissipation in Mercury's mantle. All parameters discussed in this contribution might be measured by the upcoming BepiColombo mission [1] scheduled for launch in 2018 and operated by the European Space Agency (ESA) and the Japan Aerospace Exploration Agency (JAXA).

2. Method

All constructed models consist of three chemically separated layers: A core surrounded by a mantle and covered by a crust. While the crust is kept as one single layer, the mantle and the core are further subdivided. Each sublayer is characterized by its thickness, density, temperature, pressure, viscosity and rigidity. The parameter space is spanned by the the volatile content of the core, where we account for sulfur and silicon, the temperature of the core-mantle boundary as well as by the crustal thickness and density. The remaining parameters are solved for in order to obtain self-consistent models. The construction of the models follows a two-step process. In a first step each model is initialized by a given value of each of the parameter listed above as including a set of three geodetic constraints, namely the mean density, the mean moment of inertia and the fractional part of the moment of inertia which is due to the mantle to solve for the radius of the outer core, the reference liquid core density as well as for the mantle density. A solution is only considered valid if the resulting model is hydrostatic and if the solved parameters are consistent with laboratory measurements. In the second step each solution for the structural model is provided with a set of different mantle rheologies parametrized by the unrelaxed rigidity and the grain size. Based on these, the tidal Love number k_2 is calculated and compared against the measurement. Models which are not consistent with the measurement inside its 3-σ error bar are discarded.

The nominal value used for k_2 is 0.451 ± 0.014 [4] but the error bar also accounts for the value determined by [5]. The used mean moment of inertia is 0.346 ± 0.014 [6]. The assumed C_m/C value is 0.421 ± 0.025 [7]. However, within the used error intervals the C_m/C is also consistent with the value 0.431 ± 0.021 [6].

3. Results

Typical k_2 values range between 0.45 and 0.52 implying that the measured value argues for a high mantle rigidity and / or high grain-sizes as well as a lower temperature at the core-mantle boundary in agreement with previous work [8]. In the considered range of models the tidal Love number h_2 ranges between 0.77 and 0.93. The corresponding tidal amplitudes range from 1.93 to 2.33 m at the equator and 0.24 to 0.29 m at the poles.

An important advantage of having both tidal Love numbers is that certain dependencies can be suppressed by combining them. The main parameter controlling the value of k_2 and h_2 is the existence of a liquid core. Further, the amplitude of the deformation is controlled by the mantle rheology. However, when considering the Love numbers individually, the presence of a solid inner core has only a moderate effect on the amplitude in comparison to the

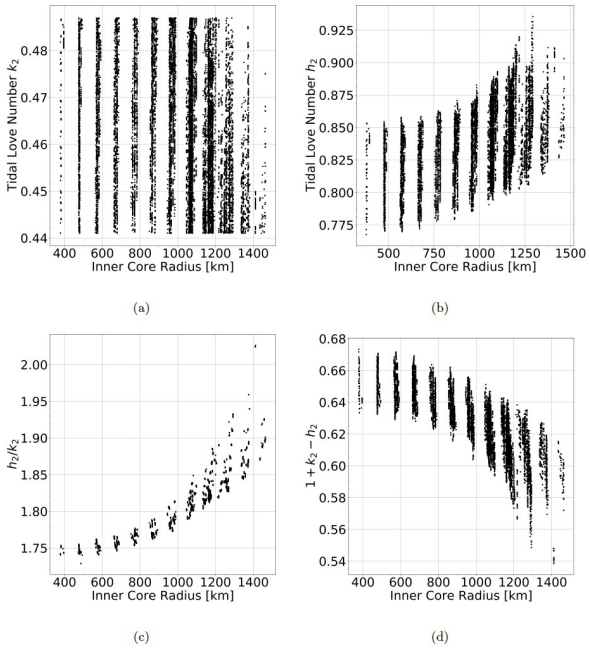

Figure 1: (a) Tidal Love number k_2 as a function of inner core size. (b) The tidal Love number h_2 as a function of the inner core size. (c) Using the ratio h_2/k_2 is less ambiguous and therefore allows setting an upper limit on the core size. (d) The same effect can be principally observed using the linear combination $1+k_2-h_2$, however provides a less strict constraint.

rheological properties of the mantle (compare to Figure 1). A linear combination as well as the ratio h_2/k_2 cancels out the ambiguity to a certain extent. What is left are the changes in the gravity field due to a redistribution of mass inside the core. Since a density contrast between a solid core an a liquid core is present, the size and density of an inner core are noticeable when combining both Love numbers. The linear combination is known as the diminishing factor, which has been proposed previously to better constrain the ice thickness of Jupiter's moon Europa [2] but is also applicable to other icy satellites e.g. Ganymede [3]. For small solid cores, the effect is barely noticeable, so in the case of the core being small a measurement of the respective ratio or linear combination would allow the determination of an upper bound for the size of the inner core but a determination of the actual inner core size would only be feasible with a significant uncertainty due to the remaining ambiguity. The ratio h_2/k_2 is affected by a similar behaviour, however is less ambiguous. Therefore, for cores > 700 km in radius the size can potentially be inferred but a measurement accuracy in the order of 1% in h_2 would be required.

Since the tidal Love numbers are complex numbers they are not only characterized by their amplitude but also by a phase which is a function of the rheologic parameters and indicates the amount of tidal dissipation. A particularity of the 3:2 resonance is that the tidal dissipation barely depends on the eccentricity. The main source of tidal dissipation on Mercury is the mantle; however the maximum values for Im(k_2) consistent with the geodetic constraints are between 0.02 and 0.03. This result is consistent with the maximum value estimated from the spin orientation [9]. The maximum tidal dissipation would then correspond to a surface flux of < 0.16 mW/m^2 .

4. Discussion

A measurement of the tidal Love number h_2 should fall most likely in the predicted range of 0.77 to 0.93. A refined measurement of the moment of inertia, C_m/C and k_2 are likely to further constrain the value. In case of a compliant measurement the remaining range of possible values is valuable to discriminate between the remaining models to get additional constraints on the inner core size. In case of a small core however, the inner core size is unlikely to be constrained any further due to the remaining ambiguity in the interior models. In case of an inner core with a radius above 1000 km the size can be constrained with an accuracy of 50 to 200 km due to the exponential growth of the h_2 over k_2 ratio. Therefore, it would also allow to reassess the moment of inertia if necessary and to provide valuable information for models addressing Mercury's core dynamic and magnetic field generation.

References

[1] Benkhoff et al. (2010), PSS 58. [2] Wahr et al. (2010), JGR 111. [3] Steinbrügge et al. (2015), PSS. 117. [4] Verma and Margot (2016) JGR: Planets 121. [5] Mazarico et al. (2014) [6] Margot et al. (2012) JGR: Planets 117. JGR: Planets 119. [7] Stark et al. (2015) GRL 42. [8] Padovan et al. (2014), JGR: Planets 119. [9] Baland et al. (2017), Icarus 291.

EPSC Abstracts
Vol. 12, EPSC2018-625-2, 2018
European Planetary Science Congress 2018

Mercury observations in 2016 and 2019, during Transits and Total Eclipse

M. Pérez-Ayúcar (1), J. Zender (2), M. Castillo (1), M. Breitfelner (1)
(1) European Space Astronomy Center (ESAC), Madrid, Spain (miguel.perez.ayucar@esa.int)

(2) European Space Technology Center (ESTEC), Noordwijk, The Netherlands (joe.zender@esa.int)

Abstract

Transits are rare astronomical events of profound historical importance (measuring the distances in the solar system). Although its scientific use has diminished since humanity roams our solar system with robotic spacecrafts, transits remain a spectacular astronomical event, with an enormous potential to engage nowadays students and general public into Planetary Sciences and Space, and also performing some unique science experiments.

In the case of Mercury, transits occur only about 13-14 times per century. It was first observed in 1631 by Pierre Gassendi, and from 2000 to 2100, 14 occasions are predicted. In this decade, only 2016 and 2019 had a transit. After that, people on Earth will have to wait until Nov 2032 to observe the event.

The educational project CESAR (Cooperation through Education in Science and Astronomy Research), in collaboration with ESA's space projects (Bepi – Colombo, Venus Express, Solar Orbiter, Proba-2) has been covering since 2012 such events (Venus transit 2012, May 2016 Mercury Transit, Total Eclipse 2017). The team is currently preparing the Nov 2019 Mercury Transit and Jul 2019 Total Eclipse.

For the Mercury Transit in May 2016, a dual observation was made from two separate locations: a twin portable telescope set-up at the IAC (Instituto de Astrofísica de Canarias) Izaña, Tenerife, Spain, and in Cerro Paranal, Chile, achieving a ground baseline parallax of around 10.000km.

For the Mercury Transit in Nov 2019, as the geometry is quite similar to 2016, a comparable set up is being organized: dual teams at Canary Islands and Chile.

For the Total Eclipse in Jul 2019, a team will travel to the European Southern Observatory (ESO) at La Silla, Chile, to record and transmit live the occultation, and record unique observations of the Mercury exosphere, while in totality.

In this paper we will report on the results from the Mercury Transit 2016, and explain the campaign and expected results from 2019.

EPSC Abstracts
Vol. 12, EPSC2018-649, 2018
European Planetary Science Congress 2018

SIMULATION OF SPACE-WEATHERED TIR SPECTRA ON MERCURY

Kay Wohlfarth (1), Arne Grumpe (1), Christian Wöhler (1), Aleksandra Stojic (2), Andreas Morlok (2), and Harald Hiesinger (2), (1) Image Analysis Group, TU Dortmund University , Germany (2) Institut für Planetologie, WWU, Münster, Germany {kay.wohlfarth, arne.grumpe, christian.woehler}@tu-dortmund.de

1. Introduction

The BepiColombo spacecraft will carry the spectrometer MERTIS which is designed to perform hyperspectral measurements of the Mercurian surface in the thermal infrared (TIR) domain (7 µm – 14 µm) [1]. TIR spectra have been used to quantify modal abundances on Mars from Thermal Emission Imaging System (TEMIS) and Thermal Emission Spectrometer (TES) data [2,3]. Spectral measurements in the TIR range of Mercury's surface are subject to the superposition of solar reflection and variable thermal emission [4]. Additionally, the regolith is affected by space weathering, which is known to have an impact on the spectral shape. In order to address combined reflectance and emittance as well as space weathering in view of the evaluation of MERTIS measurements, this work contributes in two ways: At first, we apply our space weathering simulation framework [5] to generate artificially space weathered spectra of silicates in the TIR region and compare them to laboratory weathering experiments [6]. Secondly, we employ our previous approach [7] to simulate combined reflectance and emittance spectra of space weathered silicates under conditions which are comparable to Mercury's environment. This will not only improve the accuracy of previous simulations but it is also a step towards a comprehensive model of Mercury's radiance characteristic relevant for soil characterization, spectral unmixing and modal abundance estimation.

2. Method

Space weathering simulation: In our previous work [5], the effects of space weathering are simulated by directly modeling the scattering behavior of submicroscopic iron spherules employing Mie theory. The technique falls into two steps: At first, the scattering behavior of iron is computed. Secondly, the single scattering albedo of the simulated iron is mixed with the single scattering albedo of a silicate. Subsequently, the mixed albedos are fed into Hapke's model [8] in order to generate reflectance spectra under arbitrary illumination conditions.

Combined reflectance and emittance: The wavelength-dependent radiance I which is measured at the sensor is a superposition of solar reflection and thermal emission. Solar irradiance J [W/m^2] illuminates the surface and is reflected according to the reflectance function $r(i, e, g)$. It depends on the incidence angle i, the emission angle e and the phase angle g. Additionally, thermal radiation U emerges from the surface according to Planck's law which is multiplied with the directional emissivity ϵ_d:

$$I(i, e, g, \lambda) = Jr(i, e, g, \lambda) + \epsilon_d(e, \lambda)U(T, \lambda)$$

The combined model was presented in [7]. It relies on the anisotropic reflectance model proposed in [8] and the hemispherical directional emissivity which is obtained by integrating r [7,8]. We make use of our artificially weathered spectra in order to simulate realistic radiance emerging from Mercury.

3. Results

Space weathering simulation: We carried out a space weathering simulation of an olivine sample in the TIR region for iron particle sizes of 100 nm in diameter. The results for different weight percentages are plotted in Figure 1. In the work of [6], olivine samples were irradiated by laser pulses, where two effects are observed (Figure 2): A larger number of pulses and more powerful irradiation yield a more prominent darkening effect, where the darkening effect becomes less strong with increasing wavelength. The strongest irradiation with 5 pulses of 50 mJ produces a severe darkening effect for the whole spectrum, but the authors of [6] state that this scenario is likely to be unrealistic. The comparison of our simulation with the results from [6] indicates an overall consistency: An increasing iron content accounts for a stronger darkening effect, and the effect becomes weaker with increasing wavelength. An unrealistically high amount of 10 wt% of iron causes the very dark spectrum. Note that we studied bidirectional reflectance r_d, whereas in [6] a scaled reflectance is studied. Moreover, different olivine samples were used. This explains the different scaling of the reflectance and the slightly different spectral shapes.

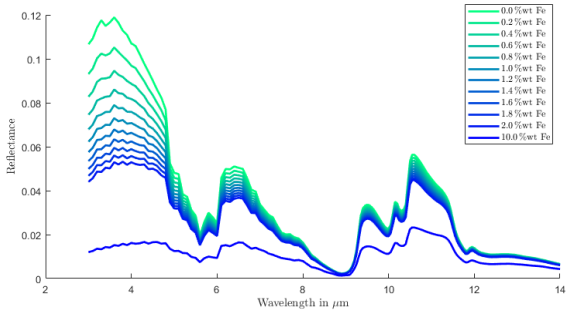

Figure 1. Simulated space weathering of olivine.

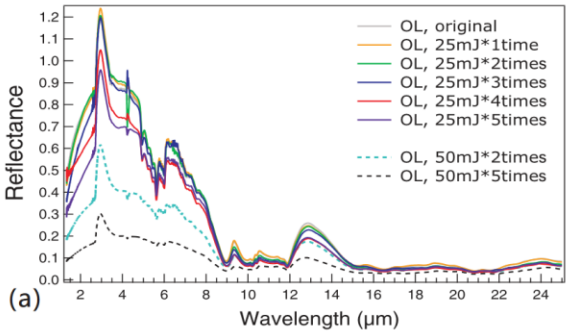

Figure 2. Space weathering experiment (from [6]).

Combined reflectance and emittance: We used a reflectance spectrum which was computationally space weathered with 2 wt% of iron and fed it into our combined reflectance and emittance framework. The spectrum was acquired at room temperature. Thus, temperature dependent changes of the spectral bands will not be observed in our simulation. In the work of [9] the latitude-dependent temperatures at perihelion and aphelion are given. We examine several keypoints ranging from (0°W|15°N) to (0°W|88°N) for perihelion and from (90°W|15°N) to (90°W|86°N) on aphelion. A higher latitude also implies that the incoming solar irradiance decreases with the cosine of the latitude. The resulting spectra are divided by the blackbody radiation and we call this quantity apparent emissivity. As depicted in Figures 3 and 4, the spectra of the apparent emissivity only show a variation with temperature for wavelengths roughly below 5 µm. This indicates that thermal emission is the dominant source of radiance emerging from Mercury in the spectral range of MERTIS.

Local Topography: In our simulations, Mercury was assumed to be a perfect sphere. In reality, the Mercurian surface exhibits a rich topography. Some surface elements in this area may face the sun, have low solar incidence angles and thus become hotter than an even surface. Surface elements which are only tangentially lit are colder. Thus, a small area with many different slopes may exhibit a mixture of different temperatures and incidence angles.

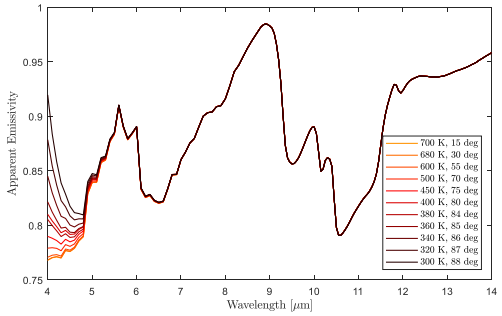

Figure 3. Simulated apparent emissivity at perihelion.

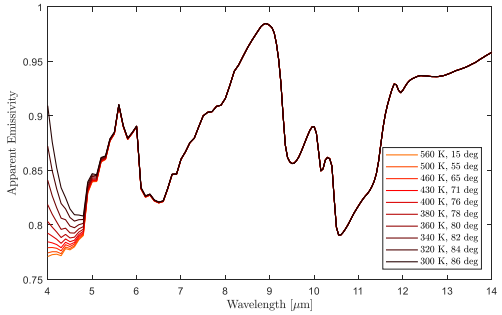

Figure 4. Simulated apparent emissivity at aphelion.

4. Conclusion

We simulated combined reflectance and emittance spectra under the influence of space weathering for realistic scenarios on the Mercurian surface. Our model enables the simulation of various conditions on the planet. The results indicate that emission is the predominant source of radiance emerging from Mercury at wavelengths beyond 5 µm. Further investigations shall combine the model with information on topographic information and local temperature, which is crucial for a physically meaningful interpretation of radiance spectra of Mercury's surface.

References

[1] Helbert, J. et al. (2005) *LPSC XXXVI*, abstract #1753, [2] Huang, J. et al. (2013) *JGR: Planets*, 118, 2146–2152. [3] Goudge, T. A. et al. (2015) *Icarus*, 250, 165–187., [4] Collins, E. F. et al. (1999) *SPIE* 3753, 286–299., [5] Grumpe, A. et al. (2018) LPSC XLIX, abstract #2533, [6] Yang, Y. et al. (2016) A&A 597 A50, [7] Wohlfarth, K. et al. (2018) LPSC XLIX, abstract #2519, [8] Hapke, B. (2002) *Icarus*, 157, 523–534. [9] Vasavada A. R. et al. (1999) *Icarus*, 141, 179–193. [12] Bauch K. et al. (2014) *Planetary and Space Science*, 101, 27-36

EPSC Abstracts
Vol. 12, EPSC2018-650, 2018
European Planetary Science Congress 2018

Concerning the Offset Dipole Magnetic Field of Planet Mercury

Daniel Heyner
(1) Institute for Geophysics and extraterrestrial Physics, Mendelssohnstr. 3, 38106 Braunschweig, Germany (d.heyner@tu-bs.de)

Abstract

The MESSENGER mission revealed an asymmetry in the magnetic field of planet Mercury. In the far field, the magnetic equator is offset northwards by 0.19 planetary radii. The magnetic field inside the magnetosphere was only measured in the northern hemisphere, thus internal and external Gauss coefficients may not be determined independently without the aid of a magnetospheric model. This magnetospheric model in turn requires an internal dipole field. The effect of taking this offset-dipole model determined from the far-field measurements as initial assumption for the magnetospheric model utilized in the spherical harmonic analysis for the internal field is examined for a possible bias. In the analysis, all magnetic field data from entire mission is used. It is found that the bias effect is mainly visible in the quadrupolar and octupolar Gauss coefficients. The resulting magnetic spectrum clearly deviates from a pure offset dipole spectrum.

EPSC Abstracts
Vol. 12, EPSC2018-653, 2018
European Planetary Science Congress 2018

MESSENGER Epithermal Neutron Map of Mercury: Possible Low-Latitude Hydrogen Variation

Jack T. Wilson, David J. Lawrence and Patrick N. Peplowski.
The Johns Hopkins University Applied Physics Laboratory, Laurel, MD 20723, USA (Jack.Wilson@jhuapl.edu).

Abstract

Based on data from the MESSENGER spacecraft we present a spatially resolved map of the epithermal neutron flux in the northern hemisphere of Mercury. The decreasing epithermal neutron flux towards the north pole is consistent with the presence of hydrogen, in the form of water-ice in permanently shaded craters, as reported in previous work. Additionally, the new low-latitude map also shows significant variability away from the pole. Specifically, a correlation between epithermal flux and mean/maximum sub-surface temperature is seen. This may indicate longitudinal variation in hydrogen abundance in Mercury's low- and mid-latitudes.

1.Introduction

The MErcury Surface, Space ENvironment, GEochemistry, and Ranging (MESSENGER) spacecraft [1] carried out an in-depth investigation of Mercury's surface composition during its 5-year mission. MESSENGER's X-Ray Spectrometer (XRS) and Gamma-Ray Spectrometer (GRS) provide element specific data. Data from these instruments have provided elemental abundances for H, K, Th, and U, as well as elemental ratios by weight of Na/Si, Mg/Si, Al/Si, S/Si, Cl/Si, Ca/Si, Ti/Si, Cr/Si, Mn/Si, and Fe/Si. However, several of these measurements are not spatially resolved and many that are suffer from incomplete coverage.

In addition to the XRS and GRS MESSENER contained a neutron spectrometer, unlike individual gamma ray lines neutron data are well sampled and spatially resolved. Neutrons are generated by nuclear spallation reactions when galactic cosmic rays interact with the surface materials of airless or nearly airless planetary bodies. These neutrons undergo moderation by the soil and atmosphere in a way that imprints compositional information into their energy spectra.

In planetary sciences neutron data are conventionally separated into three energy bands. Low-energy, thermal neutrons with energy < 0.5 eV are used to infer the macroscopic neutron absorption cross section, which contains information on the abundance of neutron absorbing elements. Epithermal neutrons, those with energies between 0.5 eV and 0.5 MeV, are primarily sensitive to the presence of hydrogen due to its strong neutron

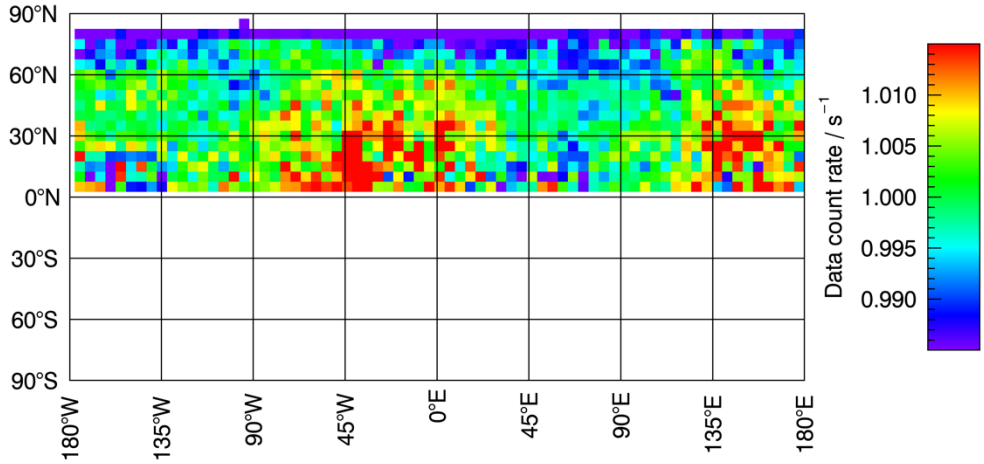

Figure 1: Northern hemisphere map of epithermal neutron count rate on Mercury relative to the mean count rate.

moderating ability, caused by the similarity in the neutron and proton mass. In the absence of hydrogen epithermal neutron flux is proportional to mean atomic mass of surface material. Fast neutron have energy > 0.5 MeV and are primarily sensitive to mean atomic mass.

Maps have been published of both the thermal [2] and fast [3] MESSENGER neutron data, but due to the large systematic errors no epithermal neutron map has yet been published. Here we will present a full-coverage map of epithermal-neutron variability in Mercury's northern hemisphere and discuss what this map implies for our knowledge of elemental composition variations across Mercury.

2.Data and Methods

All five years of MESSENGER epithermal data measured by the borated plastic sensor are used in this study. This large dataset provides sufficient statistical precision to produce a robust map of the thermal neutron flux.

The data reduction was similar to that described in [3] and references therein. That is, empirical corrections were made for variations in GCR flux, spacecraft attitude and solid angle subtended by the planet. Additionally, a correction was made for the Doppler-induced count rate variation based on the spacecraft velocity. This correction was unimportant for the fast neutron data but is important for the epithermal neutron data as the lower energy epithermal neutrons have a speed comparable to that of the spacecraft. As in [3] the efficacy of these corrections was verified by performing similar corrections on a mock data set to determine the size of residual systematic errors.

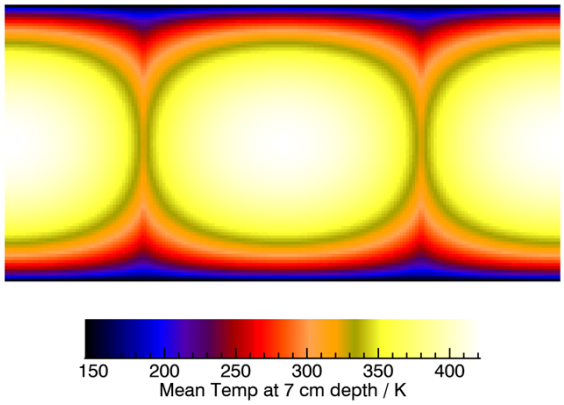

Figure 2: A global map of the mean temperature 7cm beneath Mercury's surface as modelled by [4].

3.Results and Discussion

Figure 1 shows the mapped, corrected epithermal neutron data. As expected the flux is low at the north pole implying an increased abundance of hydrogen and consistent with the presence of water ice in the permanently shaded craters. Significant additional variation is seen at equatorial to mid latitudes. Antipodal highs in epithermal flux are seen at ~30°W and ~150°E, which corresponds approximately to Mercury's hot poles as shown in Figure 2.

The low latitude modulation of epithermal flux is statistically significant and cannot be explained by any know systematic error. If the variation is interpreted as the result of hydrogen variation it implies that the Mercury's hot poles are depleted in hydrogen when compared to the cold poles. In the event that Mercury's volatiles were delivered recently one might expect to see such a correlation due to variation in the stability of hydrogen in the soil at different temperatures. We will further investigate possible physical explanations for this signature and look for confirmation of the hydrogen signal in other datasets including the GRS.

References

[1] Solomon, S. C., R. L. McNutt Jr., R. E. Gold, and D. L. Domingue, MESSENGER mission overview, Space Sci. Rev., 131, 2007, 3–39.

[2] Peplowski, Patrick N., Larry G. Evans, Karen R. Stockstill-Cahill, David J. Lawrence, John O. Goldsten, Timothy J. McCoy, Larry R. Nittler, Sean C. Solomon, Ann L. Sprague, Richard D. Starr, Shoshana Z. Weider, Enhanced sodium abundance in Mercury's north polar region revealed by the MESSENGER Gamma-Ray Spectrometer, Icarus, Volume 228, 2014, 86-95.

[3] Lawrence, David J., Patrick N. Peplowski, Andrew W. Beck, William C. Feldman, Elizabeth A. Frank, Timothy J. McCoy, Larry R. Nittler, Sean C. Solomon, Compositional terranes on Mercury: Information from fast neutrons, Icarus, Volume 281, 2017, 32-45.

[4] Vasavada, Ashwin R., David A. Paige, Stephen E. Wood, Near-Surface Temperatures on Mercury and the Moon and the Stability of Polar Ice Deposits, Icarus, Volume 141, Issue 2, 1999, 179-193.

EPSC Abstracts
Vol. 12, EPSC2018-721-1, 2018
European Planetary Science Congress 2018

Updates on geologic mapping of Kuiper (H06) quadrangle

Lorenza Giacomini (1), Valentina Galluzzi (1), Cristian Carli (1), Matteo Massironi (2), Luigi Ferranti (3) and Pasquale Palumbo (4,1).

(1) INAF, Istituto di Astrofisica e Planetologia Spaziali (IAPS), Rome, Italy (lorenza.giacomini@iaps.inaf.it);
(2) Dipartimento di Geoscienze, Università degli Studi di Padova, Padua, Italy; (3) DISTAR, Università degli Studi di Napoli Federico II, Naples, Italy; (4) Dipartimento di Scienze & Tecnologie, Università degli Studi di Napoli 'Parthenope', Naples, Italy.

1. Introduction

Kuiper quadrangle is located at the equatorial zone of Mercury and encompasses the area between longitudes 288°E – 360°E and latitudes 22.5°N – 22.5°S. The quadrangle was previously mapped for its most part by [2] that, using Mariner10 data, produced a final 1:5M scale map of the area. In this work we present the preliminary results of a more detailed geological map (1:3M scale) of the Kuiper quadrangle that we compiled using the higher resolution MESSENGER data.

2. Data and Methods

The main basemap used for mapping is the MDIS (Mercury Dual Imaging System) 166 m/pixel BDR (map-projected Basemap reduced Data Record) monochrome mosaic compiled using NAC (Narrow Angle Camera) and WAC (Wide Angle Camera) 750 nm-images. In order to better distinguish the surface morphologies, MDIS mosaics illuminated with high solar incidence angle, both from east (HIE) and west (HIW) [3] have been considered. Moreover, to characterized the spectral features and topography of the surface, we used MDIS global color mosaics [4] and DLR stereo-DEM [5]. Because Kuiper quadrangle is located in the equatorial region, the map was produced in an equirectangular projection. Then, the quadrangle has been mapped using ArcGIS at an average scale of 1:400k for a final output of 1:3M.

3. Current results

So far, the western and norther part of quadrangle have been mapped (Fig.1). The preliminary geological map shows a prevalence of crater materials (i.e. crater floor, crater ejecta). Craters were grouped into three classes, on the basis of their degradation degree [6]:

-*C3 craters*. They represent fresh craters with sharp rim and extended bright and rayed ejecta;
-*C2 craters*. Moderate degraded craters whose rim is eroded but clearly detectable. Extensive ejecta blankets are still present;
-*C1 craters*. Very degraded craters with an almost completely obliterated rim. Ejecta are very limited or absent.

Different plain units were also identified and classified as:
- *Intercrater plains*. Densely cratered terrains, characterized by a rough surface texture. They represent the more extended plains on the quadrangle;
- *Intermediate plains*. Terrains showing a gently rolling surface with a moderate density of superposed craters. Intermediate plains are limited in extension and widespread all over the mapped part of the quadrangle;
- *Smooth plains*. Poorly cratered terrain with a planar surface. The most extended smooth plain has been detected on the surrounding of Rudaki crater. In the remaining cases, the plains are limited in extension and confined on the floor of the largest craters.

Finally, several structures were mapped all over the quadrangle. Most of these features are represented by thrusts, some of which appear to form systematic alignments. In particular, two main thrust systems have been identified:
i) *Thakur system*, a 1500 km-long system including several scarps with a NNE-SSW trend, located at the edge between the Kuiper and Beethoven (H07) quadrangles;
ii) *Victoria system*, located between Kuiper and Victoria quadrangle (H02). It encompasses faults with a prevalent N-S and NNW-SSE trend, for a total length of 3500 km.

4. Conclusion and future work

At this stage, about 70% of Kuiper quadrangle has been mapped. Once the mapping activity is accomplished, the geological map will be merged

with the other mapped quadrangles [6,7,8,9,10,11] and integrated into the global 1:3M geological map of Mercury [1], which is being prepared in support to ESA/JAXA (European Space Agency, Japan Aerospace Agency) BepiColombo mission.
The following step regards specific targets of interest, detected during the mapping activity, which can be studied at higher resolution, integrating geomorphologic and spectral analysis. One of these targets will be Renoir basin that shows a variety of geologic units and features on its floor, suggesting a crater's complex evolution.

Acknowledgements

We gratefully acknowledge funding from the Italian Space Agency (ASI) under ASI-INAF agreement 2017-47-H.0. MM was also supported by European Union's Horizon 2020 research grant agreement No 776276- PLANMAP.

References

[1] Galluzzi et al.: *Mercury: Current and Future Science of the Innermost Planet*. Abstract#6075, 2018.
[2] De Hon et al.: *IMAP* #1233, 1981.
[3] Chabot et al.: *LPS XLVII*. Abstract#1256, 2016.
[4] Denevi et al.: *LPS XLVII*. Abstract#1264, 2016.
[5] Preusker et al.: *Planetary and Space Sci*., 142, 26-37.
[6] Galluzzi et al.: *Journal of Maps*, 12, 226–238, 2016.
[7] Mancinelli, et al.: *Journal of Maps*, 12, 190–202, 2016.
[8] Guzzetta et al.: *Journal of Maps*, 13, 227–238, 2017.
[9] Wright et al.: *Mercury: Current and Future Science of the Innermost Planet*. Abstract#6062, 2018.
[10] Malliband : *Mercury: Current and Future Science of the Innermost Planet*. Abstract#6091, 2018.
[11] Lewang et al.: *LPS XLIX*, Abstract#1846, 2018.

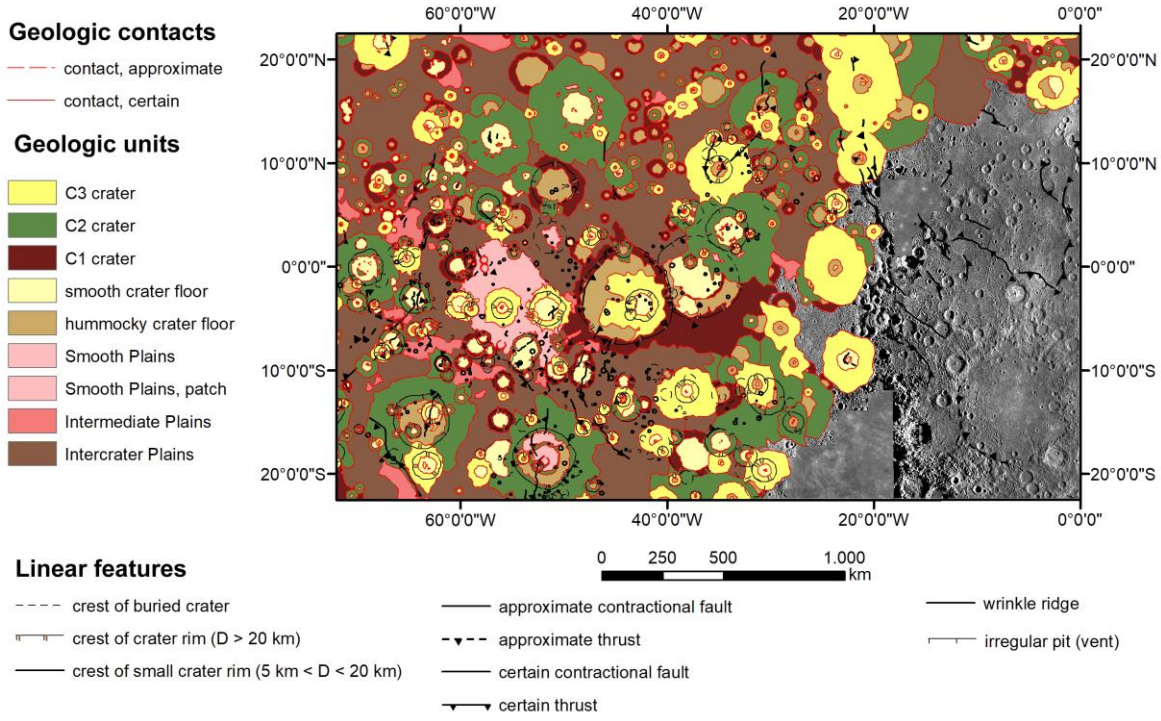

Fig.1 Current status of 1:3M geological map of Kuiper quadrangle (H06), Mercury. The basemap is a BDR mosaic of MESSENGER MDIS.

EPSC Abstracts
Vol. 12, EPSC2018-726, 2018
European Planetary Science Congress 2018

The BepiColombo Radiation Monitor (BERM)

Richard Moissl (1),
(1) European Space Astronomy Centre (ESAC), Madrid, Spain (richard.moissl@esa.int)

Abstract

This paper will present results of the preliminary calibration activities of the BepiColombo Radiation Monitor (BERM) instrument onboard BepiColombo.

Although the Radiation Monitor is not part of the scientific payload, the data from the unit can be used to complement the scientific investigations of the hermean environment. Therefore, the data of the BERM instrument will be archived along with data from scientific measurements. It is foreseen to provide auxiliary data products such as radiation flux rates at detectors and critical electronics of scientific payload onboard BepiColombo.

EPSC Abstracts
Vol. 12, EPSC2018-733, 2018
European Planetary Science Congress 2018

Mid-Infrared Spectroscopy of Planetary Analogs: A Database for Planetary Remote Sensing

Andreas Morlok (1) Stephan Klemme (2) Iris Weber (1) Martin Sohn (3) Aleksandra Stojic (1) Harald Hiesinger (1) Joern Helbert (4)
(1) Institut für Planetologie, Wilhelm-Klemm Strasse 10, 48149, Germany (morlokan@uni-muenster,de) (2) Institut für Mineralogie, Corrensstrasse 24, 48149 Münster (3) Hochschule Emden/Leer, Constantiaplatz 4, 26723 Emden, Germany (4) Institute for Planetary Research, DLR, Rutherfordstrasse 2, 12489 Berlin, Germany

Abstract

As part of an ongoing study, we report mid-infrared spectra of surface analogs for planetary bodies (Venus, Earth) for a database of spectra for planetary remote sensing.

1. Introduction

The IRIS (Infrared and Raman for Interplanetary Spectroscopy) laboratory generates spectra for a database [1] for the ESA/JAXA BepiColombo mission to Mercury. Onboard is a mid-infrared spectrometer (MERTIS-Mercury Radiometer and Thermal Infrared Spectrometer). This unique device allows to map spectral features and thus mineralogy in the 7-14 µm range, with a spatial resolution of about 500 meters [2-4]. Glass can arise through impacts and in volcanic processes and lacks an ordered microstructure and represents the most amorphous phase of a material [5,6]. It is expected to be a major component of the surface of Mercury [7]. Using synthetic materials allows us to produce infrared spectra of materials of which no rock samples are available, or average compositions of larger areas [8]. Here we present analog glass samples for the surfaces of the two largest terrestrial planets, Earth and Venus.

2. Samples & Techniques

Bulk glasses were synthesized based on the chemical composition for the surface of Venus, based on lander data [9],terrestrial MORB basalts [10] and the bulk continental crust [11]. The samples were characterized using Raman spectroscopy and EMPA.

For the mid-infrared FTIR diffuse reflectance analyses, powder size fractions 0-25 µm, 25-63 µm, 63-125 µm, and 125-250 µm were measured, using a Bruker Vertex 70 infrared system at the IRIS laboratories at the Institut für Planetologie in Münster analyses were conducted under low pressure to reduce atmospheric bands. The results will be made available via a database [1].

3. Results

Results of the EMPA analyses are presented in Tab.1. Analogs for Venus surface and MORB show mafic compositions, while the bulk continental crust has a granodioritic composition.

	(1)	(2)	(3)
Na_2O	0.06	2.76	3.1
MgO	11.6	7.9	4.3
SiO_2	50.1	50.2	61.7
Al_2O_3	17.9	15.7	15.2
K_2O	0.05	0.04	1.75
CaO	9.1	11.3	6.0
FeO	9.3	9.4	6.4
TiO_2	1.15	1.42	0.87
Cr_2O_3	0.01	0.01	0.01
MnO	0.02	0.03	0.01
Total	99.29	98.76	99.34

Table 1: EMPA analyses of glasses in the analyzed samples. (1) Venus surface (2) Earth MORB (3) Earth continental crust.

The surface analog of Venus (Fig.1a) shows a typical spectrum of amorphous material with one dominating band at 9.8 – 9.9 µm. The Christiansen Feature (CF), characteristic reflectance low is at 8.1 µm. A Transparency feature (TF) typical for the fine grained size fractions could not be identified. The Raman spectrum confirms this (Fig.1b). Similar, the bulk continental crust and average MORB basalts have spectra of glassy material. The CF is located at 7.9 µm and 8.1 – 8.2 µm, respectively. The dominating amorphous silicate feature is at 9.5 µm (crust) and 10.2 µm. The weak TF is at 11.7 µm (crust) and 11.8 µm (MORB).

4. Discussion

Similar to earlier studies of synthetic glass based on surface areas of Mercury, samples with low MgO content show spectra typical of amorphous materials with only one dominating RB band [8].

5. Summary and Conclusions

Future studies will include a wider range of planetary compositions, as well as crystallization experiments.

Acknowledgements

This work was partly supported by DLR grant 50 QW 1701 in the framework of the BepiColombo mission.

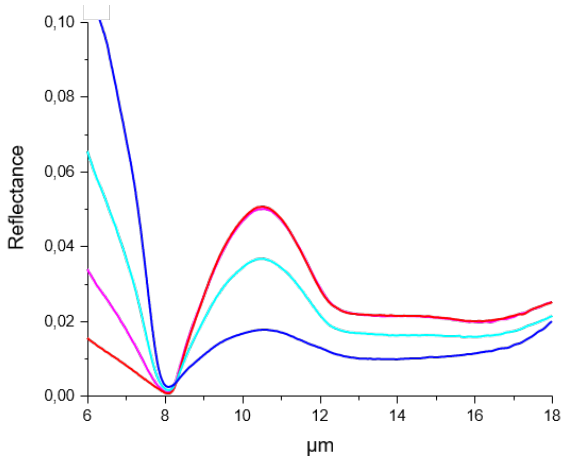

Fig. 1a: Reflectance mid-infrared spectra of surface of Venus, based on Lander data [9].

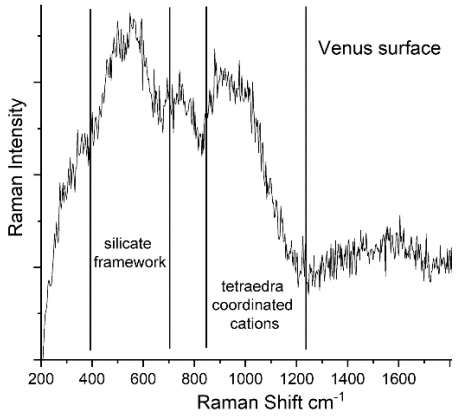

Fig. 1b: Raman spectra of glass in the Venus analog.

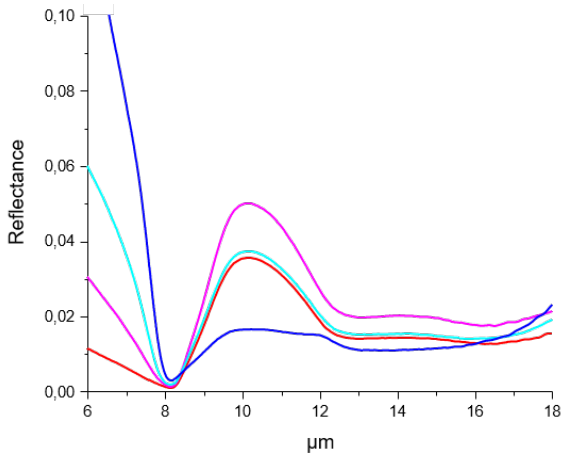

Fig. 2: Reflectance mid-infrared spectra of terrestrial MORB, based on average of several analyses [10].

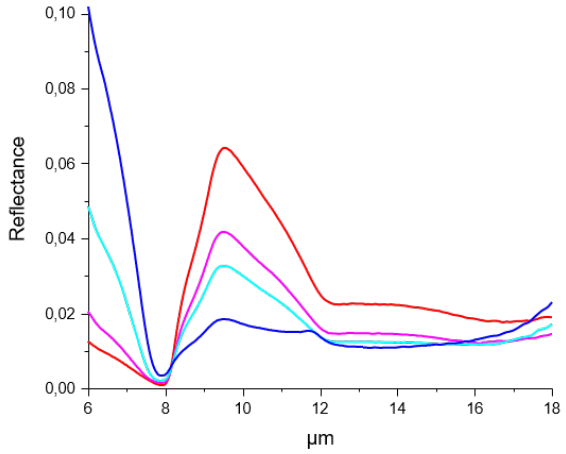

Fig. 3: Reflectance mid-infrared spectra of terrestrial continental crust [11].

References

[1]Weber, I. et al. (2018) 49th LPSC #1430 [2] Maturilli A. (2006) Planetary and Space Science 54, 1057–1064. [2] Helbert J. and Maturilli A. (2009) Earth and Planetary Science Letters 285, 347-354. [3] Benkhoff, J. et al. (2010) Planetary and Space Science 58, 2-20.[4] Hiesinger H. et al. (2010) Planetary and Space Science 58, 144–165. [5] Johnson J.R. (2012) Icarus 221, 359–364 [6] Lee R.J. et al. (2010) Journal of Geophysical Research 115, 1-9 [7] Hörz, H. and Cintala, M. (1997) Met.Plan.Science 32, 179-209 [8] Morlok, A. et al. (2017) Icarus 296, 123-138 [9] Fegley, B. et al. (2006) Treatise on Geochemistry, Vol.I, 487- 507 [10] Klein, E.M. (2003) Treatise on Geochemistry Vol.III, 433-463 [11] Rudnik R.L. (2003) Treatise on Geochemistry Vol.III, 1-64

EPSC Abstracts
Vol. 12, EPSC2018-736-1, 2018
European Planetary Science Congress 2018

Deconvolution of Mid-Infrared Telescope Spectra of Mercury using Machine Learning: Supporting MERTIS onboard ESA/JAXA BepiColombo mission

Indhu Varatharajan (1), Mario D'Amore (1), Alessandro Maturilli (1), Jörn Helbert (1), Harald Hiesinger (2)
(1) Institute for Planetary Research, German Aerospace Center DLR, 12489 Berlin, Germany (indhu.varatharajan@dlr.de), (2) Institute of Planetology, Wilhelm-Klemm-Str. 10, 48149 Münster, Germany

Abstract

The Mercury Radiometer and Thermal Imaging Spectrometer (MERTIS), onboard the ESA/JAXA BepiColombo mission to Mercury, will map the thermal emissivity at wavelength range of 7-14 µm (mid-infrared; MIR) and a spatial resolution of 500 m/pixel [1].

Mercury has been studied via MIR spectroscopy from ground/telescopic observations over three decades [2-8]. However, the total number of observations made is still quite small (Fig. 1). Over the past decade, the Planetary Spectroscopy Laboratory (PSL) at German Aerospace Center (DLR) Berlin obtained experimentally thermal emissivity measurements of analog materials under controlled and simulated surface conditions of Mercury from 100° to 500°C under vacuum conditions in support of MERTIS (Fig. 2) [9]. Using a specialized endmember spectral library created under Mercury's conditions will increase significantly the accuracy of the deconvolution model results of not only MERTIS but also telescopic observations of Mercury.

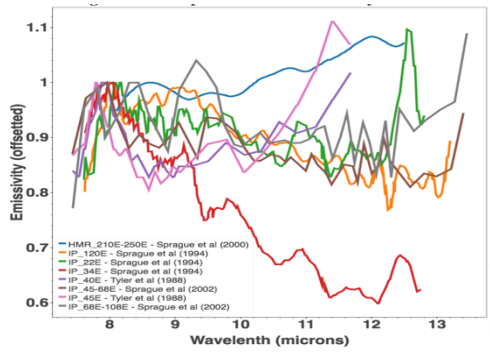

Figure 1: Published telescope spectra [3-8], digitised by the author [12].

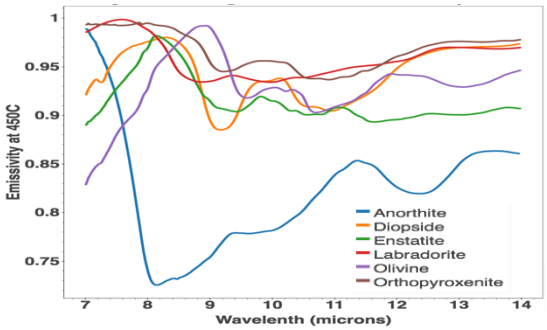

Figure 2: MIR spectra of analogue minerals under simulated conditions of Mercury at PSL.

1. Introduction

Spectroscopy is powerful technique to study the surface mineralogy of any planetary body from its orbit. By carefully understanding the spectral behavior of various planetary analogues in laboratory experiments at the planetary surface and environmental conditions, the mineral abundance and distribution globally can be mapped from orbit.

1.1 Challenges in Spectroscopy

Many factors influence the spectral behavior of a planetary surface such as grain size, phase angle of observation, slope, and abundance of the mineral. Though these factors affecting the spectra can be understood in a controlled environment, the real challenge comes in understanding the remote sensing spectra and can be split in two main parts: 1. spectral behavior of minerals in their related planetary environment, 2. understanding the mixture spectra from mineral assemblages.

2. Methods

In this study, we revisited the available telescope spectra and adapted the algorithm by [10,11] by only choosing the endmember spectral library created at PSL for unbiased model accuracy. The unmixing algorithm is based on a least square inversion of the system, Y = AX, where Y is a vector containing the telescope spectrum, A is a NxM matrix filled with the endmembers spectra (N) number of endmembers and M is a the number of spectral channels), and X is a vector containing the coefficients of each components of the input library. The solution of this linear system is given by,

$$X = (A^T A)^{-1} A^T Y \quad (1)$$

As we have a large endmember library, the selection of set of endmembers (A) is carried out by systematic exploration of whole set of combinations of four components, i.e., ${}^{N}C_4$ = N!/(4! x (N-4)!). The final accuracy of the linear fit is evaluated by computing the χ^2 residuals between the model and the data and the endmember combination giving the minimum χ^2 is the best fit to the telescope spectra. This spectral unmixing method is successfully tested on the powdered samples which include endmembers and their mixed proportion, see Fig. 3.

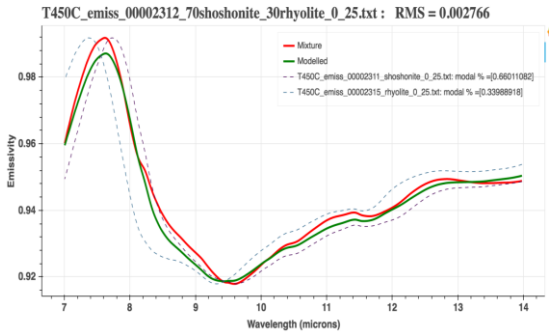

Figure 3: Linear unmixing algorithm is applied to laboratory sepctra of the mixture (solid red) containing 70% shoshonite and 30% rhyolite; and the resulting modelled spectra (green spectra) estimates to 66% shoshonite and 34 % rhyolite with RMS of 0.003.

3. On-going work

Comparison of different spectral unmixing algorithms (Monte Carlo – Bayesian algorithm, and genetic algorithm) is being tested to increase the confidence of unmixing results of the endmember counterparts.

References

[1] Hiesinger, H. and J. Helbert, The Mercury Radiometer and Thermal Infrared Spectrometer (MERTIS) for the BepiColombo mission, PSS, Vol. 58(1-2): pp. 144-165, 2010

[2] Sprague, A.L. et al: Spectral emissivity measurements of Mercury's surface indicate Mg- and Ca-rich mineralogy, K-spar, Na-rich plagioclase, rutile, with possible perovskite, and garnet, PSS, Vol. 57, pp. 364-383, 2009.

[3] Sprague, A.L. et al: Mid-Infrared (8.1–12.5 μm) Imaging of Mercury, Icarus, Vol. 147(2), pp. 421-432, 2000.

[4] Sprague, A.L. et al (2002) Mercury: Mid‐infrared (3‐13.5 microns) observations show heterogeneous composition, presence of intermediate and basic soil types, and pyroxene, MAPS Vol. 37(9), pp. 1255-1268, 2002.

[5] Sprague, A.L. et al: Mercury: Evidence for Anorthosite and Basalt from Mid-infrared (7.3-13.5 μm) Spectroscopy, Icarus, Vol. 109(1), pp. 156-16, 1994.

[6] Sprague, A.L. et al: Mercury's feldspar connection mid-ir measurements suggest plagioclase, Vol. 19(10), pp. 1507-1510, 1997.

[7] Sprague, A.L. et al: Comparison of Laboratory Emission Spectra with Mercury Telescopic Data, Icarus, Vol. 133(2), pp. 174-183, 1998.

[8] Tyler et al: Determination of rock type on Mercury and the Moon through remote sensing in the thermal infrared, GRL Vol. 15(8), pp. 808-811, 1988.

[9] Maturilli, A., et al.: Emissivity Spectra of Analogue Materials at Mercury P-T Conditions, in 48th Lunar and Planetary Science Conference, p. 1427, 2017.

[10] Ramsey and Christiansen, Mineral abundance determination: Quantitative deconvolution of thermal emission spectra, JGR, Vol. 103, pp. 577-596, 1998.

[11] Combe J.-Ph. et al: Analysis of OMEGA/Mars Express data hyperspectral data using a Multiple-Endmember Linear Spectral Unmixing Model (MELSUM): Methodology and first results, PSS, Vol. 56, pp. 951-975, 2008.

[12] A. Rohatgi, https://automeris.io/WebPlotDigitizer , 2018

EPSC Abstracts
Vol. 12, EPSC2018-763-1, 2018
European Planetary Science Congress 2018

Bi-directional reflectance and NanoFTIR spectroscopy of synthetic analogues of Mercury: Supporting MERTIS payload of ESA/JAXA BepiColombo mission

Indhu Varatharajan (1), Alessandro Maturilli (1), Jörn Helbert (1), Georg Ulrich (2), Kirsten Born (3), Olivier Namur (4), Bernd Kästner (2), Lutz Hecht (3), Bernard Charlier (5), Harald Hiesinger (6)
(1) Institute of Planetary Research, German Aerospace Center (DLR), Rutherfordstr 2, 12489 Berlin, Germany (indhu.varatharajan@dlr.de), (2) Physikalisch-Technische Bundesanstalt (PTB), Abbestr. 2-12, 12489 Berlin, Germany, (3) Museum für Naturkunde (MfN), Invalidenstr 43, 10115 Berlin, Germany, (4) Department of Earth and Environmental Sciences, KU Leuven, 3001 Leuven, Belgium, (5) University of Liege, Department of Geology, 4000 Sart-Tilman, Belgium, (6) Institut für Planetologie, Wilhelm-Klemm Strasse 10, 48149 Münster, Germany.

1. Introduction

The mid infrared (MIR) spectral region is especially sensitive to the abundance of Si-O abundance, unlike the visible-near infrared spectral region. Though the geochemical suite on the NASA MESSENGER spacecraft to Mercury revealed compositionally diverse crustal materials [eg., 1], the spectrometer suite (MASCS; VIS-IR) could not reveal the silicate mineralogy of crustal materials due to the Fe2+-poor nature of the silicate minerals on the surface of Mercury. The Mercury Radiometer and Thermal Imaging Spectrometer (MERTIS) as part of the payload of the ESA/JAXA BepiColombo mission will map the surface mineralogy globally in the thermal IR wavelength range (7-14 μm) at spatial resolution of 500 m/pixel [2].

In this study, we investigated the experimental products by [3] which represent major terranes namely the low-Mg Northern Volcanic Plains (NP-LMg), high-Mg Northern Volcanic Plains (NP-HMg), Intercrater Terrane (ICT), High-Mg Province (HMR), and Smooth Plains (SP) of Mercury. These experimental products are 5 x 5 mm^2 in area containing major minerals including forsterite, diopside, enstatite, plagioclase, and locally FeSi. Therefore, studying the spectra of bulk sample and the spectra of each mineral phases in these samples will cast a new light on understanding the spectral behaviour of the silicate mineralogy of Mercury.

2. Facilities and Methods

The study consists of three parts in which we obtain; 1. Bulk spectra of the samples (DLR-PSL), 2. High resolution elemental mapping of the samples for all terrains (MfN-SEM), 3. Nano-FTIR spectra of each mineral units (PTB-NanoFTIR).

2.1 Bulk spectra of the samples

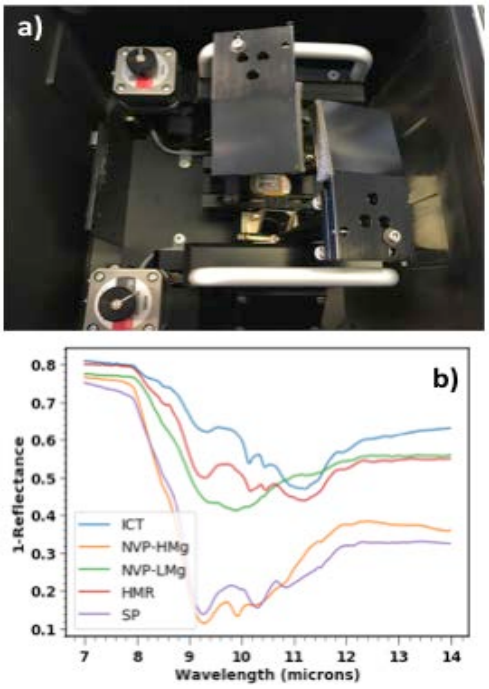

Figure 1: a) the bi-directional reflectance set-up at PSL, b) the bulk reflectance of the experimental products representing the geochemical terranes of Mercury – showing distinct spectral behavior.

Bulk bi-directional reflectance spectra of these experimental products representing Mercury terrains

are measured in IR range (1-25 µm) using a Bruker Vertex 80V at the spectral resolution of 4 cm^{-1} with the smallest aperture of 0.25 mm diameter [4-5] at PSL. The bi-directional reflectance setup is shown in Fig. 1a and the results are shown in Fig. 1b.

2.2 High-resolution elemental mapping

In order to navigate the very high resolution (nano-FTIR) spectroscopy, we first obtained the high resolution elemental composition map (Fig. 3a) of all the samples using the Secondary Electron Microscope (SEM) facility at the Museum für Naturkunde in Berlin.

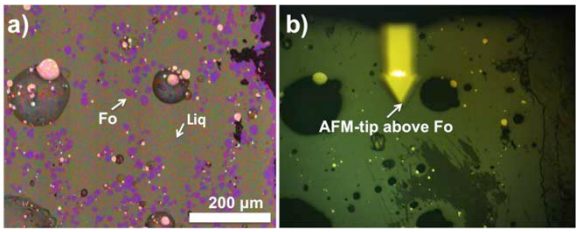

Figure 3: Sample Y0128-HMg containing 32% Forsterite (Fo). a) SEM image where pink units are Fo; b) nano-FTIR setup where cantilever tip pointing to Fo.

2.3 NanoFTIR spectra of mineral units within the sample

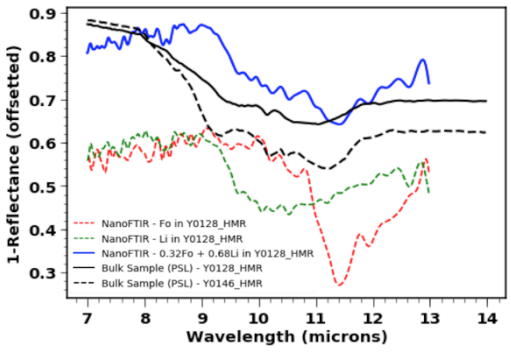

Figure 4: showing the NanoFTIR spectra of Forsterite (dashed red) and liquid/melt (dashed green); solid black is the bulk spectra of sample (shown in Fig. 3) containing 32% Fo and 68 % liquid - the linearly mixed NanoFTIR spectra using the corresponding endmembers (Fo, Li) is shown as solid blue spectra.

The use of broadband synchrotron radiation from IR-beamline of the electron storage ring (Metrology Light Source; MLS) at PTB-Berlin allows us to perform nano-FTIR (nanoscale) spectroscopy on these experimental products using a Neaspec scattering-type scanning near-field optical microscope (s-SNOM) [5-6] (Fig. 3b). This metallic probe acts as an antenna which confines the incident electric field around the tip-apex thus providing a nanoscale light source for very high-resolution imaging. Using this facility, we obtained the spectra of each mineral units guided by SEM images of the samples at the spatial resolution of <40nm for the spectral range of 5-12µm with the spectral resolution of 6.25cm^{-1}(Fig. 4).

3. Ongoing Work

Nano-FTIR spectra obtained for all terrain samples are currently being analyzed for its silicates. The spectral deconvolution algorithm will be tested on bulk spectra obtained at PSL using the endmember nano-FTIR silicate spectra. All the results will be presented at the conference.

References

[1] Vander Kaaden, K et al: Geochemistry, mineralogy, and petrology of boninitic and komatiitic rocks on the mercurian surface: Insights into the mercurian mantle, Icarus, 285, 155-168, 2017

[2] Hiesinger, H. and J. Helbert, The Mercury Radiometer and Thermal Infrared Spectrometer (MERTIS) for the BepiColombo mission, PSS, Vol. 58(1-2): pp. 144-165, 2010

[3] Namur, O. and Charlier, B. Silicate mineralogy at the surface of Mercury, *NatGeo*, Vol. 10, pp. 9–13, 2017.

[4] Maturilli, A., et al.: Emissivity Spectra of Analogue Materials at Mercury P-T Conditions, in 48th Lunar and Planetary Science Conference, p. 1427, 2017.

[5] Hermann, P. et al. Near-field imaging and nano-Fourier-transform infrared spectroscopy using broadband synchrotron radiation, *Optic Express*, 21, p.2913, 2013.

[6] Hermann, P. et al: Enhancing the sensitivity of nano-FTIR spectroscopy, *Optic Express*, 25, 16574-16587, 2017.

EPSC Abstracts
Vol. 12, EPSC2018-850, 2018
European Planetary Science Congress 2018

Spectral and lithological heterogeneities in the Shakespeare (H-03) quadrangle of Mercury

N. Bott (1), A. Doressoundiram (1), D. Perna (1,2), F. Zambon (3), C. Carli (3) and F. Capaccioni (3)
(1) LESIA - Observatoire de Paris - CNRS - Sorbonne Université - Université Paris-Diderot, 5 place Jules Janssen, 92195 Meudon, France, (2) Osservatorio Astronomico di Roma - INAF, Monte Porzio Catone, Italy, (3) Istituto di Astrofisica e Planetologia Spaziali - INAF, Roma, Italy (nicolas.Bott@obspm.fr)

Abstract

We analysed the spectral properties of the surface of Mercury in the H-03 quadrangle to define its compositional variability and identify units constrained by relevant spectral parameters.

1. Introduction

Mercury mapping campaign started to support the observational strategy of the SYMBIO-SYS instrument onboard the future BepiColombo spacecraft. A goal is to integrate the color variations due to differences in composition to the photo-interpreted geology of the innermost planet. The used data are image mosaics from the Mercury Dual Imaging System (MDIS) Wide Angle Camera (WAC) onboard MESSENGER spacecraft. Authors identified three major color units (high-reflectance plains, intermediate terrains and low-reflectance material) and two minor color units (red spots and hollows) [1].

2. Data set

The surface of Mercury is subdivided into 15 quadrangles. Some have already been mapped [2,3], others are in progress [4]. Here we focus on the H-03 quadrangle, Shakespeare, with 22.5° < latitude < 65° and 180° < longitude < 270°. We used the data of the 8 following filters: 433.2, 479.9, 558.9, 628.8, 748.7, 828.4, 898.8 and 996.2 nm. The other filters (698.8, 947.0 and 1012.6 nm) are used because they can not ensure the coverage of the quadrangle.

3. Method

To produce the color map, we used the software ISIS (USGS) and proceeded as follows: 1) Importation of raw data into ISIS (Integrated Software for Imagers and Spectrometers) format; 2) Georeferencing using SPICE kernels and a DEM of Shakespeare produced at DLR [5]; 3) Radiometric calibration; 4) Equirectangular projection; 5) Kaasalainen-Shkuratov photometric correction [6, Table 9] to report the data at standard illumination conditions (incidence i=30°, emission e=0°); 6) Coregistration of images to obtain the mosaic of Shakespeare.

4. Results

4.1 Color mapping

We applied techniques of image analysis, such as RGB color combinations (Figure 1) and Principal Component Analysis [7], to emphasize differences in spectral properties which can be correlated to differences in composition. We will expose and discuss the last updates.

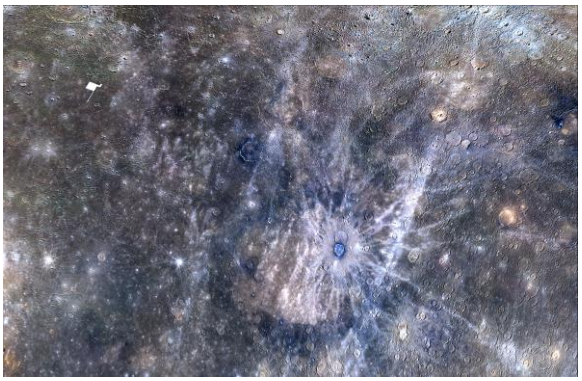

Fig. 1. RGB map of the Shakespeare quadrangle (R= 996.2 nm, G=748.7 nm and B=433.2 nm)

4.2 Spectral mapping

From the global 8-color mapping, it is possible to infer interesting spectral parameters to identify units associated to specific terrains. Considering a thresholding of the values of a spectral parameters

(reflectance at 750 nm, PC2...), we obtained indications of units, showing different terrains with probable differences in composition (Figure 2).

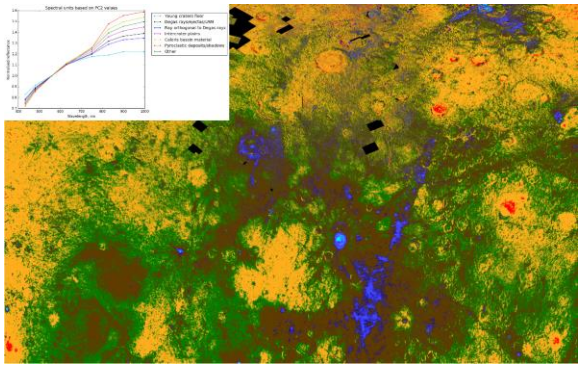

Fig. 2. Example of spectral parameter map of the Shakespeare quadrangle using a thresholding of PC2 values.

For example, it appears on the above spectral map that the floor of Degas crater (cyan) is clearly distinct from other terrains (Sobkou planitia, in yellow on the left) in term of values of PC2. As PC2 highlights the spectral slope variations, this means that the floor of this young crater has a spectral slope distinct from the rest of the quadrangle. This is confirmed on the plot of the averaged spectra of each unit defined by the threshold of this parameter (embedded graph, Figure 2). More analyses of spectral parameters will be presented.

5. Future works

This work on spectral properties of the surface material present in the Shakespeare quadrangle will be integrated to the geological map of the Shakespeare quadrangle produced by [8], and aims to define higher level units to produce a more accurate map of this quadrangle.

Acknowledgements

This work is partly supported by the Centre National d'Etudes Spatiales. D. Perna received funding from the European Union's Horizon 2020 research and innovation program under the Marie Sklodowska-Curie grant agreement n.664931.

References

[1] Blewett, D. T. et al.: Multispectral images of Mercury from the first MESSENGER flyby: Analysis of global and regional color trends, Earth and Planetary Science Letters, Vol. 285, pp. 272-282, 2009.

[2] Galluzzi, V. et al.: Geology of the Victoria quadrangle (H02), Mercury, Journal of Maps, Vol. 12, pp. 227-238, 2016.

[3] Zambon, F. et al.: Mercury compositional units inferred by MDIS. A comparison with the geology in support to the BepiColombo mission, Geophysical Research Abstracts, Vol. 18, EGU2016-16909, 2016.

[4] Giacomini, L. et al.: Geological mapping of the Kuiper quadrangle (H06) of Mercury, Geophysical Research Abstracts, Vol. 19, EGU2017-14574, 2017.

[5] Preusker, F. et al.: High-Resolution Topography from MESSENGER Orbital Stereo Imaging - The H3 Quadrangle "Shakespeare", LPS XLVIII, abstract #1441, 2017.

[6] Domingue, D. L. et al.: Application of multiple photometric models to disk-resolved measurements of Mercury's surface: Insights into Mercury's regolith characteristics, Icarus, Vol. 268, pp. 172-203.

[5] Denevi, B. W. et al.: The Evolution of Mercury's Crust: A Global Perspective from MESSENGER, Science, Vol. 324, pp. 613-618, 2009.

[7] Guzzetta, L. et al.: Geology of the Shakespeare quadrangle (H03), Mercury, Journal of Maps, Vol. 13, pp. 227-238, 2017.

EPSC Abstracts
Vol. 12, EPSC2018-868, 2018
European Planetary Science Congress 2018

Remote Sensing of Planetary Surfaces: Spectroscopy of Planetary Analogs for the BepiColombo Mission

Andreas Morlok (1) Bernard Charlier (2) Stephan Klemme (3) Olivier Namur (4) Martin Sohn (5) Iris Weber (1) Aleksandra Stojic (1) Harald Hiesinger (1) Joern Helbert (6)
(1) Institut für Planetologie, Wilhelm-Klemm Strasse 10, 48149, Germany (morlokan@uni-muenster.de) (2) University of Liege, Department of Geology, 4000 Sart-Tilman, Belgium, (3)Institut für Mineralogie, Corrensstrasse 24, 48149 Münster (4) Department of Earth and Environmental Sciences, KU Leuven, 3001 Leuven, Belgium (5) Hochschule Emden/Leer, Constantiaplatz 4, 26723 Emden, Germany (6) Institute for Planetary Research, DLR, Rutherfordstrasse 2, 12489 Berlin, Germany.

Abstract

We present mid-infrared spectra bulk powders and from in-situ studies of surface analogues for Mercury synthesized based on remote sensing data from MESSENGER.

1. Introduction

The IRIS (Infrared and Raman for Interplanetary Spectroscopy) laboratory generates spectra for the ESA/JAXA BepiColombo mission to Mercury. Onboard is MERTIS (Mercury Radiometer and Thermal Infrared Spectrometer), which allows to map spectral features in the 7-14 µm range, with a spatial resolution of about 500 meters [1-5]. Glass, which can form in impacts and in volcanic processes, lacks an ordered microstructure and represents the most amorphous phase of a material. It forms in events typical for the formation of the surface of Mercury [5-7]. Using synthetic analogs based on the observed chemical composition of planetary bodies allows us to produce infrared spectra of bodies from which no material in form of meteorites is available so far [8]. In this study, we present synthetic analogues for surface regions of Mercury based on results of the MESSENGER mission [9], and petrological experiments and modelling [10-12].

2. Samples & Techniques

Bulk glasses were synthesized based on the chemical composition for surface areas on Mercury from the MESSENGER X-ray spectrometer data [9], following a procedure described in [8]. Further glassy and crystalline analogue material was produced in petrological experiments simulating the petrologic evolution of early Mercurian magmas under controlled temperatures, pressures and oxidation states [10-12]. For this presentation, we selected spectra from the high-Mg NVP (Northern Volcanic Plains) region (Fig.1), produced at 0.1 GPa and 1210°C [10-12]. For the FTIR diffuse reflectance analyses, powder size fractions 0-25 µm, 25-63 µm, 63-125 µm, and 125-250 µm were measured from 2-18 µm. We used a Bruker Vertex 70 infrared system with a MCT detector at the IRIS laboratories at the Institut für Planetologie in Münster. Analyses were conducted under low pressure to reduce atmospheric bands. Additional FTIR microscope analyses of polished thick sections were made from the experimental runs with a Bruker Hyperion 2000 System at the Hochschule Emden/Leer. A 250×250µm sized aperture was used for all analyses.

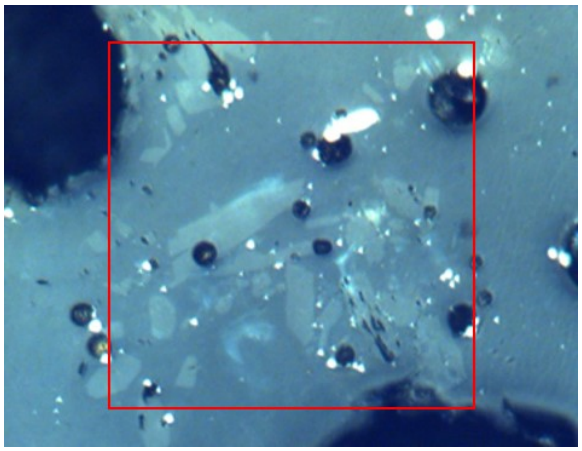

Fig.1. Optical images of the high-Mg glass sample with the composition of the Northern Volcanic Plains area. The bright parts are crystalline phases, the

darker parts are glass. The red box marks the aperture of 256×256 µm.

3. Results

The spectra of the surface regolith exhibit a strong, dominating feature at 9.8 µm, typical for glassy material (Fig.2) [8]. Two important additional characteristic bands for remote sensing, the Christiansen feature (CF; the position of lowest reflectance), and the Transparency Feature (TF; characteristic of the finest grain size fraction) are located at 8.0 µm and at 11.9 µm, respectively. The micro-FTIR analyses of the experimental sample analogs for the high-Mg NVP (Fig.3) show strong crystalline features at 9.3 µm, 9.9 µm, 10.4 µm and 11.6 µm, with minor features at 13.8 µm and 14.7 µm. The CF is at 8.1 µm, enstatite features mixed with diopside bands [13]. The spectra of glassy material is similar to the glass with the regolith composition, with a single strong band at 9.7 µm and a CF at 7.9 µm.

4. Discussion & Conclusions

Results of our ongoing study of analogue materials for the surface of Mercury show consistent spectral features for the glass and the crystalline components in relation to its chemical composition. First in-situ micro-FTIR studies of crystalline phases show a variety of pyroxene bands. These confirm earlier micro-analytical studies of the samples [10]. Future analyses will cover a wider range of bulk samples for the surface of the planet, as well as more detailed in situ studies of the phases formed in the petrological experiments under various temperature and pressure regimes. The results will be made available via a database [1].

References

[1] Weber I. et al. (2018) 49th LPSC Abstract #1430 [2] Maturili A. (2006) Planetary and Space Science 54, 1057–1064 [3] Helbert J. and Maturilli A. (2009) Earth and Planetary Science Letters 285, 347-354 [4] Benkhoff J. et al. (2010) Planetary and Space Science 58, 2-20 [5] Hiesinger H. et al. (2010) Planetary and Space Science 58, 144–165 [6] Johnson J.R. (2012) Icarus 221, 359–364 [7] Lee R.J. et al. (2010) Journal of Geophysical Research 115, 1-9 [8] Morlok A. et al. (2017) Icarus 296, 123-138 [9] Weider S.Z. et al. Earth and Planetary Science Letters 416, 109-120 [10] Namur O. and Charlier B. (2017) Nature Geoscience 10, 9-15 [11] Namur O. et al. (2016) Earth and Planetary Science Letters 448, 102-114 [12] Namur O. et al. (2016) Earth and Planetary Science Letters 439, 117-128 [13] Hamilton V. (2000) Journal of Geophysical Research, 105, 9701-9715

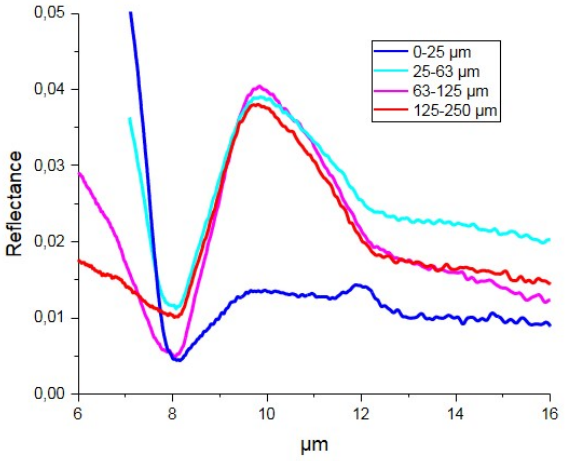

Fig.2: Mid-infrared reflectance spectra of powdered bulk glass with a composition analogue to surface regolith from Mercury [9]. The features are typical for amorphous materials, showing a featureless strong band in this region [8].

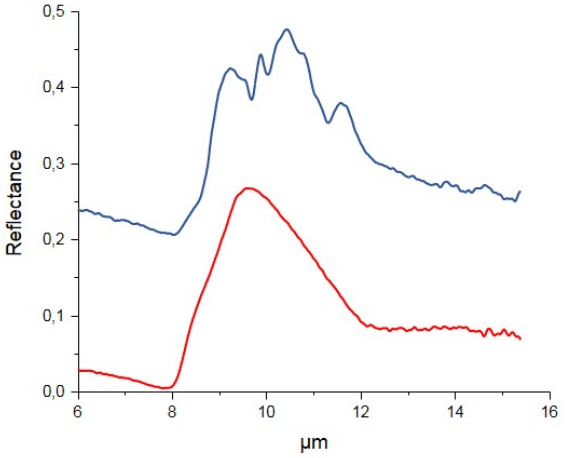

Fig.3: Micro-FTIR analyses of High-Mg Northern Volcanic Plains region (Fig.1). Blue: crystalline phases, red: glass.

Acknowledgements

This work was partly supported by DLR grant 50 QW 1701 in the framework of the BepiColombo mission. Also many thanks to Isabelle Dittmar (Emden) for helping with the micro-FTIR.

EPSC Abstracts
Vol. 12, EPSC2018-870, 2018
European Planetary Science Congress 2018

Investigating X-ray fluorescence from the surface of Mercury using MIXS

Rose Cooper (1), Manuel Gande (1), Emma Bunce (2), Adrian Martindale (2)
(1) Aberystwyth University, UK (roc17@aber.ac.uk), (2) University of Leicester, UK

Abstract

We present a model for the expected fluorescence from the exosphere and surface of Mercury, as observed by the Mercury Imaging X-ray Spectrometer (MIXS) on the upcoming BepiColombo mission. Using modified SMART-1 D-CIXS analysis routines for Lunar observations, we model the fluorescence spectra from the surface of Mercury, and compare the different surface regions. Observations of the boundaries between these regions are also conducted. X-ray fluorescence also occurs on the night side of Mercury through particle induced X-ray events (PIXE). We also model the expected fluorescence observable from this region, and consider its connection to the exosphere through surface-exosphere coupling.

1. Introduction

X-ray fluorescence is typically considered to be a laboratory technique, yet has been found to have numerous uses in planetary science. Due to the high solar flux at Mercury, it is considered a prime target for using this method for elemental abundance detection. The main focus of this work is the MIXS detectors on the BepiColumbo Mission, which is due to launch in October 2018. MIXS is comprised of two detectors, a collimated channel MIXS-C and a telescope MIXS-T [1]. Their primary aim is to measure surface elemental abundances. MESSENGER has revealed a lot more information about the geochemical composition of Mercury's, which BepiColombo will build upon.

1.1 Fluorescence model

The model used for this work was originally designed for D-C1XS on the SMART-1 Lunar mission [2], and has been adapted for this new purpose. As the fluorescence calculations originally used will still be correct [3], they require no changes. The alterations required focus mainly on the elemental abundances, proximity to the Sun, and increased solar flux.

2. Surface Fluorescence

Using surface elemental abundances from Wurz et al., (2010) we can produce fluorescence spectra for both MIXS-C and MIXT-T for a range of solar flare intensities. These can be seen in Figures 1 and 2 below.

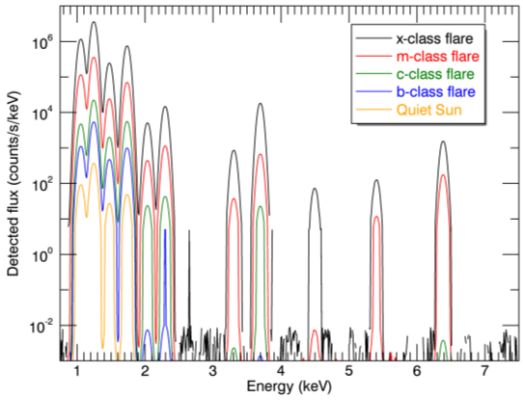

Figure 1: X-ray fluorescence spectra for Mercury's surface seen by MIXS-C during a 209s observation.

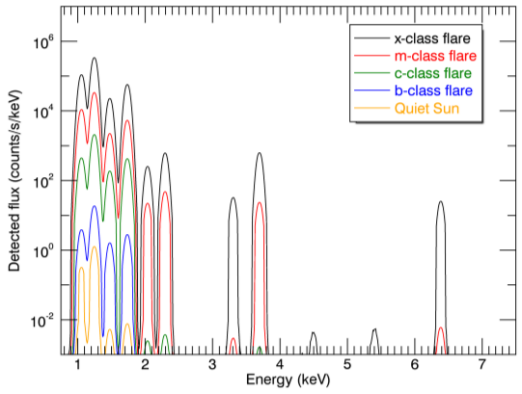

Figure 2: X-ray fluorescence spectra for Mercury's surface seen by MIXS-T during a 22.9s observation.

As the fluorescence spectra obtained by MIXS will be dependent on the composition of the region it is observing, it is possible to identify certain geochemical regions based on the spectra observed. Using the surface abundances from Lawrence et al., (2016), variations in the peak intensities of the lighter elements such as sodium, magnesium, silicon and aluminium can be detected. These are shown in Figure 3 for MIXS-C (a-c) and MIXS-T (d-f).

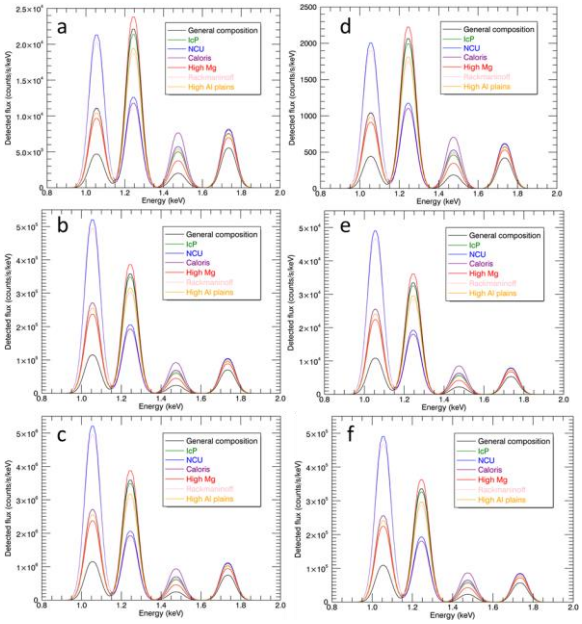

Figure 3: X-ray fluorescence spectra seen by MIXS-C (a-c) and MIXS-T (d-f) for multiple surface regions over a 10 minute observation time for: a/d) C-class flare, b/e) M-class flare, and c/f) X-class flare.

It is worth noting that some elements produce higher intensity fluorescence for a lower class flare, which will have an impact on potential observations. Following this it is also possible to observe the boundary regions between the different geochemical terranes and therefore aid in the general understanding of the geological history and development of Mercury.

3. PIXE events / Surface-Exosphere coupling

On the dayside the fluorescence is caused by solar X-rays interacting the atoms in the surface regolith. However fluorescence is also observed on the nightside of Mercury, thought to be caused by electrons precipitating onto the surface. Due to the location of the PIXE events and their connection to the cusp regions of Mercury's magnetic field, it is possible to also investigate the relationship between the surface and exosphere of Mercury. In particular there are regions of the surface which have a very high abundance of certain elements (e.g. the high Mg region in the northern plains). The model presented investigates the connection between the surface and exosphere to develop our understanding of the coupling mechanisms.

4. Summary and Conclusions

We have developed a program to model the expected fluorescence observations of Mercury's surface capable by the MIXS detector on BepiColombo. We obtain expected fluorescence spectra expected during MPO's orbit, including spectra of different geochemical terranes. X-ray fluorescence is also possible on the night side of Mercury through particle induced X-ray events. Observations of these can also be made with MIXS, which due to their location on the planet's surface can provide information regarding surface-exosphere coupling dynamics.

Acknowledgements

The authors would like to thank Adrian Martindale and the members of the Leicester University space research center for access to the MIXS grasp data, and the author of the original model Bruce Swinyard. Additional thanks to Joseph Hutton for assistance with writing the code.

References

[1] Fraser, G. W. et al: The Mercury Imaging X-ray Spectrometer (MIXS) on BepiColumbo, Planetary and Space Science, Vol. 58, pp. 79-95, 2010

[2] Grande, M. et al: The D_CIXS X-ray mapping spectrometer on SMART-1, Planetary and Space Science, Vol. 51, pp. 427-433, 2003

[3] Clark, P. E. & Trombka, J. I.: Remote X-ray spectrometer for Near and future missions: Modeling and analyzing X-ray production from source to surface, Journal of Geophysical Research, Vol. 102, pp. 16,361-16,384, 1997

EPSC Abstracts
Vol. 12, EPSC2018-890, 2018
European Planetary Science Congress 2018

Mercury's Rotational State from self-registration of Mercury Laser Altimeter profiles

Alexander Stark (1), Jürgen Oberst (1,2), Hauke Hussmann (1) and Gregor Steinbrügge (1,3)
(1) German Aerospace Center (DLR), Berlin, Germany (alexander.stark@dlr.de) (2) Institute of Geodesy and Geoinformation Science, Technische Universität Berlin, Germany (3) Institute for Geophysics, University of Texas at Austin, Austin, TX, USA

Abstract

We use Mercury Laser Altimeter (MLA) data to measure Mercury's rotational state. In four years of orbital observations MLA onboard the MErcury Surface, Space ENvironment, GEochemistry, and Ranging (MESSNEGER) spacecraft provided 3226 topographic profiles of Mercury. Counting in total more than 22 million precise range measurements this dataset represents a valuable source for the measurement of Mercury's rotational state. Indeed, Mercury's obliquity and libration amplitude represent critical constraints for models of its interior.

1. Introduction

Mercury exhibits a unique rotation state. Its rotation is tidally coupled to its orbit in a 3:2 resonance. As Mercury's mantel is decoupled from the molten outer core forced longitudinal librations, i.e. small periodic changes in the rotation rate, are observed [1,2,3]. Furthermore, driven by tidal forces the rotation axis of Mercury occupies a Cassini state, i.e. an equilibrium configuration of rotation axis with the orbital plane normal and Laplace plane normal. Both the obliquity and libration amplitude comprise information about the moments of inertia of the planet. Combined with low degree and order spherical harmonics coefficients of Mercury's gravity field one can infer the depth of the core-mantle boundary and the densities of the mantel and core.

In a recent work Mercury's rotation was measured using co-registration of MLA profiles and digital terrain models (DTMs) derived from images using stereo photogrammetry [3]. Due to the limited coverage provided by the stereo DTMs the authors have used only 50% of the MLA measurements distributed over three years of MESSENGER orbital observations. Nonetheless, Mercury's mean rotation rate, obliquity, and the libration amplitude could be determined through precise co-registration of the two complementary topographic data sets.

2. Data

The MESSENGER spacecraft orbited Mercury from March 2011 to April 2015. On its eccentric near-polar orbit the range to the surface of Mercury typically varied from about 200 km up to 15,200 km. With the pericenter located at high northern latitudes the coverage with MLA profiles is limited to the northern hemisphere of Mercury. However, at the polar region where all profiles intersect the density of MLA footprints, usually separated by about 400 m, becomes very large and allows the compilation of an accurate DTM with resolutions of a few hundred meters.

3. Method

In this work we exploit the idea of the co-registration method and perform a "self-registration" of the MLA profiles. In contrast to the co-registration approach where two data sets originate from different instruments, the self-registration approach comprises the registration of one data set to itself. In order to measure Mercury's rotational state we construct a precise, internally consistent DTM of Mercury using the self-registration approach. This reference DTM subsequently serves for the measurement of Mercury's rotational state. We focus on the high northern latitudes where the density of MLA footprints allows the construction of a DTM with a pixel resolution of 222 m. To remove the MLA profiles from residual errors in spacecraft orbit and pointing, as well as Mercury rotation, we iteratively select a random subset of MLA profiles (typically 25%) and co-register them to a DTM constructed from the remaining profiles. Thereby, we allow maximal flexibility in the co-registration parameters in order to achieve maximal compensation of all

lateral offsets between the profiles. After about 50 iterations all profiles are removed from false detections, i.e. noise considered as valid range measurements, and positioned consistently to other profiles. With the reference DTM we can now take the initial (uncorrected) laser profiles and explicitly solve for the rotational state of Mercury. In fact, as each profile was obtained within a relatively short time period (a few minutes) we can solve for the instantaneous orientation of Mercury at the observation time of the profile. By analysis of sets of profiles taken over longer time we may carry out a precise tracking of Mercury's rotation. Moreover, the procedure permits validation of the assumed rotational models, which typically is not feasible in a least-squares adjustment.

4. Discussion and Outlook

The self-registration technique is similar to the more common cross-over adjustment, where height differences of intersecting profiles are used as observables [4,5,6]. However, typical issues arising in the usage of the cross-overs are resolved in the self-registration approach. For instance, the interpolation errors due to large separation of laser footprints typically diminish the accuracy of the cross-over observables. Indeed, while the cross-over observables are determined by four footprints, in the self-registration approach all footprints of a profile are used to align it to footprints of all other profiles in its vicinity.

The self-registration method builds upon a high density of laser altimeter footprints. For spacecraft in polar orbits (as is the case for MESSENGER) laser altimeter profiles merge near the poles. Here, however, the angle of rotation about the axis causes the smallest lateral displacement. Consequently, the measurement of the rotation angle becomes challenging and is associated with a higher uncertainty. In contrast, the orientation of the rotational axis is typically very well constrained and allows precise measurement of the obliquity. The proposed method can also be used to measure tidal deformations, as the reference DTM comprises a static topography to which the periodic radial displacements caused by tides can be tracked over time. Such measurement, however, require precise sub-meter range measurements and accurate spacecraft orbit and pointing information, conditions possibly achievable with the BepiColombo Laser Altimeter (BELA) [5].

Acknowledgements

This work was supported by a research grant from Helmholtz Association and German Aerospace Center (DLR) (PD-308). We acknowledge the work by the MLA instrument and MESSENGER science teams.

References

[1] Margot, J. L. et al., *Science*, 316, 710, doi: 10.1029/2012je004161, 2007.
[2] Margot, J. L., et al., *JGR-Planets*, 117, E00L09, doi: 10.1126/science.1140514, 2012.
[3] Stark, A., et al., *GRL*, 42, 7881, doi: 10.1002/2015gl065152, 2015.
[4] Neumann, G. A. et al., *JGR-Planets*, 106, 23753, doi: 10.1029/2000je001381, 2001.
[5] Mazarico E. et al, *47th Lunar and Planetary Science Conference*. The Woodlands, Texas, Abstract number 2062, 2016.
[6] Steinbrügge, G. et al., *PSS*, in press, doi:10.1016/j.pss.2018.04.017, 2018.

EPSC Abstracts
Vol. 12, EPSC2018-908-1, 2018
European Planetary Science Congress 2018

1:3million Scale Geological Mapping of the Derain Quadrangle, Mercury

C.C. Malliband (1), D.A. Rothery (1), M.R. Balme (1), and S.J. Conway (2).
(1) School of Physical Sciences, The Open University, Milton Keynes, MK7 6AA, UK (chris.malliband@open.ac.uk), (2) CNRS, LPG, Université de Nantes, France.

1. Introduction:

We are currently undertaking detailed (1:3M) geological mapping of the Derain (H-10) quadrangle of Mercury. This is as part of a coordinated European project to produce a complete set of geological maps [e.g. 1,2,3,4,5] in advance of BepiColumbo's arrival at Mercury. This mapping will aid mission planning and provide scientific context for BepiColombo observations.

2. Data and Methods:

The map is being produced in ArcGIS 10.5 using data from NASA's MESSENGER mission. Mapping is being conducted principally using the 166 m/pixel (meters per pixel) BDR mosaic. This is complemented

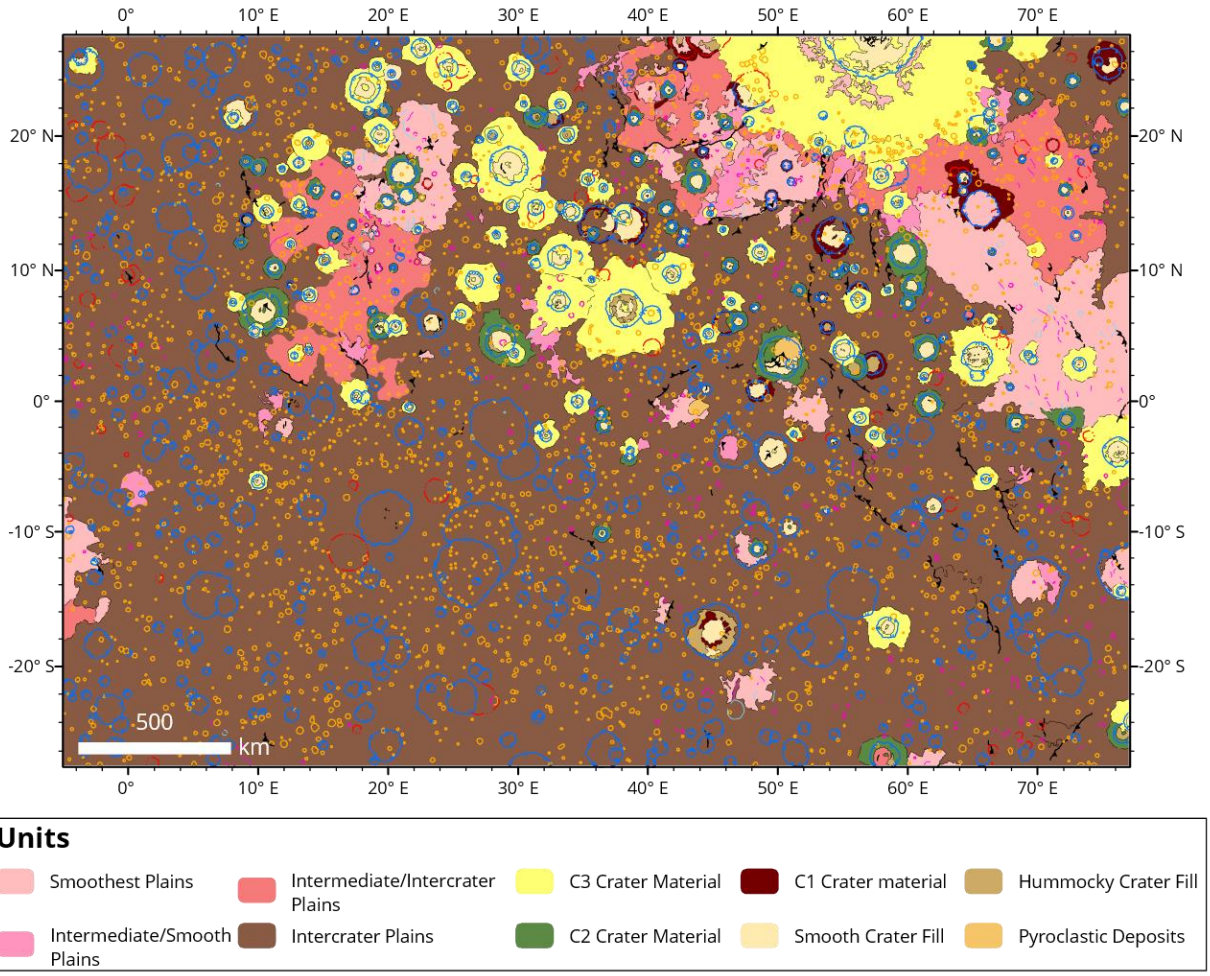

Fig 1. Working map (incomplete) of Derain quadrangle showing 3 class crater degradation scheme

by a range of other MESSENGER products, in particular: Enhanced Colour (665 m/pixel), low incidence mosaics and the Global DEM (665 m/pixel). Features of particular interest are also investigated using individual frames from MESSENGER's Narrow Angle Camera. As the map is intended for publication at 1:3M, line work is being prepared principally at 1:300k in line with prior work [e.g. 1]. We are also mapping an extra 5^{o} border beyond the Derain Quadrangle to allow better integration with adjoining maps.

3. Units:

We aim to produce mapping that complements other geological mapping underway. This includes mapping crater degradation with both the 3-Class degradation scheme [1] (as shown in Figure 1) and the 5-Class degradation scheme [6].

3.1 Plains Units:

The Derain quadrangle has a complex plains morphology, with numerous examples of small-scale smooth plains [7] and areas that do not easily classify as smooth or intercrater plains [8]. We are working to find a method to adequately display the visible geological relationships in these areas.

4. Progress and Ongoing Work:

We have completed mapping large scale plains units and most crater ejecta in the north eastern portion of the quadrangle. Plains mapping will probably be updated to ensure the best representation of complex areas. We are continuing work to extend crater classification and ejecta mapping.

Acknowledgments

CCM acknowledges project funding from the STFC and Open University Space Strategic Research Area.

References

[1] Galluzzi, V., Guzzetta, L., Ferranti, L., Achille, G. D., Rothery, D. A., & Palumbo, P. (2016). Geology of the Victoria quadrangle (H02), Mercury. Journal of Maps, 12(sup1), 227–238.

[2] Mancinelli, P., Minelli, F., Pauselli, C., & Federico, C. (2016). Geology of the Raditladi quadrangle, Mercury (H04). Journal of Maps, 12(sup1), 190–202.

[3] Guzzetta, L., Galluzzi, V., Ferranti, L., & Palumbo, P. (2017). Geology of the Shakespeare quadrangle (H03), Mercury. Journal of Maps, 13(2), 227–238.

[4] Wright J. et. al, (2018), GEOLOGICAL MAPPING OF THE HOKUSAI (H05) QUADRANGLE OF MERCURY: STATUS UPDATE. LPSC 49, Abstract #2164. The Woodlands, TX, USA, 2016.

[5] Pegg D. L. et al., GEOLOGICAL MAPPING OF THE DEBUSSY QUADRANGLE (H-14) PRELIMINARY RESULTS. Mercury: Current and Future Science 2018, Columbia, MD, USA, 2018.

[6] Kinczyk M. J. et al., A morphological evaluation of crater degradation on Mercury: Revisiting crater classification with MESSENGER data, LPSC 47, Abstract #1573. The Woodlands, TX, USA, 2016.

[7] Malliband C.C. et. al., SMALL SMOOTH UNITS ('YOUNG' LAVAS?) ABUTTING LOBATE SCARPS ON MERCURY. Mercury: Current and Future Science 2018, Columbia, MD, USA, 2018.

[8] Galluzzi V. et al., THE MAKING OF THE 1:3M GEOLOGICAL MAP SERIES OF MERCURY: STATUS AND UPDATES, Mercury: Current and Future Science 2018, Columbia, MD, USA, 2018.

EPSC Abstracts
Vol. 12, EPSC2018-932, 2018
European Planetary Science Congress 2018

The scientific outcome from BepiColombo flybys at Venus

V. Mangano (1), S. de la Fuente (2) , E. Montagnon (3), M. Casale (2), J. Benkhoff (4), J. Zender (4) , G. Murakami (5) S.Orsini (1), E. De Angelis (1), R. Rispoli (1)

(1) INAF/IAPS Roma, Italy (2) ESA/ESAC, Villanueva de la Canada, Spain (3) ESA/ESOC, Darmstadt, Germany (4) ESA/ESTEC, Noordvijk, The Nederlands, (5) JAXA/ISAS, Tokyo, Japan

Abstract

BepiColombo is a dual spacecraft mission to be launched in October 2018 to explore Mercury and carried out jointly between the European Space Agency (ESA) and the Japanese Aerospace Exploration Agency (JAXA). During its long cruise to Mercury, BepiColombo will swing-by Venus twice, in 2020 and in 2021. Though the cruise configuration does not allow all the instruments to be operative before Mercury orbit insertion, this is nonetheless a great occasion to obtain interesting scientific outcome. A 'scientific traceability matrix' is presented here.

1. Introduction

The Mercury Planetary Orbiter (MPO) payload comprises 11 experiments and instrument suites. It will focus on a global characterization of Mercury through the investigation of its interior, surface, exosphere and magnetosphere. In addition, it will test Einstein's theory of general relativity. The second spacecraft, the Mercury Magnetosphere Orbiter (MMO), will carry 5 experiments or instrument suites to study the environment around the planet including the planet's exosphere and magnetosphere, and their interaction processes with the solar wind. MPO and MMO will be launched in a composite with a propulsion element, the Mercury transfer module (MTM) and a sunshade cone to protect the MMO (MOSIF).

During the long cruise to Mercury (7.2 years), BepiColombo will have 1 flyby at the Earth in April 2020, and two fly-by's at Venus in October 2020 and August 2021, before arriving close to Mercury with the first of 6 flybys two months later. The launch and cruise configuration (MCS) will not allow full operability of all instruments onboard. In fact, MMO will be partly shielded by MOSIF, thus allowing instruments to detect signals only within a conical field-of-view around the MCS's –Z axis, and on-board the MPO all the instruments obstructed by the MTM (+Z axis) will not be able to operate. Nevertheless, all the instruments not requiring pointing or with apertures in the other directions will be operative.

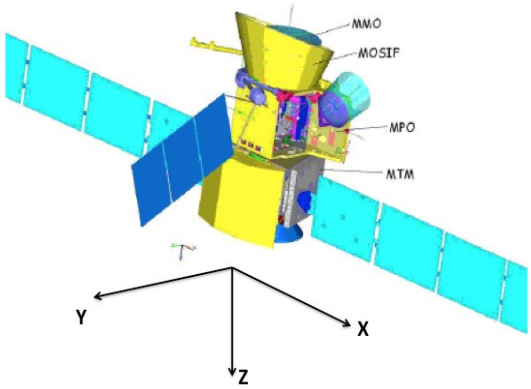

Figure 1: BepiColombo in its cruise configuration (MCS).

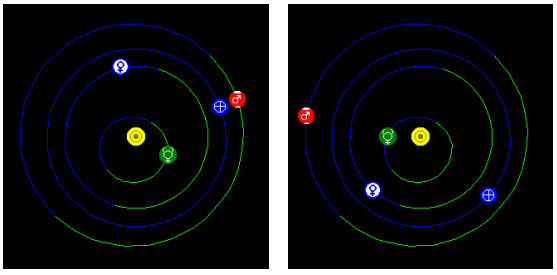

Figure 2: Inner Solar System at the time of the 1st (left) and 2nd Venus flyby (right).

2. Venus Flyby's Analysis

The MCS nominal attitude during cruise will be defined by the +Y axis pointed to the Sun and a rotation of 120 degrees/hour about the Sun vector (which results in approximately 8 full rotations/day). The two Venus flybys geometries can be summarized

in Figure 2 and 3, and will have closest approach altitude of about 11000 and 1000 km, respectively.

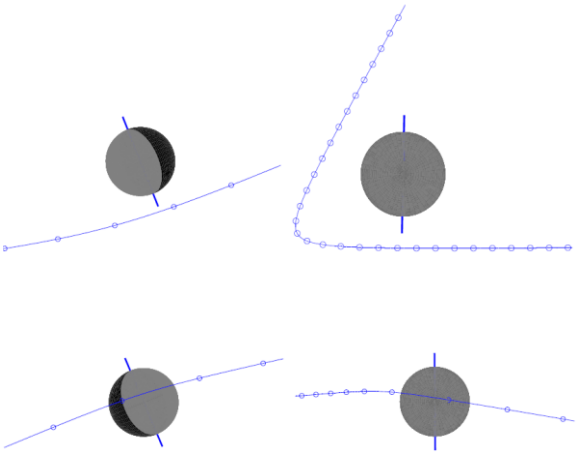

Figure 3: (up) 1st Venus flyby on Oct 12th,2020 as seen from the Earth (left) and from the Sun (right); (bottom) 2nd Venus flyby on Aug 11th, 2021.

3. BepiColombo science at Venus

8 of the 11 instruments onboard the MPO will be able to operate at Venus. They are: the accelerometer ISA, the magnetometer MAG, the two channels (spectrometer and radiometer) of MERTIS, the neutron and gamma spectrometers MGNS, the radio science experiment MORE, the EUV and FUB spectrometers of PHEBUS, the two ion detectors (MIPA and PICAM) of SERENA, and the two spectrometers of SIXS.

The big differences occurring between Mercury and Venus necessarily derive in a different use of some of the instruments in the payload. In particular, MERTIS spectrometer and radiometer, devoted to the study of the Hermean surface composition and grain size, on Venus will be used to sound clouds at 55-100 km altitude in the bands of CO_2, SO_2, H_2SO_4, and will be able to provide temperature profiles. On the contrary, PHEBUS, designed to study the exospheric composition of Mercury, will be able to measure Venusian H, He and O hot populations. MGNS at Mercury will sound surface composition, especially in terms of radioisotopes and volatile deposits; at Venus will perform atmospheric analysis to measure leakage flux of neutrons and measure gamma-rays emission. SERENA/MIPA & PICAM together with SIXS will be able to study the planetary environment in terms of solar radiation and energetic particles, as well of lower energy ion population, giving name to the particles entrapped in the local Interplanetary Magnetic Field (first flyby) and induced magnetosphere that will be measured by the magnetometer MAG.

Important support to the MPO measurements of the planetary environment around Venus (both in terms of particles population and magnetic field) will be given by the 3 (over 5) instruments onboard MMO. MPPE will be able to detect low energy ions and low and high energy electrons, and perform plasma imaging. The magnetometer MGF will corroborate MPO/MAG measurements; and PWI will measure electric field, plasma and radio waves.

4. Science and Operations

A necessary work of connection between science requirements and spacecraft constraints during the cruise phase (and swing-by in particular) was mandatory to verify real feasibility of such measurements out of the original target for which BepiColombo instruments were designed. This effort included on one side the analysis of instrument pointing requirements from ESA/ESAC and ESOC teams and the generation of a ‘pointing timeline’ to optimize the scientific outcome given the time and attitude restrictions [1]. On the other, the scientific outcome at Venus and the operation modes will be very soon consolidated in a ‘scientific traceability matrix’ that will be presented at the EPSC conference.

5. References

[1] Montagnon, E., De la Fuente, S., BepiColombo – Operational Analysis of Venus Swingby Observation Requests, BC-ESC-TN-10045, issue 1, released 13/03/17

EPSC Abstracts
Vol. 12, EPSC2018-936, 2018
European Planetary Science Congress 2018

Analytical investigations of Laser-Produced Impact Melts of Basaltic Rocks

Iris Weber (1), Andreas Morlok (1), Christopher Hamann (2), Dayl J. P. Martin (3), Katherine H. Joy (3), Roy Wogelius (3), Aleksandra Stojic (1), Harald Hiesinger (1), Jörn Helbert (4)
(1) Institut für Planetologie, Wilhelm-Klemm-Strasse 10, 48149, Münster, Germany (2) Museum für Naturkunde, Invalidenstrasse 43, 10115 Berlin, Germany (3) School of Earth and Environmental Sciences, University of Manchester, Oxford Road, Manchester M13 9PL, UK (4) Institute for Planetary Research, DLR, Rutherfordstrasse 2, 12489 Berlin, Germany (sonderm@uni-muenster.de)

1. Introduction

The Infrared and Raman for Interplanetary Spectroscopy (IRIS) laboratory at the Institute für Planetologie in Münster produces, among others, spectra for a database for the mid-infrared spectrometer MERTIS (Mercury Radiometer and Thermal Infrared Spectrometer) onboard of the ESA/JAXA BepiColombo mission to Mercury. MERTIS will be able to map spectral features of the surface in the 7-14 µm range, with an average spatial resolution of ~500 m [1-4]. Thus, the mineralogical composition of the planetary surface can be determined via remote sensing.
Mercury has been exposed to heavy impact cratering [4]. Therefore, impact products like glass are an important component of its surface. We thus are studying a series of mid-IR spectroscopy of shocked, i.e., basaltic material in the laboratory environment, in order to interpret future MERTIS measurements [5-8].

2. Samples and Techniques

In this work, the impact melting of basaltic materials was simulated by using a pulsed Nd:YAG laser at the Technische Universität Berlin [9]. The sample was irradiated along 15 mm long and 1 mm wide lines. To optimize the melt production the laser settings were: 0.9 kW for emitted power over 15 s at a wavelength of 1064 nm, a pulse frequency of 25 Hz, and a pulse duration of 2.5 ms. Afterwards the sample runs were collected, embedded in resin, sectioned, and polished. Hoffelder basalt (Hoffeld, Germany) was used as starting material. This sample is a basanitic, porphyritic rock consisting of 200–800µm size olivine ($Fo_{79\pm4}$) phenocrysts set in an aphanitic groundmass (≤100µm) of labradorite ($An_{62}Ab_{36}$), salite ($En_{39\pm3}Wo_{49\pm2}$), Fe,Ti oxides, and feldspathoids.
Detailed quantitative analyses were made with a JEOL JXA-8530F Hyperprobe electron probe micro analyser (EPMA) equipped with four wavelength dispersive spectrometers and operating at an excitation voltage of 15 kV and a beam current of 15 nA. Measurements were carried out with a spot size of 2 µm.
For IR analyses, we used a Perkin-Elmer Spotlight-400 FTIR spectrometer at the University of Manchester. Spot analyses (25×25 µm) were made in a wavelength range from 2.5–15.4 µm in the reflectance mode, using a cooled mercury-cadmium-telluride (MCT) detector. For mapping an adjoining micro spectroscopy mapping unit was used.

3. Results

EMPA analyses of one area of the Hoffelder basalt confirm the mineralogy of the sample. Large grain olivines show a Fo content between 87 and 77. In the fine-grained matrix labradorite ($An_{60\text{-}53}Ab_{43\text{-}38}$), olivine ($Fo_{73}$), pyroxene ($En_{36}Wo_{50}$), and Fe,Ti-oxides are present. The analyses of the laser-generated glass are in good agreement with the bulk composition of the sample. A summary of the measurements are given in Table 1. The BSE (backscattered electron image, Fig. 1) shows the appearance of the investigated area.
Basaltic glass shows a very simple IR spectra (Fig. 2), dominated by one broad Reststrahlen band (RB) between 10.1 and 10.5 µm, and a Christiansen feature (CF) from 8.3 to 8.5 µm. Fine-grained parts of the basalt show more variation; here the dominating RB (9.7–10.1 µm) is accompanied by additional bands from 8.9–9.4 µm and 10.2–10.4 µm. The CF is between 7.9 and 8.3 µm. Minor bands are located at longer wavelengths from 13.1 to 16.7 µm (in the bulk spectrum). Larger crystals show a wider distribution of features, in part due to crystal orientation effects. The CF is between 8.2 and 9.1 µm, various major RB are at 9.3–9.5 µm, 9.6–10 µm, 10.2– 10.4µm, 10.6–10.9 µm, 11–11.2 µm, and 11.9–12 µm, with additional minor features between 13 and 16.2 µm.

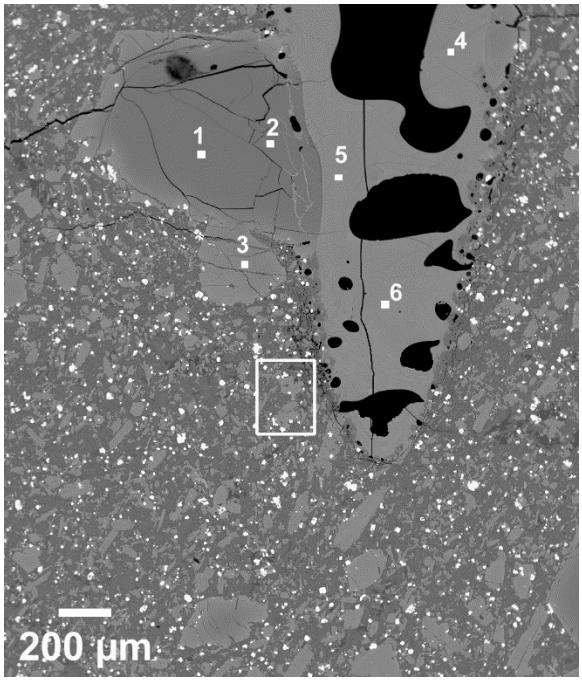

Fig. 1: BSE image of the investigated area of the treated Hoffelder basalt. Points 1–3 are the large grain olivines. Points 4–6 are in the glass. Framed is the analyzed fine-grained matrix.

Table 1: EMPA analyses of the marked areas in the BSE image of Fig. 1.

	Olivine 1,2 (Fo_{87})	Olivine 3 (Fo_{77})	Glass (4-6)	Olivine Fine grained	Feldspar Fine grained
Na_2O	0.02	0.01	2.52	0.02	4.6
MgO	46.3	39.7	12.7	36.8	0.04
SiO_2	40.0	38.5	42.4	38.1	53.5
Al_2O_3	0.05	0.03	14.5	0.02	28.7
K_2O	n.d.	n.d.	1.13	0.01	0.42
CaO	0.16	0.28	10.6	0.42	11.7
FeO	12.7	20.6	11.2	23.7	0.70
TiO_2	0.05	0.04	2.65	0.09	0.14
Cr_2O_3	0.01	0.03	0.04	0.03	n.d.
MnO	0.17	0.42	0.18	0.57	0.03
Total	99.46	99.61	97.92	99.66	99.74

References

[1] Maturili A. (2006) Planetary and Space Science 54, 1057–1064 [2] Helbert J. and Maturilli A. (2009) Earth and Planetary Science Letters 285, 347-354 [3] Benkhoff, J. et al. (2010) Planetary and Space Science 58, 2-20 [4] Hiesinger H. et al. (2010) Planetary and Space Science 58, 144–165 [5] Morlok A. et al. (2017) Icarus 296, 123-138 [6] Morlok A. et al. (2016) Icarus 278, 162-179 [7] Martin, D.J.P. (2017) Meteoritics & Planetary Science 52, 1103-1124 [8] Pernet-Fisher, J.F. (2017) Scientific Reports 78 [9] Hamann C. et al. (2016) Journal of Geophysical Research 43, 10602-10610 [10] DuFresne C.D.M. et al. (2009) American Mineralogist 94, 1580-1590 [11] Weber I. et al. (2018) 49th LPSC Abstract #1430

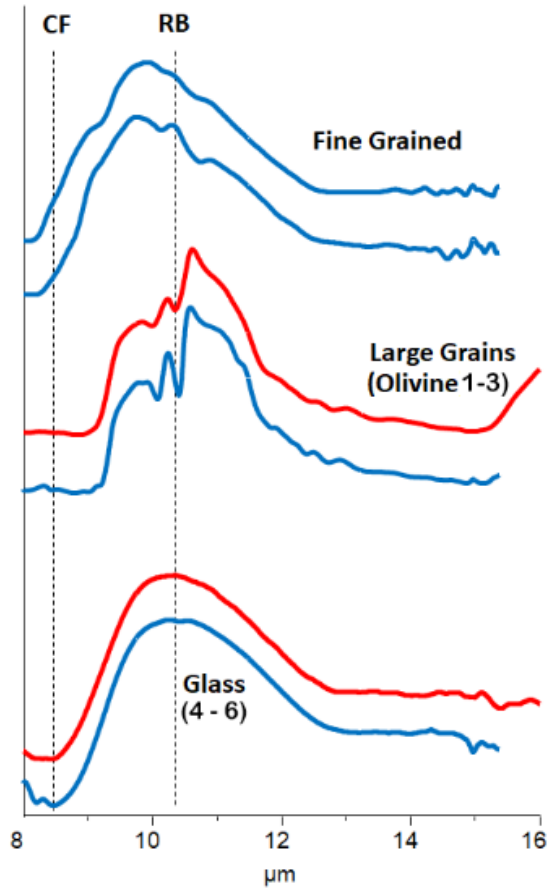

Fig. 2: Resulting micro-FTIR spectra from the pristine and melted parts of the basalt slab. Red = single point analyses (25 × 25 µm), blue = phases identified using PCS analyses.

4. Discussion and Conclusions

IR spectra of the melt glass are consistent with those of basaltic glass in earlier studies [5,10].
Mid-infrared investigations give distinctive signatures for the melted and un-melted components in the sample. This helps to discriminate impact-shocked lithologies in basalt from pristine igneous material. However, as glass will be only a part of the mineral mixture of the surface; further components will have to be taken into account.
Our results are available via a web-accessible database, which will be extended continuously [11].

Acknowledgements

This work is partly supported by the DLR (funding 50QW1702 in the framework of the BepiColombo mission) and the DFG (MEMIN Research Unit FOR 887).

EPSC Abstracts
Vol. 12, EPSC2018-973-2, 2018
European Planetary Science Congress 2018

Simulation of MPO orbit reconstruction using Doppler observations and comparison with laser altimetry observations

Alireza Hosseiniarani (1), Stefano Bertone (2), Daniel Arnold (2), Adrian Jäggi (2), Nicolas Thomas (1)
(1) Physics Institute, University of Bern, Switzerland (seyedalireza.hosseiniarani@space.unibe.ch),
(2) Astronomical Institute, University of Bern, Switzerland

Abstract

The BepiColombo Laser Altimeter (BELA) [1] will fly on board the European Space Agency's BepiColombo Mercury Planetary Orbiter (MPO). In this study, we present the MPO orbit reconstruction based on Doppler data with different settings on the arc lengths, arcs initial conditions, dynamical model, observation mode and orbit determination process and we compare the results of the orbit reconstruction with laser altimetry observables at crossover points.

1. Introduction

BepiColombo is Europe's first mission to Mercury [2]. It will set off in 2018 on a journey to the smallest terrestrial planet in our Solar System, Mercury. The mission comprises two spacecraft: MPO and MMO. The BepiColombo Laser Altimeter (BELA) is one of the instruments of MPO. The orbit of MPO spacecraft can be determined using Doppler tracking data [3]. But the contribution of laser altimetry observation at crossover points can potentially improve the accuracy of the determined orbit [4].

2. Modelling

For modeling the orbit of MPO around Mercury, we use a full force model containing all the gravitational and non-gravitational forces. The propagated orbit has been verified against orbits provided by DLR and ESA. Our simulations of Doppler tracking measurements include 2-way X-band and K-band Doppler measurements, station and planetary eclipses and the relativistic corrections and atmospheric effects.

To model the laser altimetry observation, we detect the location of crossover points based on the orbit and we simulate a series of laser altimetry observations around these points. Then we add both random and systematic errors to the observables based on the developed BELA instrument model [5] to have a realistic simulation.

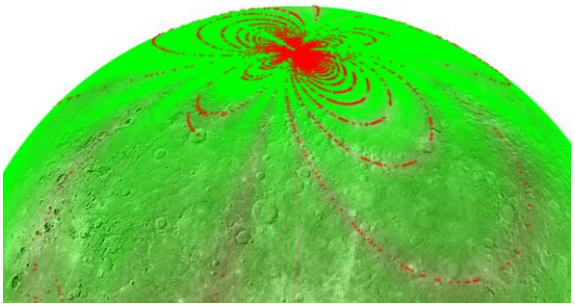

Figure 1: The distribution of crossover points in the first two months of mission (green lines are altimetry ground tracks and red points are crossover points)

For this study we use the planetary extension of the Bernese Software (BSW [6]). The latter is an advanced space data processing software developed at the Astronomical Institute of the University of Bern (AIUB).

3. Doppler Orbit reconstruction

We perform some orbit reconstruction tests using just the Doppler data with different settings on the arc lengths, arcs initial conditions, dynamical model, observation mode and orbit determination process in the Bernese software and we compare the results. For these tests, we use a full force model (Gravitational model w d/o 50, SRP, IR, Albedo) to produce synthetic Doppler data and a reduced force model with errors on the initial state vector as the knowledge of the orbit.

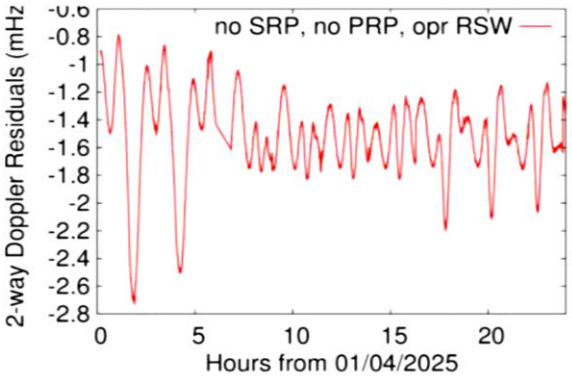

Figure 2: 2-way Doppler residuals in a simple orbit reconstruction test (RMS = 0.9 mHz over 60 days)

The goal of these tests is to find the best possible orbit determination accuracy that can be achieved using only Doppler data and the impact of different settings on the results. We also compare the results of Doppler-only orbit reconstruction with the altimetry crossover observables.

4. Summary and Conclusions

One of the final goals of this work is to study the impact of laser altimetry data in the form of crossovers to improve the orbit of the spacecraft. To achieve this, here we perform and present some orbit reconstruction tests using just the Doppler data with different settings and compare the results with previous studies. Finally, we compare the determined orbit with the laser altimetry crossover observables. such comparison can be used as both a validation/quality measure for the different tests and as a first step for including altimetry crossovers in the orbit recovery.

Acknowledgements

This study has been funded with the support of the Swiss National Foundation (SNF) and NCCR PlanetS.

References

[1] Thomas, N. et al: The BepiColombo Laser Altimeter (BELA): Concept and baseline design, PSS, 2007001.

[2] Benkhoff, J. et al: BepiColombo—Comprehensive exploration of Mercury: Mission overview and science goals, PSS, 2010

[3] S. Cicalò et al: The BepiColombo MORE gravimetry and rotation experiments with the ORBIT14 software, MNRAS, 2016.

[4] Rowlands D.D. et al: The Use of Laser Altimetry in the orbit and Attitude determination of Mars Global Surveyor, GRL, 1999

[5] Hosseiniarani, A.: Improved modelling of BELA altimetry observation for MPO orbit reconstruction, EGU, 8–13 April 2018, Vienna, Austria

[6] Dach, R. et al: Bernese GNSS Software Version 5.2. AIUB, 2015.

EPSC Abstracts
Vol. 12, EPSC2018-1001, 2018
European Planetary Science Congress 2018

Potential Identification of Sublimation-Driven Downslope Mass Movements on Mercury

C.C. Malliband (1), S.J. Conway (2), D.A. Rothery (1), and M.R. Balme (1),
(1) School of Physical Sciences, The Open University, Milton Keynes, MK7 6AA, UK (chris.malliband@open.ac.uk), (2) CNRS, LPG, Université de Nantes, France

1. Introduction

Mass movement has been recognised on many solar system bodies. Evidence of mass movement on Mercury has previously been limited to a single documented example, found in the pyroclastic vent NE of Rachmaninoff crater (Nathir Facula). Here we present the identification of a further three examples.

2. Identified Examples

2.1 Mass movement in Nathair Facula Vent

Attention was drawn to the slope features in the Nathair Facula vent (NE of Rachmaninoff crater) (Fig. 1) on the MESSENGER web-site, but so far as we are aware there has been no formal study. The features are downslope erosion-deposition systems with an alcove at the head, chute and a fan at the base. Feature heads appear to develop in a stratigraphic layer of brighter material (Fig. 1B). This brighter

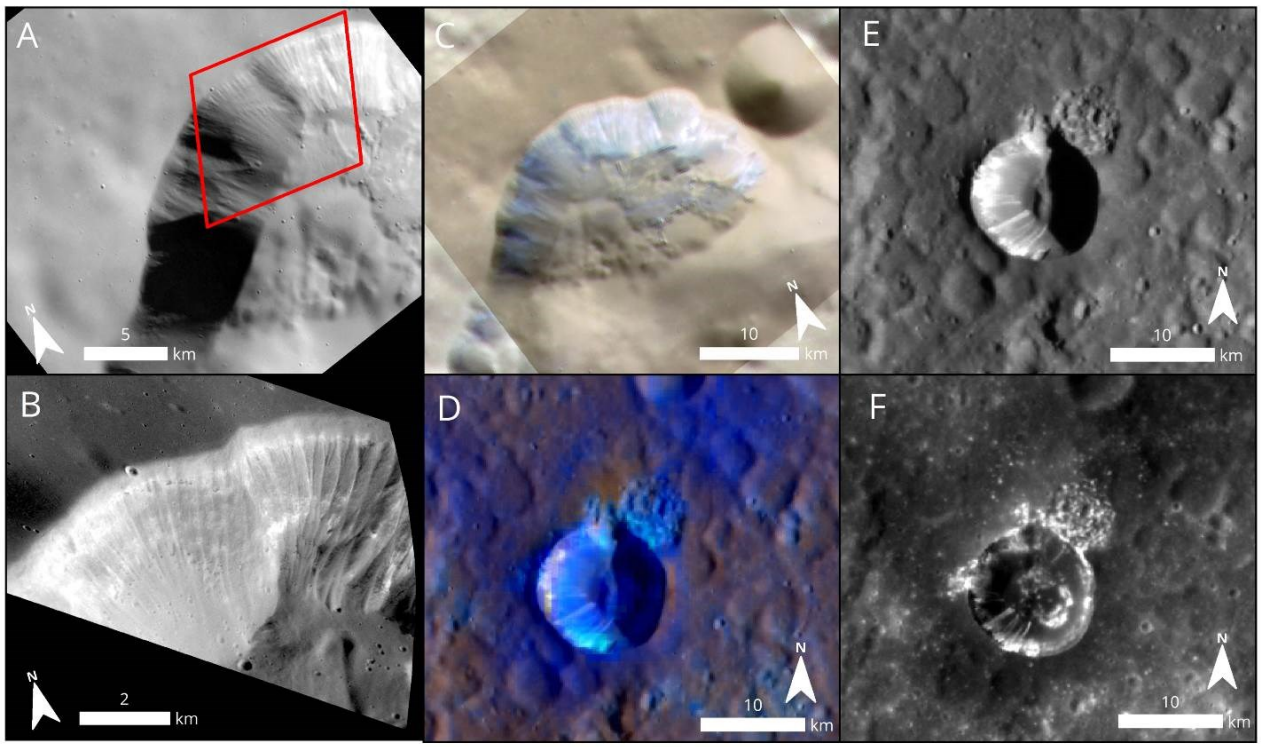

Fig. 1: A,B,C Gully-like slope features in vent NE of Rachmaninoff. A:Context image centered on 36°N, 63.8°E showing widespread slope features. Box shows location of B. (NAC: EN1003843866M) B: High resolution (6.4m/pixel) image showing source at bright layer (NAC: EN1028933034M) C: Enhanced color. D, E, F. Newly discovered slope features at 8°S, 55°E. D, enhanced color; E, high incidence angle (NAC: EN0252295266M) F, low incidence angle. Note bright, possibly hollow forming, material, high in crater wall (NAC: EN1028933034M).

material appears to be related to hollows [1].

2.2 Slope features in unnamed crater (≈285 km N of Nabokov)

The newly identified slope features are in a ≈12 km diameter simple impact crater. The crater is surrounded by low reflectance material and has an area of hollows on the NE crater rim. The slope features start just below the crater rim, in a bright stratigraphic layer. This may be similar to the hollow forming layer in Nathir Facula vent.

2.3 Possible slope features in Berkel crater and peak ring element in Rustaveli crater.

We have identified a third possible set of downslope oriented high albedo slope features in Berkel crater. This is a complex crater and the features of interest are located on the rim terraces. These features also appear to start in a bright layer below the crater rim. This is the least confident identification.

We are also investigating a possible slope feature on a peak ring element in Rustaveli crater. This is visible only in low altitude imagery.

3. Current work

We are examining other areas with steep slopes and catalogued hollows, and are performing a global survey to identify any further examples. We will compare the topography of these features to erosion-deposition systems on the Moon [2, 3], Mars [4,5], and Vesta [6]. Currently our working hypothesis is that these downslope movements are triggered by sublimation.

Acknowledgements

CCM acknowledges project funding from the STFC and Open University Space Strategic Research Area.

SJC is supported by the French Space Agency CNES, in preparation for BepiColombo.

References

[1] Blewett, D. T., Chabot, N. L., Denevi, B. W., Ernst, C. M., Head, J. W., Izenberg, N. R., et al. (2011). Hollows on Mercury: MESSENGER Evidence for Geologically Recent Volatile-Related Activity. Science, 333(6051), 1856–1859.

[2] Bart, G. D. (2007). Comparison of small Lunar landslides and Martian gullies. Icarus, 187(2), 417–421.

[3] Kokelaar B. P., Bahia R. S., Joy K. H., Viroulet S., & Gray J. M. N. T. (2017). Granular avalanches on the Moon: Mass‐wasting conditions, processes, and features. Journal of Geophysical Research: Planets, 122(9), 1893–1925.

[4] Conway, S. J., Balme, M. R., Kreslavsky, M. A., Murray, J. B., & Towner, M. C. (2015). The comparison of topographic long profiles of gullies on Earth to gullies on Mars: A signal of water on Mars. Icarus, 253, 189–204.

[5] Brusnikin, E. S., Kreslavsky, M. A., Zubarev, A. E., Patratiy, V. D., Krasilnikov, S. S., Head, J. W., & Karachevtseva, I. P. (2016). Topographic measurements of slope streaks on Mars. Icarus, 278, 52–61.

[6] Scully, J. E. C., Russell, C. T., Yin, A., Jaumann, R., Carey, E., Castillo-Rogez, J., et al. (2015). Geomorphological evidence for transient water flow on Vesta. Earth and Planetary Science Letters, 411, 151–163.

EPSC Abstracts
Vol. 12, EPSC2018-1081-1, 2018
European Planetary Science Congress 2018

MHD instabilities at the Mercury's magnetopause

Stavro L. Ivanovski (1,2), Anna Milillo (1), Monio Kartalev (2) and Stefano Massetti (1)
(1) INAF-IAPS, via Fosso del Cavaliere 100, 00133 Rome, Italy (stavro.ivanovski@iaps.inaf.it); (2) Geospace Consult Ltd, Institute of Mechanics, Bulgarian Academy of Sciences, Acad. G. Bontchev St., bl. 4, 1113 Sofia, Bulgaria

Abstract

Based on a flexible numerical incompressible magnetohydrodynamic (MHD) approach implemented for studying a coupled Kelvin-Helmholtz (KH) and tearing mode (TM) instabilities [1], we investigate the applicability of this mixing-boundary-layer MHD approach to the Mercury's magnetopause and by means of numerical simulations perform parameters study using the MESSENGER data [2].

We report results from numerical simulations of the coupled Kelvin-Helmholtz (KH) and tearing mode (TM) instability on the dayside magnetopause layer. Numerical tests with different sets of dimensionless input parameters are performed. The computational domain in this context is taken to lie on the equatorial magnetopause region.

Introduction

How the transport of momentum and plasma occurs across a boundary remains a question of outstanding scientific interest. Kelvin-Helmholtz (KH) waves and magnetic reconnection are believed to be the key drivers of plasma transport and planetary magnetospheres are excellent laboratories to investigate them. The ESA/JAXA BepiColombo mission will be launched in October 2018 and among its scientific objectives is the investigation of the physical conditions in which magnetic reconnection occurs. In the phase of preparation of the BepiColombo data, we take advantage of two datasets of MESSANGER data and use them to study numerically the development of MHD instabilities that can imply magnetic reconnection phenomena at Mercury's magnetopause.

1. The Model

The model, used to describe the flow dynamics of the magnetopause mixing layer in a fluid limit, is earlier proposed by [1]. The simulation domain consists of a rectangular region in (x,z)-plane, which is defined on locally introduced Cartesian grid, neglecting the realistic curvature, with co- ordinate x pointing direction along the velocity of the incident magnetosheath flow; z is in the direction downward to the Mercury's center (from the magnetosheath to the magnetosphere) and y-direction is ensuring a right-handed coordinate system. The governing MHD equations are for incompressible, viscous, electrically-conductive fluid with the following restriction: the derivatives of all the parameters along y-direction are assumed to be zero.

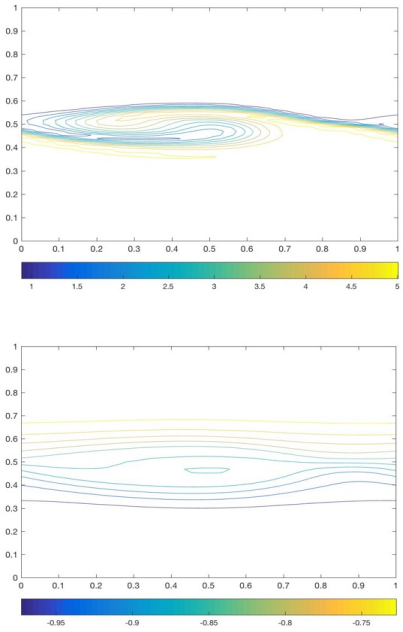

Figure 1. KH and TM instabilities of density (top) and B_y (bottom) in the case of high-shear

magnetopause reconnect, 24 November 2011, based on the MESSENGER data [2].

2. Results and conclusions

A full 3D MHD system of equations for incompressible and conducting fluid is reduced only by neglecting the partial derivatives in one direction. Two MESSENGER data case studies were simulated by means of numerical modelling of coupled Kelvin-Helmholtz (KH) and tearing mode (TM) instabilities at the dayside Mercury magnetopause mixing layer.

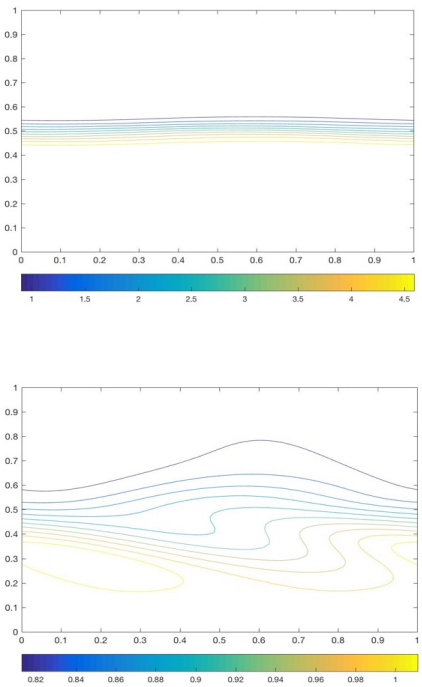

Figure 2. Density (top) and B_x **(**bottom**)** in the case of low-shear magnetopause reconnect, 21 November 2011, based on the MESSENGER data [2].

We were only focused on investigating the observed magnetic reconnection in terms of developed instability configurations: the high shear magnetic reconnection was clearly evidenced in the time evolution of the simulated MHD instabilities. In the case of high-shear magnetopause reconnect, i.e. on 24 November 2011, we obtained the typical vortex features that exhibit magnetic reconnection in the developed KH and TM instabilities (Figure 1). While in the case of low-shear magnetopause reconnection, i. e. 21 November 2011, we obtained no manifestation of magnetic reconnection (Figure 2).

Acknowledgements

This work is supported by the SERENA ASI-INAF agreement.

References

[1] Ivanovski et al. 2011, JTAM, vol. 41, No. 3, pp. 31–42.
[2] DiBraccio et al. 2013, JGR, 118, 997-1008

EPSC Abstracts
Vol. 12, EPSC2018-1092, 2018
European Planetary Science Congress 2018

Spectroscopy of minerals analogs of Mercury under the hermean conditions: The effect of the temperature

N. Bott (1), R. Brunetto (2), C. Carli (3), F. Capaccioni (3), A. Doressoundiram (1), Y. Langevin (2), D. Perna (1,4), F. Poulet (2), G. Serventi (3), M. Sgavetti (3), F. Borondics (5), and C. Sandt (5)
(1) LESIA - Observatoire de Paris - CNRS - Sorbonne Université - Université Paris-Diderot, 5 place Jules Janssen, 92195 Meudon, France, (2) Institut d'Astrophysique Spatiale - CNRS - Université Paris-Sud, Orsay, France, (3) Istituto di Astrofisica e Planetologia Spaziali - INAF, Roma, Italy, (4) Osservatorio Astronomico di Roma - INAF, Monte Porzio Catone, Italy, (5) Synchrotron SOLEIL, Saint-Aubin, France (nicolas.Bott@obspm.fr)

Abstract

We present a preliminary study to focus on the effects of the extreme conditions occurring on Mercury on minerals analogs, in particular taking into account the strong variations of temperature.

1. Introduction

A major result of the MESSENGER mission was to reveal the volcanic hermean surface poor in iron [1], but unexpectedly rich in volatile elements [2]. The high abundance of sulfur on Mercury is particularly interesting, because its sublimation is suggested to trigger the formation of hollows [3]. Laboratory experiments whose aim is to study the evolution of sulfides in the conditions of Mercury's surface are in progress [4]. However, to understand the spectral properties of the surface need to consider how minerals can be affected by the hermean environment. The effects of temperature and space weathering on minerals have been already studied [5,6] but rarely on Mercury's analogs [7].

2. Samples and setups

We began our activities measuring a loose powder (75-100 µm) of plagioclase Pl3 [8] and 5 mm diameter pellets with the same plagioclase powder. To simulate the hermean high T conditions, we used a LINKAM (nitrogen purged) cell to heat and cool our samples which allows to measure VIS-IR (0.4-15 µm) spectra as a function of temperature (298-623K in our case). Finally, we used two setups for our spectroscopic analyses: 1) a visible-near infrared spectrometer Maya2000 Pro coupled with a microscope through optical fibers; 2) a near to mid infrared spectrometer coupled with an Agilent microscope, installed at the SMIS (Spectroscopy and Microscopy in the Infrared using Synchrotron) beamline of the synchrotron SOLEIL.

3. Analytical method

In a typical heating experiment, the powder or the pellet was placed inside the purged heating cell and reflectance spectra were recorded every 50K of increasing temperature. The heating ramp was 5K/min, with a 10-20 min plateau to record the spectrum at a given temperature. A similar cooling cycle was then performed and spectra were measured as a function of decreasing temperature from 623K to 302K.

4. Preliminary results

Figure 1 shows the thermal infrared where the Christiansen feature (CF) and the Reststrahlen absorption bands (RB) of silicates are studied.

A preliminary qualitative analysis showed a shift towards greater wavelengths for several RB peaks (e.g. at ~9.0 and ~10.5 µm) as a function of increasing T, whereas the CF does not shift. A more quantitative analysis will be presented and discussed.

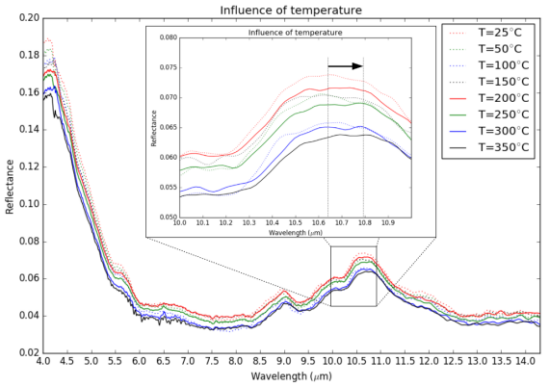

Fig. 1. Mid infrared spectra of a pellet of plagioclase taken at different temperatures (from 298 K to 623 K).

5. Future activities

In the next future, we plan to perform more heating experiments to study the evolution of natural minerals, as well as synthetic Mercury-like glasses [7] at temperature during day time. In addition, we consider to take measurements in cold conditions as it is the case on the floor of polar craters of Mercury. Finally, we plan to irradiate our samples with 40 keV ion beams with different fluences as a simulation of slow solar wind irradiation of Mercury.

Acknowledgements

This work is partly supported by the Centre National d'Études Spatiales. The microspectroscopy activities are supported by grants from Région Ile-de-France (DIM-ACAV) and SOLEIL. D. Perna received funding from the European Union's Horizon 2020 research & innovation program under the Marie Sklodowska-Curie grant agreement n.664931

References

[1] Peplowski P. N. et al.: Mapping iron abundances on the surface of Mercury: Predicted spatial resolution of the MESSENGER Gamma-Ray Spectrometer, Planetary and Space Science, Vol. 59, pp. 1654-1658, 2011.

[2] Nittler L. R. et al.: The Major-Element Composition of Mercury's Surface from MESSENGER X-ray Spectrometry, Science, Vol. 333, pp. 1847-1850, 2011.

[3] Blewett D. T. et al.: Mercury's hollows: Constraints on formation and composition from analysis of geological setting and spectral reflectance, Journal of Geophysical Research, Vol. 118, pp. 1013-1032, 2013.

[4] Varatharajan I. et al.: Emissivity of Ca-Sulfide in Mid-Infrared Under Simulated Extreme Thermal Environment of Mercury, LPI abstract #2047, 2018.

[5] Suto H. et al.: Low-temperature single crystal reflection spectra of forsterite, Monthly Notices of the Royal Astronomical Society, Vol. 370, pp. 1599-1606, 2006.

[6] Brunetto R. et al.: Ion irradiation of Allende meteorite probed by visible, IR, and Raman spectroscopies, Icarus, Vol. 237, pp. 278-292, 2014.

[7] Morlok A. et al.: IR spectroscopy of synthetic glasses with Mercury surface composition: Analogs for remote sensing, Icarus, Vol. 296, pp. 123-138, 2017.

[8] Serventi G. et al.: Spectral variability of plagioclase-mafic mixtures (1): Effects of chemistry and modal abundance in reflectance spectra of rocks and mineral mixtures, Icarus, Vol. 226, pp. 282-298, 2014.

EPSC Abstracts
Vol. 12, EPSC2018-1099, 2018
European Planetary Science Congress 2018

Unveling Mercury surface composition: results from MESSENGER and future outlooks from the SIMBIO-SYS Visible and Infrared Hyperspectral Imager (VIHI)

F. Zambon (1), G. Filacchione (1), F. Capaccioni (1), C. Carli (1), M. T. Capria (1) and G. Cremonese (2) and the SIMBIO-SYS Team
(1) INAF-IAPS Istituto di Astrofisica e Planetologia Spaziali, Via del Fosso del Cavaliere, 100, I-00133 Rome, (2) INAF - Osservatorio Astronomico di Padova

Introduction

October 2018 marks the lunch of BepiColombo, the first ESA/JAXA mission devoted to the study of Mercury. Because of its extreme environment, only other two spacecrafts explored Mercury, Mariner 10, which carried out only few flybys of the planet, about 37 years ago, and the NASA MESSENGER mission entered in orbit around Mercury in March 2011. During four years of operating life, MESSENGER allowed for mapping the entire surface of Mercury at different spatial scales, revealing aspects hitherto hidden, but arising new questions. In this regard, the future BepiColombo mission, will answer questions still unsolved. BepiColombo mission consists of two modular orbiters: a Mercury Planetary Orbiter (MPO) provided by ESA and a Mercury Magnetospheric Orbiter (MMO) by the Japan Aerospace eXploration Agency (JAXA). The Spectrometer and Imagers for MPO BepiColombo-Integrated Observatory SYStem (SIMBIO-SYS) consists of three channels the high-resolution imager (HRIC), the stereo imaging system (STC) and the visible-near-infrared imaging spectrometer (VIHI), all together these three instruments will give new information regarding the surface composition and the geology of Mercury [1].

Mercury's surface composition: MDIS-WAC and MASCS-VIRS onboard MESSENGER mission

Mapping Mercury's surface composition was one of the goal of the MESSENGER mission, for this purpose the Mercury Dual Imaging System (MDIS), and the Mercury Atmospheric and Surface Composition Spectrometer (MASCS) were included in the spacecraft [2]. MDIS, the MESSENGER camera, consists of two instruments: a Narrow Angle Camera (NAC) centered at ∼747 nm, which acquired high-resolution images for the geological analysis, and the Wide Angle Camera (WAC), provided with 11 filters dedicated to the compositional analysis, operating in a range of wavelengths between ∼395 and ∼1040 nm. MASCS-VIRS is a spectrograph fixed concave grating with focal length of of 210 mm, composed by a solid-state detector with 512 elements silicon for the visible channel (215-1050 nm), and a indium-gallium-arsenide near infrared detector (850-1450 nm) of 256 elements [3]. Both MDIS and MASCS cover the overall Mercury surface revealing color variations which correspond with variation in composition. The first MASCS-VIRS global RGB map (Fig. 1) shows regional variation in reflectance or spectral slopes [4]. In particular, reflectance spectra show no clear evidence of any absorption bands, including the band centered near 1 μm that would be associated with the presence of ferrous iron in silicates, indicating a very low iron content (2-3 wt% FeO or less). Furthermore, the compositional analysis supported by the X-ray and gamma-ray observations confirm the results obtained by VIRS [4]. Similarly, the MDIS-WAC color maps revealed a color variation related to differences in spectral slopes, which allow for discriminating different type of terrains and features, such as smooth plains, intercrater plains and pyroclastic deposits [5]. On the other hand, thanks to MDIS color filter data, an absorption feature centered in the 629 nm filter has been observed in reflectance spectra of Dominici's south wall/rim hollows [6], and a broad, shallow band near 600 nm is found in the Low Reflectance Material (LRM) [7]. In this standpoint, the availability of the data acquired by MESSENGER may therefore be considered an opportunity not only for the planning and the selection of scientific targets for BepiColombo, and in particular for SIMBIO-SYS, but also to improve the knowledge of Mercury surface from the geological and compositional point of view. In this regard, we are working to produce quadrangles color mosaics (Fig. 2) and high resolution color mosaics of smaller areas to define color products and obtain an "advanced" geologic map. The mapping process permits integration of different geological surface information [8] to better understand the planet crust formation and evolution. Merging data from different instruments provides

additional information about lithological composition, contributing to the construction of a more complete geological map.

SIMBIO-SYS and the Visible and Infrared Hyperspectral Imager (VIHI)

SIMBIO-SYS is the first integrated suite containing two cameras and an imaging spectrometer. STC will perform the global mapping in stereo mode, providing the DTM of the entire surface, and color images of a small percentage of the planet, HRIC channel has the primary task to provide images at 5m/pixel scale from periherm (400 km from planet surface), in different bands in the visible, while VIHI channel is an advanced hyperspectral imager realized to study Mercury's surface composition [1]. VIHI channel concept is based on a collecting Schmidt telescope and a diffraction grating spectrometer (Littrow configuration) joined at the telescope focal plane where the spectrometer entrance slit is located [9]. The image of the slit is dispersed by the diffraction grating on a 2-D 256x256 pixels cadmium-mercury-telluride (HgCdTe) detector [9]. Conversely to MASCS-VIRS, which is a pointer spectrometer, VIHI is an imaging spectrometer covering a spectral range between 400 and 2000 nm, with a spectral sampling of 6.25 nm/band, and a FOV of 64 mrad with 256 pixels having each a IFOV of 250 μrad. Since the instrument shall operate in push-broom mode, these characteristics allow to acquire a 25.6 km-wide swath on ground at 100 m/pixel resolution from a 400 km polar orbit. According to the Bepi-Colombo mission science requirements, VIHI must complete a global mineralogical mapping with spatial resolution better than 500 m and local mapping of selected regions of about 10% of the surface with a spatial sampling of 100 m [9]. Considering the characteristics of the instrument and the mission requirements, VIHI will allow for producing compositional map of Mercury never achieved before. VIHI has been fully characterized during an extensive pre launch campaign where the geometric, spectral, radiometric and linearity responses have been determined for the expected range of operative temperatures [10,11]

Acknowledgements

This work was supported by the Italian Space Agency (ASI) within the SIMBIO-SYS project (ASI- INAF contract no. I/022/10/0).

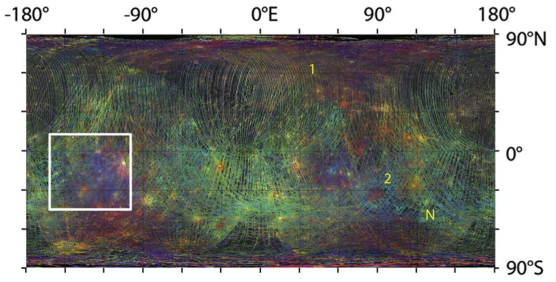

Figure 1: Color composite in simple cylindrical projection maps obtained by MASCS-VIRS data (See [4]). Red channel is the reflectance at 575nm, green channel is 415/750 nm, while Blue channel is 310/390 nm ratio.

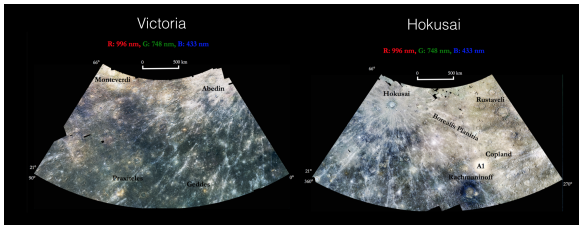

Figure 2: RGB (R: 996nm, G: 748 nm; B: 433 nm) maps of Victoria and Hokusai quadrangle obtained from MDIS-WAC data.

References

[1] Flamini, E. et al., 2010, PSS, 58 (2010) 125-143.

[2] Solomon, S. C. et al., 2008, Science 321 (59)

[3] Espiritu, R. and Malaret, E., 2012, http://pds–geosciences.wustl.edu/messenger/mess–$e_{vh} - -mascs - -2 - -virs - -edr - -v1/messmas_1001/document/virsedrsis.pdf$

[4] Izenberg, N. R. et al., 2014, Icarus 228, 364-374

[5] Denevi , B. W. et al., 2009, Science, 324

[6] Vilas, F. et al., 2016, Geophys. Res. Lett., 43, 1450-1456

[7] Klima, R. L. et al., 2018, 49th Lunar and Planetary Science Conference 2018 (LPI Contrib. No. 2083)

[8] Galluzzi, V. et al., 2016, Journal of Maps.

[9] Capaccioni, F. et al., 2010, IEEE TRANSACTIONS ON GEOSCIENCE AND REMOTE SENSING, 48 (11)

[10] Filacchione, G. et al., 2017, Review of Scientific Instruments 88, 094502

[11] Altieri, F. et al., 2017 Review of Scientific instruments, 88, 094503.

EPSC Abstracts
Vol. 12, EPSC2018-1104, 2018
European Planetary Science Congress 2018

Preliminary color map of the Borealis (H-01) quadrangle of Mercury

N. Nguyen (1,2), N. Bott (1) , A. Doressoundiram (1) ,
(1)LESIA - Observatoire de Paris, Meudon, France, (2)University of Science and Technology of Hanoi, Vietnam
(ngoc.nguyen@obspm.fr)

1. Introduction

This study is part of the Mercury mapping campaign to support the observational strategy of the future BepiColombo mission. The target is the color map of the north polar region - Borealis quadrangle from the multi-band images of Mercury Dual Imaging System Wide Angle Camera (MDIS-WAC) of Messenger mission. Three principal component (high-reflectance plains, intermediate terrains and low-reflectance material) and two minor color units (red spots and hollows) were identified based on the reflectance and the slope of spectra [1].

2. Data set

The surface of Mercury is subdivided into 15 quadrangles. This study focuses on the Borealis (H-01) quadrangle of Mercury, extends from 65° to 90° in latitude and from 0° to 360° in longitude. The data of MDIS-WAC was taken with 12 different bands in visible and near-infrared; however, we just use the data of 8 filters: 433.2, 479.9, 558.9, 628.8, 748.7, 828.4, 898.8 and 996.2 nm (respectively F, C, D, E, G, L, J and I filter) for the scientific analysis.

3. Method

The software ISIS (Integrated Spectrographic Innovative Software) of USGS is used to produce the color map of Borealis. The image processing follows: 1/ Importing the raw data into ISIS format; 2/ Georeferencing to update information of the spacecraft position, pointing, the sun position, etc; 3/ Performing radiometric calibration to remove the bias, the dark current and the flat field; 4/ Polar stereographic projection with 450 m/pixel resolution; 5/ Applying Kaasalainen-Shkuratov photometric correction to normalize the data with lab conditions (incidence angle i=30°, phase angle φ=30° and emission angle e=0°); 6/ Coregistration of each image with filter G; 7/ Stacking and trimming the images to obtain the mosaic of Borealis.[2]

4. Preliminary results and future work

The preliminary RGB map of the Borealis obtained with filters at 996.2, 748.7, and 479.9 nm, respectively, is in Figure 1.

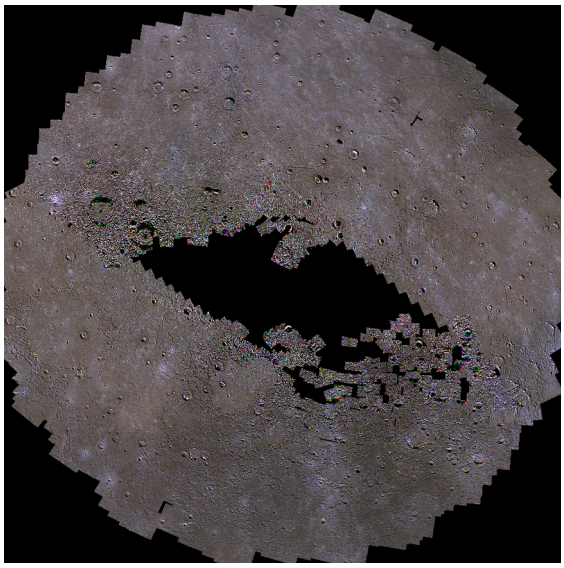

Figure 1: RGB map of the Shakespeare quadrangle (R=996.2 nm, G=748.7 nm and B=479.9 nm)

We will present an analysis of this map. Several method will be applied for example K-means, principal component analysis to classify the surface of the Borealis, similar to N. Bott and F. Zambon in other quadrangles of the Mercury mapping campaign.

Then, the color map will be combined with its geology and the data of Mercury Dual Imaging System (MDIS) to find out regions of interest for the BepiColombo mission.

Acknowledgements

This work is partly supported by the Centre National d'Etudes Spatiales (CNES).

References

[1] Blewett, D. T. et al.: Multispectral images of Mercury from the first MESSENGER flyby: Analysis of global and regional color trends, Earth and Planetary Science Letters, Vol. 285, pp. 272-282, 2009.
[2] N. Bott et al.: The Shakespeare (H-03) quadrangle of Mercury: from color mapping to distinction of lithological heterogeneity, Mercury: Current and Future Science 2018 LPI Contrib. No. 2047, 2018.

EPSC Abstracts
Vol. 12, EPSC2018-1114, 2018
European Planetary Science Congress 2018

Exploraion of the innermost planet Mercury's environment by BepiColombo

Go Murakami (1), Hajime Hayakawa (1) and Masaki Fujimoto (1)
(1) Institute of Space and Astronautical Science, Japan Aerospace Exploration Agency, Sagamihara, Japan
(go@stp.isas.jaxa.jp)

Abstract

Mercury, the innermost planet in the solar system, has the weak planetary magnetic field and forms its magnetosphere. Mercury's magnetosphere is one of the best targets to study a planetary environment exposed to extreme stellar wind. The first Mercury orbiter MESSENGER explored this region and discovered a wide variety of phenomena. However, due to the highly ecliptic orbit with north-south asymmetry and limited capability for plasma measurements, many science topics still remain unsolved. The Mercury Magnetospheric Orbiter (MMO) for the BepiColombo mission will be launched in October 2018. MMO has a complete package of plasma instruments. Here we present how it can contribute to deepen our understanding Mercury's environment by addressing the puzzles raised by MESSEGNER

Introduction

Mercury has the weak planetary magnetic field stands against the intense solar wind in the close proximity of the Sun. Mercury's plasma environment is quite different in the parameters from the well-studied terrestrial magneto-sphere. In addition, recently many Earth-type exoplanets orbiting in habitable zones very close to cool stars (M-dwarfs) were found. Such exoplanets are exposed to extreme stellar winds and ultraviolet radiations. Thus Mercury's magnetosphere is one of the best targets to study planetary environments. Exploring Mercury which is the innermost planet in the solar system plays a key role to understand such extreme environment.

The first Mercury orbiter MESSENGER explored this region and discovered a wide variety of phenomena. For example, Mercury's magnetosphere is much more dynamic than one had predicted. However, due to the highly ecliptic orbit with north-south asymmetry and limited capability for plasma measurements, many science topics still remain unsolved.

The next Mercury exploration mission BepiColombo, which is the international joint project between ESA and JAXA, will be launched in October 2018 and will arrive at Mercury in December 2025. The JAXA's spacecraft Mercury Magnetospheric Orbiter (MMO) is equipped to study the space environment of Mercury. MMO is mainly designed for plasma observations with the complete package of plasma instruments consortium and is expected to extract essential elements of space plasma physics that become visible in the Hermean environment. In addition, ESA's Mercury Planetary Orbiter (MPO) also has several instruments for plasma measurements, so we can investigate Mercury's environment with two points measurements.

BepiColombo/MMO

The MMO spacecraft will have a ecliptic polar orbit with a period of 9.3 hours, a periapsis of 590 km, and a apoapsis of 11640 km. The orbital plane is same as that of MPO. The MMO will be spin-stabilized with a rotation rate of 15 rpm and a spin axis almost perpendicular to the orbital plane of Mercury around the Sun.

MMO has a complete package of plasma environment measurements: Magnetic Field measurement (MGF), Plasma Wave Instrument (PWI), and Mercury Plasma Particle Experiment (MPPE). These instrument will be operated as a plasma measurement consortium. In addition, two more instruments are installed onboard MMO to investigate Mercury's exosphere and dust environment: Mercury Sodium Atmospheric Spectral Imager (MSASI) and Mercury Dust Monitor (MDM). The instruments onboard MMO are listed in Table 1. It also includes

the comparison with the similar instruments onboard MESSENGER.

Table 1: Science instruments list onboard MMO

	BepiColombo/MMO				MESSENGER	
Plasma (SW, MS)	MPPE	MEA	Low-energy electrons	3eV-26keV	-	
		MIA	Low-energy ions	15eV-29keV	FIPS	50eV-13keV 1-40 amu/e
		MSA	Ion mass spectroscopy	1eV-38keV 1-60 amu/e m/ Δm = 40 (<13keV) m/ Δm = 10 (>13keV)		
		HEP-ion	High-energy ions	30keV-1.5MeV	EPS	25keV-1MeV
		HEP-ele	Hihg-energy electrons	30keV-700keV	EPS	25keV-1MeV
		ENA	Plasma imaging	10eV-3.3keV	-	
	MGF		Magnetic field	DC - 64Hz L: <0.25Hz, M: 8Hz	MAG	DC - 20Hz
	PWI		Electric field, plasma wave, radio wave	DC - 10MHz (E) few - 640kHz (B)	-	
Exosphere	MSASI		Na-exosphere image	Spatial resol.: 3-30km R = 65000	MASCS	Spatial reol.: 25-800km R = 1000
Dust	MDM		Dust environment	10s pg*km/s	-	

Almost all of tests in ESA's test center (ESTEC) have successfully finished and soon the spacecraft will be shipped to the launch site in French Guiana. So now we can focus on science observation planning.

MMO has large constraints on science operations, such as thermal issue and limited telemetry rate. Due to the thermal issue each science instrument cannot always be turned on. In addition, due to the low telemetry rate in average, only a part (~20-30%) of science mission data with high resolution can be downlinked. Therefore, in order to maximize the scientific results and outcomes to be achieved by MMO, we are now working to optimize the science observation and downlink plans in detail.

EPSC Abstracts
Vol. 12, EPSC2018-1129, 2018
European Planetary Science Congress 2018

SERENA particle package: the link between the environment and Mercury ready to launch on board BepiColombo

Stefano Orsini (1), Anna Milillo (1) Stefano Livi (2), Herbert Lichtenegger (3), Stas Barabash (4), Elisabetta De Angelis (1), Esa Kallio (5), Peter Wurz (6), Angelo Olivieri (7), Christina Plainaki (7), Alessandro Aronica (1), Francesco Lazzarotto (1), Rosanna Rispoli (1) and the SERENA Team
(1) INAF/IAPS, Rome, Italy; (2) SouthWest Research Institute (SwRI), USA; (3) Institut für Weltraumforschung (IWF), Austria; (4) Swedish Institute of Space Physics (IRF), Sweden; (5) Bern University (UniBe), Switzerland; (6) Finnish Meteorological Institute (FMI), Finland; (7) Italian Space Agency (ASI), Italy (stefano.orsini@iaps.inaf.it).

Abstract

At October 2018 the ESA-JAXA BepiColombo mission to Mercury will be launched from Kourou site. The particle sensor package, Search for Exospheric Refilling and Emitted Natural Abundances (SERENA) on MPO is a key experiment for the investigation of the Mercury environment. SERENA is composed by for units devoted to the detection of neutral and ionised particles in the Hermean environment; the interaction between energetic plasma particles, solar radiation and micrometeorites with the Hermean surface gives rise to both thermal and energetic neutral particle populations in the near-planet space; such populations will be recorded by the SERENA Neutral Particle Analysers (NPA): a mass spectrometer and a Energetic Neutral Atom (ENA) imager (STROFIO and ELENA). The photo-ionised or charged component of the surface release processes as well as the precipitating and circulating plasma in the Hermean magnetosphere will be recorded by the SERENA ion spectrometers (IS): two ion sensors (PICAM and MIPA).
The experiment and the scientific objectives will be presented together with the performances of each unit: ELENA, STROFIO, PICAM and MIPA, also in the context of joint investigation with other BepiColombo instruments.

1. Introduction

The proximity of Mercury to the Sun makes its environment particularly extreme. Mercury's weak intrinsic global magnetic field supports a small, but dynamic, magnetosphere. The plasma in Mercury's space environment coexists with the planet's exosphere and strongly interacts with the surface. In fact, Mercury's environment is a complex and tightly-coupled system where the magnetosphere, exosphere, and surface experience temporal and spatial variations linked to each other [1].
For this reason, having the possibility of simultaneous information on the external conditions and the close-to-planet environment would greatly help in the definition of the active processes. SERENA [2], observing the environment from the MPO spacecraft is a key experiment being the link between the measurements in the solar wind or in the tail from the MMO and the surface observations from the MPO.

2. SERENA package

SERENA four sensors are: ELENA (Emitted Low Energy Neutral Atoms), STROFIO (Exososphere Mass Spectrometer), PICAM (Planetary Ion CAMera), MIPA (Miniature Ion Precipitation Analyzer) (Figure 1).

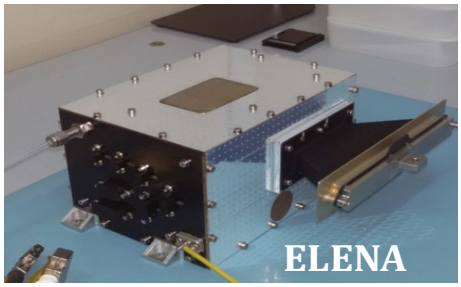

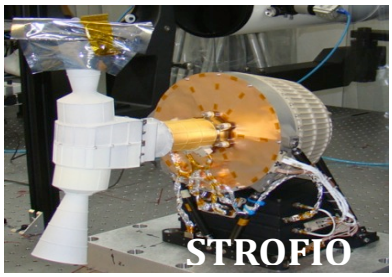

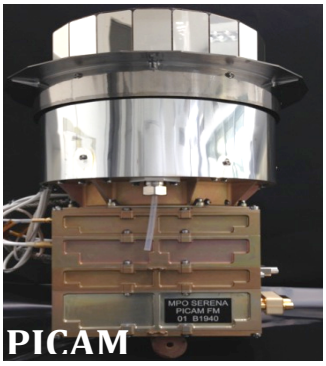

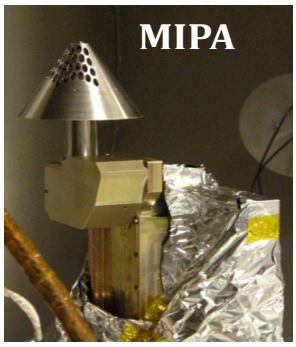

Figure 1: SERENA four sensors: ELENA, STROFIO, PICAM and MIPA.

Acknowledgements

SERENA is primarily supported by the Italian Space Agency (SERENA ASI-INAF agreement), with contributions of other international partners for the provision of STROFIO, PICAM, and MIPA.

References

[1] Milillo et al., BepiColombo Special Issue on Planetary and Space Science, doi:10.1016/ j.pss.2008.06.005, Vol 58, pp 40–60, 2010.

[2] Orsini et al., BepiColombo Special Issue on Planetary and Space Science, doi:10.1016/ j.pss.2008.06.005, Vol 58, pp 385-395, 2010 ,

EPSC Abstracts
Vol. 12, EPSC2018-1139-1, 2018
European Planetary Science Congress 2018

Constraining the interior structure of Mercury by geodesy data

Marie-Hélène Deproost (1,2), Attilio Rivoldini (2) and Tim Van Hoolst (1,2)
(1) KU Leuven, Belgium, (2) Royal Observatory of Belgium (marie-helene.deproost@oma.be)

Abstract

Geodetic properties of planets are strongly related to their interior structure and can be used to infer Mercury's deep structure. The moments of inertia of the planet and the core, deduced from combination of Mercury's gravity field and rotation, constrain the mass distribution inside the planet, giving information on the core and mantle densities and on the position of the core-mantle boundary. Additional constraints on the core size and on the rigidity of the shell and density can be obtained from tides.

In this study we combine the 88-day libration amplitude, the obliquity, the gravitationnal field, and the tidal Love number k_2 in order to constrain Mercury's interior structure, and in particular its core and inner core sizes. Our interior models are in agreement with thermal evolution calculations of the planet. We consider iron-rich cores with light elements and mantle bulk compositions in agreement with the reducing formation conditions of Mercury. Recent thermoelastic and melting properties of the constituents are used.

Acknowledgements

This work was financially supported by the Belgian Federal Science Policy Office (BR/143/A2/COMEIN)

EPSC Abstracts
Vol. 12, EPSC2018-1184, 2018
European Planetary Science Congress 2018

The ISA accelerometer, in view of BepiColombo launch

V. Iafolla, E. Fiorenza, C. Lefevre, D.M. Lucchesi, M. Lucente, C. Magnafico, R. Peron, F. Santoli
Istituto di Astrofisica e Planetologia Spaziali (IAPS-INAF), Roma, Italy (valerio.iafolla@iaps.inaf.it)

Abstract

The BepiColombo Italian Spring Accelerometer (ISA) is a component of the dedicated suite of instruments which will perform the so-called Radio Science Experiments in order to study gravitational field, internal structure and rotational state of the planet Mercury, and to verify important predictions of the general theory of relativity. Its main role is the measurement of non-gravitational accelerations acting on the surface of the Mercury Planetary Orbiter spacecraft, thereby enabling to work on a virtually drag-free satellite. In this talk the concept, design and development of the instrument are reviewed, along with its main scientific products. The development and testing of the data processing procedures, as well as the definition of the instrument operations for the various mission phases, are also presented, with special emphasis on the activities foreseen for the cruise phase.

1. Introduction

The ESA mission BepiColombo (BC) is a challenging programme aimed at the exploration of planet Mercury and its space environment [1, 13]. It comprises two spacecraft, the Mercury Planetary Orbiter (MPO) and the Mercury Magnetospheric Orbiter (MMO) that will be launched in the second half of 2018 and will reach Mercury after almost seven years of cruise. The MPO spacecraft will be dedicated mainly to the study of the geology and geophysics of the planet itself; it will host a suite of instruments devoted to the so-called Radio Science Experiments (RSE) in which, by precisely tracking the MPO orbital motion and carefully modelling its dynamics, the gravitational field and rotation state of the planet could be reconstructed, along with a series of tests of general relativistic effects. For a deep discussion of the RSE concept and its realisation, see [9, 10, 5, 11, 12].

The parameters of interest (related as said to Hermean geophysics and to fundamental physics) can be extracted from the observational data using a procedure of orbit determination and parameter estimation, usually called POD (precise orbit determination). A model for the orbital dynamics of the spacecraft is fitted to the tracking data, in this case distance and velocity (called also *range* and *range-rate*) of the spacecraft with respect to one or more Earth-bound stations. The model should be sufficiently accurate to describe the orbital dynamics at a level comparable to the information content of tracking. It has to be noticed that, while the majority of the forces acting on the spacecraft in orbit around Mercury comes from its gravitational attraction as well as from the attraction of the other bodies of the Solar System, a non-negligible part is constituted by surface forces resultant from the interaction of the spacecraft body with particles and fields in the near-Mercury environment (the so-called *non-gravitational perturbations*). A precise modelisation of these forces is not easy [7]: an effective alternative is the direct measurement of the total resulting acceleration via an on-board accelerometer. This is the BC choice, employing the ISA (Italian Spring Accelerometer) accelerometer [3, 4, 2]. ISA is a three-axis accelerometer: it features three sensing elements arranged in a suitable geometrical configuration, each one sensing a one-dimensional component of the overall signal. These three channels can then be properly combined in order to obtain the total acceleration vector acting on a given reference point (called *vertex*). The time series of acceleration values so measured is then an input to the POD: the MPO becomes therefore a sort of *a posteriori* drag-free satellite.

2. Scientific objectives and accelerometer role

The BC RSE can be roughly divided into three different but nevertheless deeply connected experiments, respectively gravimetry, rotation and relativity. The gravimetry and rotation experiments aim to determine respectively the global Mercury gravity field and its rotational state, to constrain models of the planet internal structure. Goal of the relativity experiment is to test selected predictions of the general relativity theory (namely the perihelion precession and the Shapiro

time delay), constraining several PPN (parameterized post-Newtonian) parameters. An effective POD is the key for the achievement of these objectives.

The ISA accelerometer will directly measure the surface accelerations acting on the MPO spacecraft, to be subsequently used in the POD procedure. These accelerations are mainly due to photons from the Sun or from the planet surface being reflected-absorbed-diffused by the surface of the spacecraft, and to radiation anisotropically emitted by the spacecraft body. they are rather difficult to model, depending in a complex way on the spacecraft attitude and on the (possibly time-dependent) optical properties of its surfaces. A simple, *cannonball*, model for the strongest effect (*direct solar radiation pressure* — see e.g. [8, 6]) can only provide order-of-magnitude estimates of the force. More elaborate models (that would take into account the response of the various parts, as solar panels and antennae) could reasonably hope to achieve an accuracy of at most 10 % of the total expected signal [7]; this is not enough for the RSE purposes, and this is indeed the motivation for measuring them directly with an accelerometer.

An ideal accelerometer is a device which measures the three components of an acceleration vector acting on a defined reference point, usually the center of mass (CoM) of the spacecraft. Such an ideal instrument, placed just at the spacecraft CoM, measures only the non-gravitational accelerations: it is completely insensitive to gravitational effects. A real, extended accelerometer could sense also spurious effects, due e.g. to gravitational gradients. The induced measured spurious signal has to be properly accounted for (filtered out / modelled). This task is generally known as *data reduction*.

References

[1] J. Benkhoff, J. van Casteren, H. Hayakawa, M. Fujimoto, H. Laakso, M. Novara, P. Ferri, H. R. Middleton, and R. Ziethe. BepiColombo—Comprehensive exploration of Mercury: Mission overview and science goals. *Plan. Space Sci.*, 58:2–20, January 2010.

[2] V. Iafolla, E. Fiorenza, C. Lefevre, D. M. Lucchesi, M. Lucente, C. Magnafico, R. Peron, and F. Santoli. The BepiColombo ISA accelerometer: Ready for launch. In *2016 IEEE Metrology for Aerospace (MetroAeroSpace)*, pages 538–544, June 2016.

[3] V. Iafolla, E. Fiorenza, C. Lefevre, A. Morbidini, S. Nozzoli, R. Peron, M. Persichini, A. Reale, and F. Santoli. Italian Spring Accelerometer (ISA): A fundamental support to BepiColombo Radio Science Experiments. *Plan. Space Sci.*, 58:300–308, January 2010.

[4] V. Iafolla and S. Nozzoli. Italian spring accelerometer (ISA) a high sensitive accelerometer for "BepiColombo" ESA CORNERSTONE. *Plan. Space Sci.*, 49:1609–1617, December 2001.

[5] L. Imperi and L. Iess. Testing general relativity during the cruise phase of the BepiColombo mission to Mercury. *Metrology for Aerospace (MetroAeroSpace)*, (2015 IEEE):135–140, 2015.

[6] D. M. Lucchesi. Reassessment of the error modelling of non-gravitational perturbations on LAGEOS II and their impact in the Lense-Thirring determination. Part I. *Plan. Space Sci.*, 49:447–463, April 2001.

[7] D. M. Lucchesi and V. Iafolla. The Non-Gravitational Perturbations impact on the Bepi-Colombo Radio Science Experiment and the key rôle of the ISA accelerometer: direct solar radiation and albedo effects. *Celestial Mech. Dyn. Astr.*, 96:99–127, October 2006.

[8] A. Milani, A. M. Nobili, and P. Farinella. *Non-gravitational perturbations and satellite geodesy*. Adam Hilger, Bristol, 1987.

[9] A. Milani, A. Rossi, D. Vokrouhlický, D. Villani, and C. Bonanno. Gravity field and rotation state of Mercury from the BepiColombo Radio Science Experiments. *Plan. Space Sci.*, 49:1579–1596, December 2001.

[10] A. Milani, D. Vokrouhlický, D. Villani, C. Bonanno, and A. Rossi. Testing general relativity with the BepiColombo radio science experiment. *Phys. Rev. D*, 66(8):082001, October 2002.

[11] G. Schettino, S. Cicalò, S. Di Ruzza, and G. Tommei. The relativity experiment of MORE: Global full-cycle simulation and results. *Metrology for Aerospace (MetroAeroSpace)*, (2015 IEEE):141–145, 2015.

[12] G. Schettino, L. Imperi, L. Iess, and G. Tommei. Sensitivity study of systematic errors in the Bepi-Colombo relativity experiment. In *2016 IEEE*

Metrology for Aerospace (MetroAeroSpace), pages 533–537, June 2016.

[13] T. Spohn, F. Sohl, K. Wieczerkowski, and V. Conzelmann. The interior structure of Mercury: what we know, what we expect from Bepi-Colombo. *Plan. Space Sci.*, 49:1561–1570, December 2001.

EPSC Abstracts
Vol. 12, EPSC2018-1186-1, 2018
European Planetary Science Congress 2018

Bedrock layering revealed by hollows on Mercury

Valentina Galluzzi (1), Lorenza Giacomini (1), Alice Lucchetti (2), Maurizio Pajola (2), Pasquale Palumbo (3,1), Gabriele Cremonese (2)
(1) INAF-IAPS, Istituto di Astrofisica e Planetologia Spaziali, Rome, Italy (valentina.galluzzi@iaps.inaf.it), (2) INAF-OAPD, Osservatorio Astronomico di Padova, Padua, Italy, (3) Dipartimento di Scienze e Tecnologie, Università degli Studi di Napoli "Parthenope", Naples, Italy.

Abstract

We performed a thorough analysis of MESSENGER MDIS-NAC images with a resolution higher than 10 m/pixel located on top of central peaks and peak rings of Mercury. Sporadically, these frames capture hollows on top of the peaks revealing a not-previously detected layered structure at their floors. Here we investigate their origin and possible significance.

1. Introduction

The Mercury Dual Imaging System (MDIS), on-board the NASA MESSENGER (Mercury Surface, Space, ENvironment, GEochemistry, and Ranging) spacecraft, provided over 250,000 images, ~26,000 of which were gathered at a resolution better than 10 m/pixel by the Narrow Angle Camera (NAC). NAC images with such resolution are found at high-northern latitudes, where MESSENGER elliptical orbit reached its minimum altitude of 200 km, constantly decreasing during its final crashing phase. Such high-resolution images are key to uncover the morphology, texture and structure of the Hermean surface, however, Mercury is extensively covered with regolith that does not permit to look directly at the pristine bedrock. The areas where such exposed bedrock is most likely detected are usually located on steep scarps, such as crater walls, or crater central peaks and peak rings, where mass wasting processes cause regolith removal. In particular, crater central peaks often reveal the sub-surface lithology that was uplifted, tilted and strained by the impact process [1]. Moreover, on Mercury, regolith removal might occur also via hollows formation which are supposed to form because of a process of sublimation or volatile loss [2,3]. In order to find the bedrock exposures, we checked all NAC images with a resolution better than 10 m/pixel that captured locations of interest, such as those described above, with particular attention to those craters that also encompass hollows. Nonetheless, chances of finding such evidence are very low because of the scarce coverage of such high-resolution images that need to capture both peaks and hollows.

2. Exploring the data

We investigated more than 26,000 MDIS/NAC frames with a resolution better than 10 m/pixel (hereafter called HR-NAC), and manually selected all those footprints located on top, or nearby, steep scarps such as crater central uplifts, crater walls, fault scarps and hollows on a GIS environment. This work was repeated twice by different people -to avoid missing any useful frame- by dividing the selected footprints into categories (i.e., central peaks, fault scarps, etc.). Secondly, we batch-processed the selected frames with the USGS ISIS3 software to visually check the images on the GIS starting from the central peak category.

3. Layering revealed

We found more than 900 HR-NAC footprints located on the categories of interest. More than 300 of these are related to crater central peaks and peak rings. After importing the latter frames into the GIS, we verified that only few tens of these show a texture that could be seemingly be related to bedrock exposure. However, three peak-related HR-NAC frames surprisingly revealed evidence of putative layered and uplifted mega-blocks outcropping on the floor of some hundreds-meters wide hollows (e.g., Figure 1). Although it is quite common to observe tilted layered blocks in correspondence of crater uplifts on Earth and Mars [e.g., 1,4], it was never observed on Mercury before. In fact, observing such features implies the existence of layered bedrock before the crater formed. No evidence of layering was provided for Mercury so far, however, it is possible that the surface's widespread lava flows have undergone a layering process, whether a) flow interruptions occurred causing a bedding discontinuity, or b) the high temperature difference at the surface of Mercury caused a cyclic cooling of the lava flow surface. By measuring the putative layers drawn in Figure 1 (right) we estimate an almost

constant layer width of 10-16 m. We aim at repeating the measurements also on other similar features found elsewhere on Mercury.

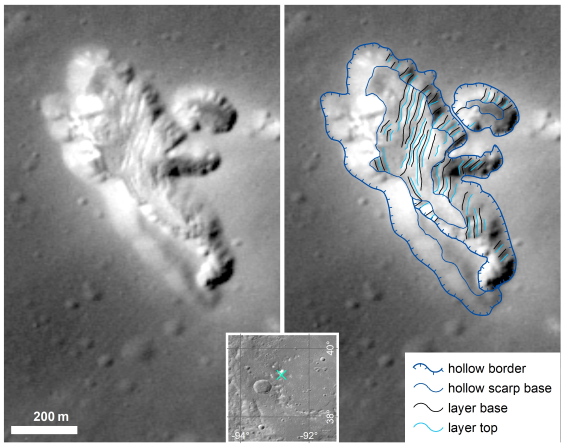

Figure 1: Hollow located on Al-Hamadhani western peak ring (inset) as shown by the 4 m/pixel MDIS/NAC frame EN1066825461M (left). We used a polyline layer to mark the main morphological features, including the putative tilted layers (right).

4. Summary and future work

We found evidence of putative layered Hermean bedrock outcropping on the floor of some hollows located in correspondence with crater central peaks and peak rings. This was possible thanks to an accurate analysis of hundreds of MDIS/NAC images with a resolution better than 10 m/pixel. The occurrence of such features revealed to be less than 1% of the coverage provided by HR-NAC frames. This depends on several conditions that must occur together: 1) the HR-NAC frame must be on top of a crater uplift; 2) the crater uplift must have hollows causing regolith removal; 3) the bedrock of the analyzed area had to be layered prior to the impact. Since Mercury has no sedimentary rocks on its surface, the origin of such layering must be investigated and could be linked to lava flow evolution. Another cause of the observed lineaments could be due to rock parallel and systematic fracturing. With this work we aim at understanding the origin and evolution of such discontinuities. To this end, we are checking other HR-NAC frames occurring also on other locations such as crater walls, fault scarps and other hollows occurring away from crater uplifts. Finally, we will compare our results with what is usually observed on Earth or Mars.

Acknowledgements

We gratefully acknowledge funding from the Italian Space Agency (ASI) under ASI-INAF agreement 2017-47-H.0. We also acknowledge the use of MESSENGER MDIS image mosaics processed by NASA/Johns Hopkins University Applied Physics Laboratory/Carnegie Institution of Washington.

References

[1] Caudill, C.M. et al.: Layered MegaBlocks in the central uplifts of impact craters, Icarus, Vol. 221, pp. 710-720, 2012.

[2] Blewett, D.T. et al.: Mercury's hollows: Constraints on formation and composition from analysis of geological setting and spectral reflectance, JGR Planets, Vol. 118, pp. 1013-1032, 2013.

[3] Thomas, R.J. et al.: Hollows on Mercury: Materials and mechanisms involved in their formation, Icarus, Vol. 229, pp. 221–235, 2014.

[4] Kenkmann, T. et al.: Structural geology of impact craters, Journal of Structural Geology, Vol. 62, pp. 156-182, 2014.

EPSC Abstracts
Vol. 12, EPSC2018-1209, 2018
European Planetary Science Congress 2018

Time-varying magnetic fields of Mercury

Ingo Wardinski, Benoit Langlais and Erwan Thébault
(1) Laboratoire de Geodynamique et de Planetologie, Universite de Nantes, France (ingo.wardinski@univ-nantes.fr)

Abstract

In this study we derive spherical harmonic models of Mercury's magnetic field from measurements of the MESSENGER mission. The models describe large scale external and internal magnetic fields. The Gauss coefficients of the magnetic fields mainly show periodic temporal variations that are related to Mercury's orbital period around the sun. These periods are found for external and internal field variations, where internal field variations appear as internal variation, but may also originate in regions below MESSENGER and above Mercury's surface. It is known that magnetospheric fields are due to interactions of the planet's internal magnetic field and the interplanetary (solar) magnetic field. Previous research suggested internal field variations to be generated by an induction effect in Mercury's core. Such process may show a time lag between the causing external field variation and the core response. However, we do not find such time lag, which may be due to the limited temporal resolution of our analyzes. Furthermore, our new results suggest that magnetic fields may also be generated in Mercurys exosphere. Most likely by transient current systems. Possible mechanisms that generate these transient exospheric magnetic fields include wind-driven electrical current systems, and the diamagnetic effect. These results may hold implications for the production of electrically charged particles in Mercury's exosphere at altitudes upward 400 km above the Planet's surface, but also for the electrical conductivity of Mercury's mantle and crust.

1. Introduction

The planet Mercury is characterized by a peculiar internal magnetic field. Although it has a deep origin as for the Earth, it is much weaker, strongly axisymmetric, and has a much larger quadrupole-to-dipole ratio at its surface than on the Earth [1, 2, 3]. The current data coverage (by MESSENGER, between March 2011 and April 2015) is too limited to derive a global model with a high spatial resolution. However, the duration of the mission, in excess of 16 Hermean years, makes it possible to study if there are any temporal changes on the global scale. We investigate these variations of internal and external origin, as modeled from the measurements once a mean magnetic field model has been subtracted. In this study we analyze these variations and correlate them with the orbital parameters.

2. MESSENGER data and mean model

MESSENGER orbited around Mercury During this interval it flew at low altitude (below 1000 km) mainly over the northern hemisphere. This led to an uneven distribution for topics related to the description and understanding of the Hermean magnetic field. Due to this data distribution it is only possible to compute low degree and order spherical harmonic global models (e.g., [1-2]), or local models (over the northern hemisphere) with a better resolution (e.g., [3]). All these models are temporally averaged, and describe the mean magnetic field of Mercury. For self-consistency we start with the raw magnetic field measurements and compute a mean magnetic field model up to degree and order 3. We consider only night-side measurements below 1000-km altitude. The derived model is very similar to that of [3]. We then subtract the measurements from this model in order to focus on the time-varying residuals. Time-varying model Measurements are sorted into temporal bins so that each contains 8 consecutive orbits (provided that there are no significant gaps between orbits). For each subset, a SH degree and order 1 internal and external magnetic field model is computed. The misfit of each subset significantly improves, going from about 50 nT (after removal of a mean global magnetic field) to about 20 nT (after modeling of the considered subset).

3. Results

The results consist in a time series of 6 times 450 coefficients, for the internal (g10, g11, and h11) and ex-

ternal (q10, q11, and s11) parts. We show on Figure. 1 time series of the external and internal axial dipole terms.

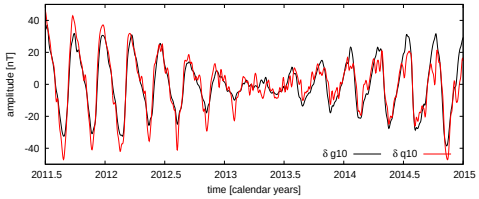

Figure 1: Time series of Gauss coefficients g10 (black) and q10 (red) over the duration of the MESSENGER mission.

4. Summary and Conclusions

External and internal magnetic field variations are highly correlated and present a periodic temporal variability. Their main period is 88 days; i.e., the duration of one Hermean revolution around the Sun. This periodic variation seems to be modulated by an additional term, which cancels out in the beginning during the first half of 2013. This corresponds to the time when MESSENGER's periapsis was the closest to the pole. Similar observations are made for the equatorial dipole terms, although the main periods are different, with two overlapping ones at 58 and 176 days (i.e., one day and two years or one solar day). In this paper we will show several statistical analyzes, which all confirm these figures. These correlated time variations of internal and external origin are very intriguing and their exact origin is under investigation. The fact that most periods are associated with the orbital parameters of Mercury make an external origin more likely, with possibly different source regions.

Acknowledgements

This work is supported by a grant of the Agence Nationale de la Recherche, ANR-13-BS05-0012, and by CNES in the frame of the BepiColombo project.

References

[1] Anderson, B. J., Johnson, C. L., Korth, H., Winslow, R. M., Borovsky, J. E., Purucker, M. E., Slavin, J. A., Solomon, S. C., Zuber, M. T., & McNutt, Jr., R. L., 2012. Low-degree structure in Mercury's planetary magnetic field, *Journal of Geophysical Research (Planets)*, **117**, E00L12.

[2] Johnson, C. L., Purucker, M. E., Korth, H., Anderson, B. J., Winslow, R. M., Al Asad, M. M. H., Slavin, J. A., Alexeev, I. I., Phillips, R. J., Zuber, M. T., & Solomon, S. C., 2012. MESSENGER observations of Mercury's magnetic field structure, *Journal of Geophysical Research (Planets)*, **117**, E00L14.

[3] Thebault, E., Langlais, B., Oliveira, J., & Amit, H., 2016. A time-averaged model of the Hermean's magnetic field, 15. Symposium on Study of the Earth's Deep Interior.

EPSC Abstracts
Vol. 12, EPSC2018-1216-2, 2018
European Planetary Science Congress 2018

Ground-Based BepiColombo Support with the Rapid Imaging Planetary Spectrograph (RIPS)

Carl Schmidt (1,2), Jeffrey Baumgardner (1), Luke Moore (1) and Tom Bida (3)
(1) Boston University, Boston, USA (schmidtc@bu.edu) (2) LATMOS, CNRS, Paris, FR (3) Lowell Observatory, Flagstaff, USA (bida@lowell.edu)

Abstract

Coupling between Mercury's exosphere and magnetosphere is complex and poorly understood. Accordingly, this will be a focused topic study for BepiColombo instruments like MSASI, PHEBUS, SERENA and others. The mission's two orbiters have tight operational constraints, however, largely due to the extreme thermal environment. Ground-based imaging of the exosphere lends valuable support to this effort by offering a global synoptic view of the measurements made *in situ.*

We present "first light" results from the Rapid Imaging Planetary Spectrograph (RIPS). This instrument uses extremely high cadence to overcome the blurring effects of the Earth's atmosphere. The technique easily resolves the brightness enhancements observed near Mercury's magnetic cusps, which are potentially sensitive to particle precipitation and space weather effects. Global sodium and potassium imaging are viable by reconstruction from thousands spectra while scanning over the disk. First results on March 15, 2018 show clear enhancements of comparable brightness near the northern and southern cusp footprints and are broadly consistent with adaptive optics results (Baumgardner et al., 2008, Schmidt et al., 2016)

1. Exosphere Observations

Ground-based observations of Mercury are intrinsically difficult due to its proximity to the Sun. The single-point measurements from the MESSENGER/MASCS instrument paint a very static picture of the exosphere with only seasonal variations (Cassidy et al., 2015). Ground-based measurements instead suggest a very dynamic exosphere that is strongly coupled to the magnetosphere (e.g., Potter and Morgan, 1990; Leblanc et al., 2009). This inconsistency can most likely be attributed to a combination of the difficultly of ground-based observations of objects in close proximity to the Sun, and the limited viewing geometry provided by the MESSENGER orbit.

RIPS will be able to monitor the sodium and potassium exospheres when Mercury is well separated from the Sun. First light results produced a spectral resolution of ~80,000, which is ideal for separating potassium emissions from telluric absorption, utilizing the planet's Doppler shift. Cross-sections of emissions in the tail structure are also viable within a given night, provided the telescope pointing is stable on minute timescales. The instrument will be installed on the AEOS 3.7m telescope in June and on the McDonald 2.1m telescope in December 2018.

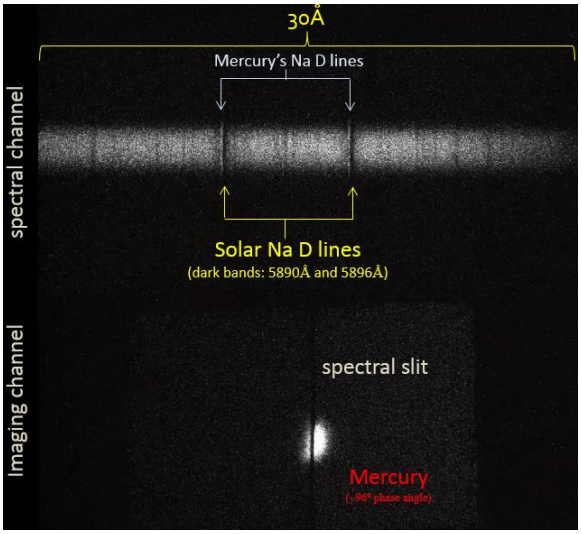

Figure 1: Characteristic 0.05 second frame from the Perkins 1.8m telescope on March 15, 2018. Over the 15 min, nearly 5000 such frames were taken, allowing excellent reconstruction of the exosphere from the top ~2% of frames with best spatial registration.

References

[1] Baumgardner, J.; Wilson, J.; Mendillo, M., Imaging the sources and full extent of the sodium tail of the planet Mercury, *GRL* (2008).

[2] Schmidt, C.; Reardon, K.; Killen, R. M.; Gary, D. E.; Ahn, K.; Leblanc, F.; Baumgardner, J. L.; Mendillo, M.; Beck, C.; Mangano, V. Absorption by Mercury's Exosphere During the May 9th, 2016 Solar Transit. *AGU Conf. Proc.* (2016).

[3] Cassidy, T. A.; Merkel, A. W.; Burger, M. H.; Sarantos, M.; Killen, R. M.; McClintock, William E.; Vervack, R. J. Mercury's seasonal sodium exosphere: MESSENGER orbital observations, *Icarus* (2015).

[4] Potter, A. E.; Morgan, T. H., Evidence for magnetospheric effects on the sodium atmosphere of Mercury, *Science* (1990).

[5] Leblanc, F.; Doressoundiram, A.; Schneider, N.; Massetti, S.; Wedlund, M.; López Ariste, A.; Barbieri, C.; Mangano, V.; Cremonese, G. Short-term variations of Mercury's Na exosphere observed with very high spectral resolution, *GRL* (2009).

EPSC Abstracts
Vol. 12, EPSC2018-1276, 2018
European Planetary Science Congress 2018

BepiVR: Virtual Reality for BepiColombo outreach

Romolo Politi (1), Emanuele Simioni (2), Gabriele Cremonese (2), Valentina Galluzzi (1), Carmelo Magnafico (1), Valeria Mangano (1), Fabrizio De Marchi (3), Cristina Re (2), Domenico Romano(1)
(1) IAPS-INAF, Rome, Italy, (2) OAPD-INAF, Padua, Italy, (3) University of Rome "La Sapienza", Rome, Italy (Romolo.Politi@inaf.it)

Abstract

We present the project for an application for Android to introduce the public to the ESA BepiColombo mission, by using the Virtual Reality (VR) technology. VR technology demonstrated its versatility and power in graphic or industrial ambient in the last years and it earned the consideration of science community, in particular in geospatial and astronomic field. We will describe the contents that will be disseminated by the application, some technical and scientific concepts and a demo of the videos that can potentially be produced to demonstrate the high level of involvement that the VR technology can provide.

1. Introduction

The ESA cornerstone mission BepiColombo - to be launched in October 2018 to Mercury - is one of first ESA mission that will benefit of immersive experience for visualization of the data analysis. Some instruments, like the stereo camera of the instrument suite SIMBIO-SYS [1] , are already devoted to produce data that fit perfectly with this kind of approach. In addition, the synergy of different instruments onboard BepiColombo can also benefit of this tool (i.e. by visualizing the ionized and neutral particles around Mercury together with the planetary magnetic field, or dual measurements of the magnetic field itself as observed simultaneously from the two spacecraft MPO and MMO) This new technology could be used also as a valid support to the public outreach associated to the BepiColombo mission, by offering an appealing experience and giving the opportunity to transmit to the public a wide variety of information on the mission, on Mercury characteristics and different environments, and on the many scientific questions still open about the planet Mercury. Here we present the concept of the novel application, with a focus on the contents that we want to transmit to the user, a conceptual scheme of the information offered, and a demo of the video to be considered as a teaser for our application.

2. The Contents

We can organize the information into four different categories: the mission; the Mercury planet, the cruise and the scientists work.

2.1. The Mission

We display a 3D model of the spacecraft, the Mercury Composite Spacecraft (MCS), with the possibility to explode it in its three main modules: Mercury Magnetospheric Orbiter (MMO), Mercury Planetary Orbiter (MPO) and Mercury Transfer Module (MTM). From the modules hosting the payload it will be possible to extract each single instrument, open it and see a simple functional scheme, with an introduction at the phenomena measured (at different difficulty levels as defined by the user), and the technology used for the measure.
A special dashboard will help the user to understand the scientific objectives of the mission and how the answers can contribute to increase our knowledge. A special section will be devoted to the technology challenges faced. It will be possible to explore, also, the information about the launch vehicle.

2.2. The Mercury Planet

Data acquired from the previous missions will be implemented to create a VR reconstruction of some of the many different environments of Mercury (i.e. exosphere, magnetosphere, surface and interior) in order to describe the heritage of the previous explorations and explain the open issues to which BepiColombo aims to provide an answer.
We are discussing about the possibility to use a virtual assistant that can drive the user on a standard path through the information, with the possibility to personalize the experience by the interaction with it.

2.3. The Cruise

A 3D diagram of the BepiColombo route to Mercury will be shown and accompanied by some sheets to describe the various phases and explain the details of some special maneuvers (like the gravity assists or the electric thrusted arcs) and the physics behind them. During the swing-bys at the Earth and at Venus, windows could be opened to give additional information on the Earth-Moon system, and on a reconstruction of Venus as derived from the ESA mission Venus Express.

2.4. The Scientists Work

We will be planning a "Who's Who" section with the personal card of the scientists involved in the mission, starting from Giuseppe (Bepi) Colombo, the Italian engineer and mathematician inspirer of the mission. We are also exploring the possibility of an interview with some protagonists using 3D videos, especially the Principal Investigators of the instruments on board the spacecraft.
A section will be dedicated also to describe the genesis of a space instrumentation starting from the first idea of a scientist, through the engineering development of prototypes and up to the final flight model and its integration on the satellite.

We are starting to develop the application for smartphones that will use the Android SDK technology. This approach, in our opinion, can maximize the audience. The possibility to host the information on a mobile device give the opportunity to have a high dissemination rate. The developing of the application without the requirement of an active viewer, that mean very low costs for the viewer i.e. using a Google Cardboard™, could be an added value for the application. We are evaluating also the possibility to create an option for a multi-user experience. In this case the computation load will be really high, and it could not be delegate to a smartphone, but to a little computation farm, using the smartphone as a simple display. It is clear that this option could be used only in controlled environment.

3. The Teaser

The teaser of the application is a stereogrammetric 3D video, created by Blender application [2]. It can be downloaded from the page [3]. Figure 1 gives an idea of the high level of immersion that can be achieved.

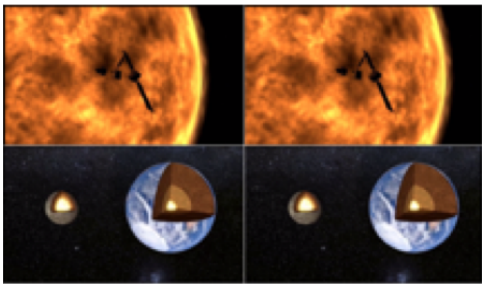

Figure 1: Frames Side by Side of the teaser showing the separation of the BepiColombo modules after the cruise phase (upper part) and the comparison between Earth and Mercury interior structure (bottom).

4. Conclusions

The application proposed has a high involvement of the audience, as well shown by the demo. The navigation interface (the first step in the application development) is presently under design, and a first version will be available for the meeting. With the present poster, we are also asking the support of the instrument teams to obtain all the information about their instruments and the related science to be included in the application. Presently, this work is supported by the BepiColombo Italian team for public outreach Bep-it

Acknowledgements

This work has been developed with the support of ASI, ESA and Airbus.

References

[1] Flamini, E., Capaccioni, F., Cremonese, G., Palumbo, P., Formaro, R., Mugnuolo, R., ... & Team, S. S. (2016). SIMBIO-SYS for BepiColombo: status and issues. Memorie della Societa Astronomica Italiana, 87, 171.

[2] Kent, B.R., 2015. 3D Scientific Visualization with Blender®. Morgan & Claypool Publishers,San Rafael, CA, 105 p.

[3] https://youtu.be/wX5pMHCKeT0